



UNIVERSIDAD NACIONAL AUTÓNOMA DE MEXICO

Unidad Académica de los Ciclos Profesional y Posgrado
del Colegio de Ciencias y Humanidades
Instituto de Geofísica
Posgrado en Geofísica

**CARACTERISTICAS SISMOTECTONICAS DE LA
SUBDUCCION DE LAS PLACAS DE RIVERA Y
COCOS EN EL SUR DE MEXICO**

T E S I S

**PARA OPTAR AL GRADO DE DOCTOR EN GEOFISICA
(SISMOLOGIA Y FISICA DEL INTERIOR DE LA TIERRA)**

P R E S E N T A

MARIO HERNAN PARDO PEDEMONTE

Ciudad Universitaria

Diciembre, 1993

**TESIS CON
FALLA DE ORIGEN**

**TESIS CON
FALLA DE ORIGEN**



Universidad Nacional
Autónoma de México



UNAM – Dirección General de Bibliotecas Tesis Digitales Restricciones de uso

DERECHOS RESERVADOS © PROHIBIDA SU REPRODUCCIÓN TOTAL O PARCIAL

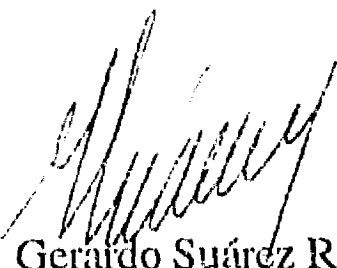
Todo el material contenido en esta tesis está protegido por la Ley Federal del Derecho de Autor (LFDA) de los Estados Unidos Mexicanos (México).

El uso de imágenes, fragmentos de videos, y demás material que sea objeto de protección de los derechos de autor, será exclusivamente para fines educativos e informativos y deberá citar la fuente donde la obtuvo mencionando el autor o autores. Cualquier uso distinto como el lucro, reproducción, edición o modificación, será perseguido y sancionado por el respectivo titular de los Derechos de Autor.

RESUMEN

Se analizan las características de la subducción de las placas de Rivera y Cocos bajo la placa de Norte América en el sur de México, al oeste de 94°W , utilizando hipocentros y mecanismos focales de sismos registrados por redes locales y telesísmicas. La sismicidad base de origen interplaca en zonas de subducción, normalizada por área y tiempo, resulta ser proporcional a la edad de la placa en la trinchera y a la velocidad de convergencia. En el caso de México, dicha sismicidad base aumenta hacia el sureste a lo largo de la trinchera, debido a las variaciones de edad y velocidad de convergencia de las placas de Rivera y Cocos. El análisis de profundidades y mecanismos de foco de sismos en la región de Guerrero, indica que la subducción de la placa de Cocos en México central es subhorizontal entre los 110 y 275 km de la trinchera y que la zona inferior de la placa continental se encuentra bajo un régimen de esfuerzo tensional. La subducción de la placa de Rivera bajo el bloque de Jalisco en el oeste de México, resulta ser muy inclinada (50° bajo los 40 km de profundidad), diferente de la geometría de la subducción observada en Guerrero y similar a la subducción de la placa de Cocos bajo la placa del Caribe en América Central. El volcán de Colima y el frente volcánico andesítico paralelo a la trinchera en la región de Jalisco, pueden ser asociados a la subducción de la placa de Rivera. Se determina un modelo integral de la geometría de las placas de Rivera y Cocos bajo la placa de Norte América, al oeste de la subducción de la dorsal de Tehuantepec. La geometría de subducción muestra una placa de Cocos subduciendo con bajo ángulo de inclinación bajo Norte América, con condiciones de frontera de placas con geometría más inclinada en los bordes, que corresponden a la placa de Rivera bajo Norte América hacia el oeste y la placa de Cocos bajo la placa del Caribe hacia el este. Este modelo explica la sismicidad y el campo de esfuerzos regional en el sur de México. La máxima profundidad del contacto sismogénico es de ~ 30 km en la placa de Cocos y ~ 40 km en la placa de Rivera. No se observan cambios laterales en la geometría de la zona acoplada interplaca al menos hasta los 30 km de profundidad, aunque subducen en la zona rasgos batimétricos importantes. Los cambios laterales notables en la geometría de la placa oceánica en subducción, sólo se observan luego que la placa oceánica se desacopla de la placa continental, sugiriendo que a partir de la transición de la zona de acoplamiento las características de edad y velocidad de convergencia comienzan a ser parámetros importantes en la dinámica de la placa oceánica. Los cambios observados en el buzamiento de la placa oceánica en profundidad, se correlacionan con la subducción de rasgos batimétricos importantes en la zona, los que se asocian a límites de regiones con diferentes características sismotectónicas. Considerando la geometría de la placa en

subducción, la distribución de sismicidad, mecanismos focales y la profundidad máxima de eventos sísmicos, se propone dividir el sur de México en cuatro regiones: 1) Jalisco, limitada por la subducción del graben de El Gordo hacia el este y con subducción inclinada de la placa de Rivera, similar a la de la placa de Cocos bajo el Caribe; 2) Michoacán, entre la subducción del graben de El Gordo y la zona de fractura de Orozco, considerada como una transición entre la subducción inclinada en Jalisco y la subhorizontal en Guerrero; 3) Guerrero, entre las zonas de fractura de Orozco y O'Gorman, con subducción subhorizontal; y 4) Oaxaca, entre la zona de fractura de O'Gorman y la subducción de la dorsal de Tehuantepec, considerada como una transición entre la subducción subhorizontal en Guerrero y la subducción inclinada bajo América Central hacia el este. Los cambios en la geometría de la subducción que ocurren en torno a los límites de las regiones propuestas, parecen ser contorsiones suaves sin fallamiento de la litósfera oceánica en subducción. En el caso del límite entre las placas de Cocos y Rivera, se observa un cambio rápido en el buzamiento de la placa oceánica. Los datos disponibles no permiten resolver si existe en esta zona una fractura o una contorsión en la placa oceánica. Los contornos de 80-100 km de profundidad de la geometría de la subducción en el sur de México se correlacionan bien con el frente de la faja volcánica transmexicana, indicando una relación directa del frente volcánico con la subducción. Por lo tanto, la orientación oblicua con respecto a la trinchera ($\sim 16^\circ$) de la faja volcánica transmexicana se debe probablemente a la geometría de las placas de Rivera y Cocos en subducción bajo la placa de Norte América en el sur de México. Análisis estadísticos de datos de movimientos de placa derivados de lineamientos de anomalías magnéticas, vectores de deslizamiento de mecanismos focales y azimuts de fallas transformadas, indican que los supuestos bloques de Jalisco y del Sur de México, si es que existen, tienen un movimiento lento menor que 5 mm/a y un movimiento insignificante relativo a las placas circundantes, respectivamente.

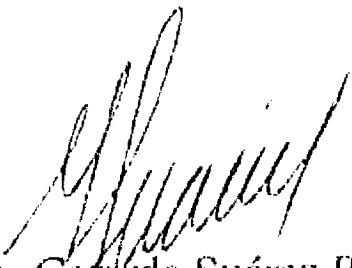


VºBº. Dr. Gerardo Suárez Reynoso
Director de Tesis

ABSTRACT

The subduction of the Rivera and Cocos plates beneath the North American plate in southern Mexico, west of 94°W , is analysed using hypocenters and focal mechanisms of earthquakes recorded by local and teleseismic networks. The interplate background seismicity in the subduction zones, normalized by area and time, appears to be proportional to the age of the oceanic slab at the trench and to the convergence velocity. In the case of Mexico, this background seismicity increases towards the southeast along the trench due to the variations on the age and convergence velocities of the Rivera and Cocos plates. Analysis of depths and focal mechanisms of earthquakes in the Guerrero region, shows that the subducted Cocos plate in central Mexico becomes subhorizontal between 110 and 275 km from the trench reaching a depth of about 50 km, and that the bottom of the overriding continental plate is in tensional stress regime. In western Mexico, the Rivera plate subducts beneath the Jalisco block with a steep angle (50° below a depth of 40 km), different from the subduction geometry observed in Guerrero, but similar to the one observed at the Cocos plate subduction beneath the Caribbean plate in Central America. In the Jalisco region, the Colima volcano and the andesitic volcanic front, parallel to the trench, can be explained by the subduction of the Rivera plate. An integrate model of the geometry of the Rivera and Cocos plates subducted beneath the North American plate, west of the Tehuantepec ridge, was determined. The subduction in southern Mexico may be approximated as a relatively young and buoyant Cocos plate with an almost subhorizontal geometry, bounded at the edges by steep subduction geometry of the Rivera plate beneath North America to the west, and the Cocos plate beneath the Caribbean plate to the east. This model explains the seismicity and the regional stress distribution in southern Mexico. The maximum seismogenic depth of the interplate contact is ~ 30 km for the Cocos plate and ~ 40 km for the Rivera plate. No lateral changes in the dip of the coupled intraplate geometry are observed, at least down to a depth of 30 km, although important bathymetric features are subducted along the trench in the zone. Lateral changes in the dip of the subducted plate geometry are observed once it is decoupled from the overriding plate, suggesting that the age and convergence velocity of the oceanic plate become important parameters in the dynamics of the slab downdip of the decoupling zone. The principal lateral changes in the dip of the downgoing plate apparently correlated with the subduction of important bathymetric features in the zone, which can be associated to boundaries of regions with different seismotectonics characteristics. Based on the geometry of the subducted oceanic plate, the seismicity and focal mechanisms distribution, and the maximum depth of seismicity, a

segmentation of southern Mexico in four regions is suggested: 1) Jalisco, bounded to the east by the subduction of El Gordo graben, showing a steep subduction geometry of the Rivera plate, similar to the one observed for the subduction of the Cocos plate beneath the Caribbean plate; 2) Michoacan, between the subduction of the El Gordo graben and the Orozco fracture zone. It can be considered as a transition zone between the steep subduction in Jalisco and the almost subhorizontal subduction in Guerrero; 3) Guerrero, between the Orozco and O'Gorman fracture zones, showing a subhorizontal subduction geometry; and 4) Oaxaca, between the O'Gorman fracture zone and the subduction of the Tehuantepec ridge, considered as a transition zone between the subhorizontal subduction geometry in Guerrero and the steep subduction geometry of the Cocos plate beneath the Caribbean plate in Central America. The changes in the dip of the downgoing slab suggest smooth contortions, except at the Rivera-Cocos boundary zone where a rapid change in dip is observed. However, the available data is not sufficient to resolve if a tear fault or a contortion in the slab exist here. The 80-100 km depth contour of the subducted slab shows a good correlation with the front of the Trans Mexican Volcanic Belt, indicating a direct relation of this volcanic belt with the subduction of the oceanic plate. Thus, the observed oblique direction ($\sim 16^\circ$) of the volcanic belt relative to the trench is mainly due to the geometry of the subducted Rivera and Cocos plates beneath the North American plate in southern Mexico. Application of statistical analysis to plate motion data derived from marine magnetic anomaly lineations, earthquakes slip vectors and transform fault azimuths, indicate that the presumed Jalisco and Southern Mexico blocks, if they exist, have a slow rate of relative motion less than 5 mm/yr and an insignificant motion relative to the surrounding plates, respectively.



V°B°. Dr. Gerardo Suárez Reynoso

Director de Tesis

INDICE

Resumen	1
I. Introducción	5
II. Sismicidad Base y grado de Acoplamiento en Zonas de Subducción. (Background Seismicity and Strength of Coupling in the Subduction Zones).	12
III. Geometría de la Zona de Benioff y Estado de Esfuerzos en la Placa Continental en México Central (Geometry of the Benioff Zone and State of Stress in the Overriding Plate in Central Mexico)	29
IV. Geometría Inclínada de la Subducción de la Placa de Rivera Bajo el Bloque de Jalisco en el Oeste de México (Steep Subduction Geometry of the Rivera Plate Beneath the Jalisco Block in Western Mexico)	41
V. Forma de la Subducción de las Placas de Rivera y Cocos en el Sur de México: Implicaciones Sísmicas y Tectónicas (Shape of the Subducted Rivera and Cocos Plates in Southern Mexico: Seismic and Tectonic Implications).	54
VI. Análisis Estadístico sobre la Existencia y Movimientos Relativos de los Bloques de Jalisco y Sur de México (Statistical Examination of the Existence and Relative Motions of the Jalisco and Southern Mexico Blocks).	95
VII. Conclusiones	126

RESUMEN

Se analizan las características de la subducción de las placas de Rivera y Cocos bajo la placa de Norte América en el sur de México, al oeste de 94°W , utilizando hipocentros y mecanismos focales de sismos registrados por redes locales y telesísmicas. La sismicidad base de origen interplaca en zonas de subducción, normalizada por área y tiempo, resulta ser proporcional a la edad de la placa en la trinchera y a la velocidad de convergencia. En el caso de México, dicha sismicidad base aumenta hacia el sureste a lo largo de la trinchera, debido a las variaciones de edad y velocidad de convergencia de las placas de Rivera y Cocos. El análisis de profundidades y mecanismos de foco de sismos en la región de Guerrero, indica que la subducción de la placa de Cocos en México central es subhorizontal entre los 110 y 275 km de la trinchera y que la zona inferior de la placa continental se encuentra bajo un régimen de esfuerzo tensional. La subducción de la placa de Rivera bajo el bloque de Jalisco en el oeste de México, resulta ser muy inclinada (50° bajo los 40 km de profundidad), diferente de la geometría de la subducción observada en Guerrero y similar a la subducción de la placa de Cocos bajo la placa del Caribe en América Central. El volcán de Colima y el frente volcánico andesítico paralelo a la trinchera en la región de Jalisco, pueden ser asociados a la subducción de la placa de Rivera. Se determina un modelo integral de la geometría de las placas de Rivera y Cocos bajo la placa de Norte América, al oeste de la subducción de la dorsal de Tehuantepec. La geometría de subducción muestra una placa de Cocos subduciendo con bajo ángulo de inclinación bajo Norte América, con condiciones de frontera de placas con geometría más inclinada en los bordes, que corresponden a la placa de Rivera bajo Norte América hacia el oeste y la placa de Cocos bajo la placa del Caribe hacia el este. Este modelo explica la sismicidad y el campo de esfuerzos regional en el sur de México. La máxima profundidad del contacto sismogénico es de ~ 30 km en la placa de Cocos y ~ 40 km en la placa de Rivera. No se observan cambios laterales en la geometría de la zona acoplada interplaca al menos hasta los 30 km de profundidad, aunque subducen en la zona rasgos batimétricos importantes. Los cambios laterales notables en la geometría de la placa oceánica en subducción, sólo se observan luego que la placa oceánica se desacopla de la placa continental, sugiriendo que a partir de la transición de la zona de acoplamiento las características de edad y velocidad de convergencia comienzan a ser parámetros importantes en la dinámica de la placa oceánica. Los cambios observados en el buzamiento de la placa oceánica en profundidad, se correlacionan con la subducción de rasgos batimétricos importantes en la zona, los que se asocian a límites de regiones con diferentes características sismotectónicas. Considerando la geometría de la placa en subducción, la distribución de sismicidad, mecanismos focales y

la profundidad máxima de eventos sísmicos, se propone dividir el sur de México en cuatro regiones: 1) Jalisco, limitada por la subducción del graben de El Gordo hacia el este y con subducción inclinada de la placa de Rivera, similar a la de la placa de Cocos bajo el Caribe; 2) Michoacán, entre la subducción del graben de El Gordo y la zona de fractura de Orozco, considerada como una transición entre la subducción inclinada en Jalisco y la subhorizontal en Guerrero; 3) Guerrero, entre las zonas de fractura de Orozco y O'Gorman, con subducción subhorizontal; y 4) Oaxaca, entre la zona de fractura de O'Gorman y la subducción de la dorsal de Tehuantepec, considerada como una transición entre la subducción subhorizontal en Guerrero y la subducción inclinada bajo América Central hacia el este. Los cambios en la geometría de la subducción que ocurren en torno a los límites de las regiones propuestas, parecen ser contorsiones suaves sin fallamiento de la litósfera oceánica en subducción. En el caso del límite entre las placas de Cocos y Rivera, se observa un cambio rápido en el buzamiento de la placa oceánica. Los datos disponibles no permiten resolver si existe en esta zona una fractura o una contorsión en la placa oceánica. Los contornos de 80-100 km de profundidad de la geometría de la subducción en el sur de México se correlacionan bien con el frente de la faja volcánica transmexicana, indicando una relación directa del frente volcánico con la subducción. Por lo tanto, la orientación oblicua con respecto a la trinchera ($\sim 16^\circ$) de la faja volcánica transmexicana se debe probablemente a la geometría de las placas de Rivera y Cocos en subducción bajo la placa de Norte América en el sur de México. Análisis estadísticos de datos de movimientos de placa derivados de lineamientos de anomalías magnéticas, vectores de deslizamiento de mecanismos focales y azimuts de fallas transformadas, indican que los supuestos bloques de Jalisco y del Sur de México, si es que existen, tienen un movimiento lento menor que 5 mm/a y un movimiento insignificante relativo a las placas circundantes, respectivamente.

ABSTRACT

The subduction of the Rivera and Cocos plates beneath the North American plate in southern Mexico, west of 94°W , is analysed using hypocenters and focal mechanisms of earthquakes recorded by local and teleseismic networks. The interplate background seismicity in the subduction zones, normalized by area and time, appears to be proportional to the age of the oceanic slab at the trench and to the convergence velocity. In the case of Mexico, this background seismicity increases towards the southeast along the trench due to the variations on the age and convergence velocities of the Rivera and Cocos plates. Analysis of depths and focal mechanisms of earthquakes in the Guerrero region, shows that the subducted Cocos plate in central Mexico becomes subhorizontal between 110 and 275 km from the trench reaching a depth of about 50 km, and that the bottom of the overriding continental plate is in tensional stress regime. In western Mexico, the Rivera plate subducts beneath the Jalisco block with a steep angle (50° below a depth of 40 km), different from the subduction geometry observed in Guerrero, but similar to the one observed at the Cocos plate subduction beneath the Caribbean plate in Central America. In the Jalisco region, the Colima volcano and the andesitic volcanic front, parallel to the trench, can be explained by the subduction of the Rivera plate. An integrate model of the geometry of the Rivera and Cocos plates subducted beneath the North American plate, west of the Tehuantepec ridge, was determined. The subduction in southern Mexico may be approximated as a relatively young and buoyant Cocos plate with an almost subhorizontal geometry, bounded at the edges by steep subduction geometry of the Rivera plate beneath North America to the west, and the Cocos plate beneath the Caribbean plate to the east. This model explains the seismicity and the regional stress distribution in southern Mexico. The maximum seismogenic depth of the interplate contact is ~ 30 km for the Cocos plate and ~ 40 km for the Rivera plate. No lateral changes in the dip of the coupled intraplate geometry are observed, at least down to a depth of 30 km, although important bathymetric features are subducted along the trench in the zone. Lateral changes in the dip of the subducted plate geometry are observed once it is decoupled from the overriding plate, suggesting that the age and convergence velocity of the oceanic plate become important parameters in the dynamics of the slab downdip of the decoupling zone. The principal lateral changes in the dip of the downgoing plate apparently correlated with the subduction of important bathymetric features in the zone, which can be associated to boundaries of regions with different seismotectonics characteristics. Based on the geometry of the subducted oceanic plate, the seismicity and focal mechanisms distribution, and the maximum depth of seismicity, a segmentation of southern Mexico in four regions is suggested: 1) Jalisco,

bounded to the east by the subduction of El Gordo graben, showing a steep subduction geometry of the Rivera plate, similar to the one observed for the subduction of the Cocos plate beneath the Caribbean plate; 2) Michoacan, between the subduction of the El Gordo graben and the Orozco fracture zone. It can be considered as a transition zone between the steep subduction in Jalisco and the almost subhorizontal subduction in Guerrero; 3) Guerrero, between the Orozco and O'Gorman fracture zones, showing a subhorizontal subduction geometry; and 4) Oaxaca, between the O'Gorman fracture zone and the subduction of the Tehuantepec ridge, considered as a transition zone between the subhorizontal subduction geometry in Guerrero and the steep subduction geometry of the Cocos plate beneath the Caribbean plate in Central America. The changes in the dip of the downgoing slab suggest smooth contortions, except at the Rivera-Cocos boundary zone where a rapid change in dip is observed. However, the available data is not sufficient to resolve if a tear fault or a contortion in the slab exist here. The 80-100 km depth contour of the subducted slab shows a good correlation with the front of the Trans Mexican Volcanic Belt, indicating a direct relation of this volcanic belt with the subduction of the oceanic plate. Thus, the observed oblique direction ($\sim 16^\circ$) of the volcanic belt relative to the trench is mainly due to the geometry of the subducted Rivera and Cocos plates beneath the North American plate in southern Mexico. Application of statistical analysis to plate motion data derived from marine magnetic anomaly lineations, earthquakes slip vectors and transform fault azimuths, indicate that the presumed Jalisco and Southern Mexico blocks, if they exist, have a slow rate of relative motion less than 5 mm/yr and an insignificant motion relative to the surrounding plates, respectively.

I. INTRODUCCION

La sismicidad y la tectónica del sur de México están caracterizadas por la subducción de las placas de Rivera y Cocos bajo la placa de Norte América a lo largo de la trinchera Mesoamericana. El rasgo principal observado en la geometría de la subducción en esta zona es la variación lateral del ángulo de buzamiento de la litósfera oceánica en subducción [Molnar and Sykes, 1969; Stoiber y Carr, 1973; Dean y Drake, 1978; Nixon, 1982; Bevis y Isacks, 1984; Burbach et al., 1984].

En la placa continental, el rasgo principal lo constituye la existencia de la faja volcánica transmexicana, cuya orientación no paralela a la trinchera ($\sim 16^\circ$) ha dado origen a hipótesis controversiales sobre su génesis, desde las que favorecen una asociación directa entre la subducción y el volcanismo [e.g., Molnar and Sykes, 1969; Demant and Robin, 1975; Nixon, 1982; Burbach et al., 1984; Suárez and Singh, 1986; Singh and Mortera, 1991], a las que sugieren que no existe relación con la subducción, sino que con antiguas zonas de debilidad en la corteza del sur de México provenientes de antiguos episodios de deformación [e.g., Mooser, 1972, Gastil and Jensky, 1973, Shurbet and Cebull, 1984; Johnson and Harrison, 1989].

El sur de México incluye la zona de subducción de Rivera hacia el oeste y está limitada por la subducción de la dorsal de Tehuantepec hacia el este. La historia tectónica de la zona para los últimos 25 m.a. incluye al menos tres grandes reorganizaciones en los movimientos de la placa oceánica. En cada reorganización la antigua placa de Farallón, que evolucionó primero como la placa de Guadalupe, fue reducida a las actuales placas de Rivera y Cocos, cambiando la posición de los centros de esparcimiento del fondo oceánico, primero hacia los montes marinos Mathematician entre los 12.5 y 11 m.a., y luego a la actual posición de la dorsal del Pacífico occidental entre los 6.3 y 3.5 m.a. [Mammerickx y Klitgord, 1982]. La velocidad absoluta relativa a los puntos calientes de la placa de Norte América es de 3.0 cm/a y la de la placa del Caribe es de 1.9 cm/a [Gripp y Gordon, 1990].

La velocidad relativa de las placas de Rivera y Cocos con respecto a Norte América varía a lo largo de la trinchera debido a la cercanía de los polos de rotación a cada placa. Esta velocidad, en relación a otras zonas de subducción, es muy lenta (2 cm/a) en el caso de Rivera-Norte América [DeMets y Stein, 1990] y en el caso de Cocos-Norte América esta velocidad es moderada (~ 6 cm/a) [DeMets et al., 1990].

Para el sur de México se han planteado varios modelos preliminares de la geometría de la subducción basados en la sismicidad [Stoiber and Carr, 1973; Hanus and Vanek, 1978; Havskov et al., 1982; Burbach et al., 1984; Bevis and Isacks, 1984; Suárez et al., 1990; Singh and Mortera, 1991; Ponce et al., 1992]. También se han planteado modelos de la

distribución regional de esfuerzos asociada a la subducción de la placa de Cocos basados en mecanismos focales, principalmente de primeras llegadas de ondas P, de sismos importantes ocurridos en la zona [Molnar and Sykes, 1969; Dean and Drake, 1978; Burbach et al., 1984; LeFevre and McNally, 1985]. Sin embargo, en la mayoría de estos estudios, la geometría de la subducción de las placas de Rivera y Cocos bajo Norte América (NW de 94°W), y el campo de esfuerzos asociado, han sido pobremente definidos debido a la baja actividad sísmica de eventos de profundidad intermedia (profundidad focal > 40 km) y a la escasez de estaciones sismológicas en el sur de México.

En este estudio se analizan las características sismotectónicas de la subducción de las placas de Rivera y Cocos bajo Norte América en el sur de México, utilizando hipocentros bien localizados y mecanismos de foco de sismos en la zona.

Sismicidad de Fondo y Grado de Acoplamiento en Zonas de Subducción

Numerosos estudios han intentado explicar las características observadas en zonas de subducción en términos de algunos parámetros que supuestamente controlan la morfología de las placas en subducción y la magnitud máxima posible de sismos intraplaca [e.g. Cross y Pilger, 1972; Ruff y Kanamori, 1980; Jarrard, 1986]. Los principales parámetros de la litósfera oceánica parecen ser la edad de la placa en la trinchera y la velocidad de convergencia relativa a la placa continental.

En el Capítulo II, se presenta un estudio [Singh et al., 1992] sobre la posible relación de la sismicidad base en zonas de subducción, definida como el número de sismos superficiales ($h \leq 70$ km) con magnitud $m_b \geq 5$ que ocurren en un área de 1000 km² por año, excluyendo los eventos que ocurren un mes antes y tres meses después de un sismo con magnitud $M_s \geq 7$. El motivo del estudio fue el comprender la baja sismicidad base observada en el oeste de México, especialmente en las regiones de Michoacán y Jalisco, caracterizadas por la ocurrencia de grandes terremotos (Michoacán, 1985, $M_s=8.1$; Jalisco, 1932, $M_s=8.2$), placas en subducción relativamente jóvenes (< 10 m.a.) y velocidades de convergencia bajas (< 5.5 cm/a) relativas a otras zonas de subducción.

Geometría de la Zona de Benioff y Estado de Esfuerzos en la Placa Continental en México Central.

La morfología de la zona de subducción en México central ha sido pobremente definida debido a la baja actividad sísmica de eventos de profundidad intermedia ($h > 40$ km) y a la falta de una cobertura adecuada de estaciones sismológicas. Estudios anteriores en la zona sólo han sido posibles en la región oeste (100°W-101°W) donde existen datos de buena calidad de la red sismológica de Guerrero [Suárez et al., 1990]. Estos autores concluyen

que el ángulo de subducción de la placa de Cocos bajo el continente es prácticamente subhorizontal y plantean la existencia de una zona doble en esfuerzos bajo la zona en que se desacoplan las placas oceánica y continental, asociada a la flexión de la placa de Cocos.

En el Capítulo III, se presenta un estudio basado en hipocentros y mecanismos focales de sismos en México central [Singh y Pardo, 1993], en el cual se corrobora la geometría de la subducción de Suárez *et al.* [1990], extendiéndola más hacia el interior del continente y se postula la posibilidad de que la placa continental esté sometida a un régimen de esfuerzos tensional. Además, se analizan posibles hipótesis para explicar la geometría observada de la placa en subducción.

Geometría Inclinada de la Subducción de la Placa de Rivera Bajo el Bloque de Jalisco en el Oeste de México.

La existencia de la placa de Rivera fue sugerida inicialmente por Atwater [1970]. Esta placa es cinemáticamente diferente de las placas de Norte América y Cocos [Eissler y McNally, 1984; DeMets y Stein, 1990] y se ha postulado que el graben de El Gordo, localizado en el fondo marino en la prolongación de la zona de fractura de Rivera, constituye el límite entre las placas de Cocos y Rivera [Bandy, 1992]. Historicamente se han documentado al menos seis grandes terremotos en la zona, incluyendo el gran evento de Jalisco en 1932, $M_s=8.2$ [Eissler y McNally, 1984; Singh *et al.*, 1985].

El Capítulo IV presenta el análisis de la geometría de la subducción de la placa de Rivera [Pardo y Suárez, 1993], utilizando hipocentros de microsismicidad registrada con redes locales, relocalización de hipocentros con datos telesísmicos [Dewey, 1981] y modelación de formas de ondas de período largo de las fases P, SV y SH [Nábelek, 1984]. Se observa un ángulo de buzamiento inclinado en la placa de Rivera ($\sim 50^\circ$), que es muy diferente a la inclinación prácticamente subhorizontal en Guerrero, y similar al observado en la subducción de la placa de Cocos bajo la placa del Caribe en Centro América [Burbach *et al.*, 1984]. Esta geometría explica la existencia del Volcán de Colima, bajo el cual la placa de Rivera alcanza los 100 km de profundidad, y se postula una posible relación del frente volcánico andesítico paralelo a la trinchera observado hacia el noroeste [Lange y Carmichael, 1991; Wallace *et al.*, 1992], con la subducción de la placa de Rivera..

Forma de la Subducción de las Placas de Rivera y Cocos en el Sur de México: Implicaciones Sísmicas y Tectónicas

En el Capítulo V, se presenta un modelo integral de la geometría de la subducción de la placas de Cocos y Rivera en el sur de México [Pardo y Suárez, 1993]. Este modelo explica

la sismicidad y el campo de esfuerzos regional en el sur de México, la relación de la subducción con la faja volcánica transmexicana y su dirección oblicua relativa a la trinchera.

Considerando la geometría de la placa oceánica en subducción a lo largo del sur de México, sus cambios notables en el buzamiento de la placa oceánica (correlacionados con la subducción de rasgos batimétricos importantes en la zona), y la profundidad máxima de sismos en la zona, se postula una división del sur de México en cuatro regiones con diferentes características sismotectónicas: Jalisco, Michoacán, Guerrero y Oaxaca.

Los contornos de profundidad 80-100 km de la geometría de la subducción de la placa oceánica se correlacionan bien con el frente de la faja volcánica transmexicana, indicando una relación directa de esta faja volcánica con la subducción. La dirección oblicua relativa a la trinchera de la faja volcánica transmexicana se debe principalmente a la forma de la subducción de las placas de Rivera y Cocos bajo Norte América en el sur de México.

Análisis Estadístico sobre la Existencia y Movimientos Relativos de los Bloques de Jalisco y Sur de México

Se ha postulado una posible fragmentación de la litósfera continental de México al sur de la faja volcánica transmexicana en dos bloques litosféricos, los bloques de Jalisco y del Sur de México.

En el Capítulo VI [*Bandy y Pardo, 1993*], la existencia y movimientos relativos de estos bloques se analizan aplicando el test estadístico F a datos de movimientos de placas derivados de lineamientos de anomalías magnéticas, vectores de deslizamiento de mecanismos focales y azimuts de fallas transformadas. La hipótesis por verificar es la significancia en el cierre de un circuito de placas utilizando los datos mencionados.

Aplicando esta técnica al circuito de placas Pacífico-Cocos-Norte América, se obtiene que no existen diferencias significativas (al 99% de confianza) en el cierre de este circuito. Luego, si es que existe el bloque del Sur de México, su movimiento relativo a las placas circundantes es insignificante y puede ser considerado como parte de la placa de Norte América.

Los resultados de aplicar esta técnica al circuito de placas Rivera-Pacífico-Norte América, indican que existe diferencia significativa en el cierre del circuito. Se postulan dos posibles interpretaciones: 1) El bloque de Jalisco existe en forma independiente relativo a las placas circundantes, con un movimiento relativo lento (< 5 mm/a) con respecto a Norte América; 2) Las diferencias en el cierre del circuito de placas se deben principalmente a efectos de cambios recientes en el movimiento relativo entre las placas de Rivera y Pacífico. En este caso, el bloque de Jalisco sería parte de la placa de Norte América.

REFERENCIAS

- Atwater, T., Implications of plate tectonics for the Cenozoic tectonic evolution of western North America, *Geol. Soc. Am. Bull.*, 81, 3513-3536, 1970.
- Bandy, W.L., Geological and Geophysical investigation of the Rivera-Cocos plate boundary: Implications of plate fragmentation, *Ph.D. Thesis, Texas A&M University, Colege Station, Texas*, 1992.
- Bandy, W.L. and M. Pardo, Statistical examination of the existence and relative motions of the Jalisco and southern Mexico blocks, Submitted to *Tectonics*, 1993.
- Bevis, M. and B.L. Isacks, Hypocentral trend surface analysis: Probing the geometry of Benioff zones, *J. Geophys. Res.*, 89, 6153-6170, 1984.
- Burbach, G., C. Frolich, W. Pennington and T. Matumoto, Seismicity and tectonics of the subducted Cocos plate, *J. Geophys. Res.*, 89, 7719-7735, 1984.
- Cross, R.H. and T.A. Pilger, Controls of subduction geometry, location of magmatic arcs, and tectonics of arc and back-arc regions, *Geol. Soc. Am. Bull.*, 93, 545-562, 1982.
- Dean, B.W. and C.L. Drake, Focal mechanism solutions and tectonics of the Middle America arc, *J. Geol.*, 86, 111-128, 1978.
- Demant, A. and C. Robin, Las fases del volcanismo en México; una síntesis en relación con la evolución geodinámica desde el Cretácico, *Rev. Inst. Geol., UNAM*, 75, 70-82, 1975.
- DeMets, C. and S. Stein, Present-day kinematics of the Rivera plate and implications for tectonics in southwestern Mexico, *J. Geophys. Res.*, 95, 21, 931-21, 948, 1990.
- DeMets, C., R.G. Gordon, D.F. Argus, and S. Stein, Current plate motions, *Geophys. Res. J. Int.*, 101, 425-478, 1990.
- Dewey, J.W., Seismicity studies with the method of Joint Hypocenter Determination, *Ph.D. Thesis, University of California, Berkeley*, 1971.
- Eissler, H. and K.C. McNally, Seismicity and tectonics of the Rivera plate and implications for the 1932 Jalisco, Mexico, earthquake, *J. Geophys. Res.*, 89, 4520-4530, 1984.
- Gastil, R.G. and W. Jensky, Evidence for strike-slip displacement beneath the Trans-Mexican volcanic belt, *Stanford Univ. Publ. Geol. Sci.*, 13, 171-180, 1973.
- Gripp, A. and R. Gordon, Current velocities relative to the hotspots incorporating the NUVEL-1 global plate motion model, *Geophys. Res. Lett.*, 17, 1109-1112, 1990.
- Hanus, V. and J. Vanek, Subduction of the Cocos plate and deep active fracture zones of Mexico, *Geofis. Inter.*, 17, 14-53, 1978.
- Havskov, J., S.K. Singh and D. Novelo, Geometry of the Benioff zone in the Tehuantepec area in southern Mexico, *Geofis. Int.*, 21, 325-330, 1982.

- Jarrard, R.D., Relations among subduction parameters, *Rev. of Geophys.*, 24, 217-284, 1986.
- Johnson, C.A. and C.G.A. Harrison, Tectonics and volcanism in central Mexico: A Landsat Thematic Mapper perspective, *Remote Sens. Envir.*, 28, 273-286, 1989.
- Lange, R. and I. Charmichael, A potassic volcanic front in western Mexico: The lamprophyric and related lavas of San Sebastian, *Geol. Soc. Am. Bull.*, 103, 928-940, 1991.
- LeFevre, L.V. and K.C. McNally, Stress distribution and subduction on aseismic ridges in the middle America subduction zone, *J. Geophys. Res.*, 90, 4495-4510, 1985.
- Mammerickx, J. and K. Klitgord, Northern East Pacific Rise: Evolution from 25 m.y.B.P. to the present, *J. Geophys. Res.*, 87, 6751-6759, 1982.
- Molnar, P. and L. R. Sykes, Tectonics of the Caribbean and Middle American region from focal mechanisms and seismicity, *Geol. Soc. Am. Bull.* 80, 1639-1684, 1969.
- Mooser, F., The Mexican volcanic belt: Structure and tectonics, *Geoffs. Int.*, 12, 55-70, 1972.
- Nábelek, J.L., Determination of earthquake source parameters from inversion of body waves, *Ph.D. thesis, 346 pp., Mass. Inst. of Technol., Cambridge, 1984.*
- Nixon, G. T., The relationship between Quaternary volcanism in central México and the seismicity and structure of subducted oceanic lithosphere, *Geol. Soc. Am. Bull.*, 93, 514-523, 1982.
- Pardo, M. and G. Suárez, Steep subduction geometry of the Rivera plate beneath the Jalisco block in western Mexico, in press: *Geophys. Res. Lett.*, 1993.
- Ponce, L., Gaulon, G. Suárez, and E. Lomas, Geometry and state of stress of the downgoing Cocos plate in the Isthmus of Tehuantepec, Mexico, *Geophys. Res. Lett.*, 19, 773-776, 1992.
- Ruff, L. and H. Kanamori, Seismicity and the subduction process, *Phys. Earth Planet. Interiors*, 23, 240-252, 1980
- Shurbet, D.H. and S.E. Cebull, Tectonic interpretation of the Trans-Mexican volcanic belt, *Tectonophys.*, 101, 159-165, 1973.
- Singh, S.K., L. Ponce, and S.P. Nishenko, The great Jalisco, Mexico, earthquake of 1932: Subduction of the Rivera Plate, *Bull. Seismol. Soc. Am.*, 75, 1301-1313, 1985.
- Singh, S.K., and F. Mortera, Source time functions of large Mexican subduction earthquakes, morphology of the Benioff zone, age of the plate, and their tectonic implications, *J. Geophys. Res.*, 96, 21487-21502, 1991.
- Singh, S.K., D. Comte, and M. Pardo, Background seismicity and strength of coupling in the subduction zones, *Bull. Soc. Seism. Am.*, 82, 2114-2125, 1992.

- Singh, S.K. and M. Pardo, Geometry of the Benioff zone and state of stress in the overriding plate in Central Mexico, *Geophys. Res. Lett.*, 20, 1483-1486, 1993.
- Stoiber R.E. and M.J. Carr, Quaternary volcanic and tectonic segmentation of Central America, *Bull. Volcanol.*, 37, 304-325, 1973.
- Suárez, G. and S.K. Singh, Tectonic interpretation of the Trans-Mexican Volcanic Belt-Discussion, *Tectonophys.*, 127, 155-160, 1986.
- Suárez, G., T. Monfret, G. Wittlinger, and C. David, Geometry of subduction and depth of the seismogenic zone in the Guerrero gap, Mexico, *Nature*, 345, 336-338, 1990.
- Wallace, P., I. Carmichael, K. Richter, and T. Becker, Volcanism and tectonism in western Mexico: A contrast of style and substance, *Geology*, 20, 625-628, 1992.

II. Sismicidad Base y grado de Acoplamiento en Zonas de Subducción
(Publicado en: *Bull. Seism. Soc. Am.*, 82, 2114-2125, 1992)

**BACKGROUND SEISMICITY AND STRENGTH OF
COUPLING IN THE SUBDUCTION ZONES**

S. K. SINGH, D. COMTE¹, AND M. PARDO¹

Instituto de Geofísica, U.N.A.M., C. U., 04510 México, D. F.
(¹also at Universidad de Chile, Depto. de Geofísica, Casilla 2777, Santiago, Chile)

ABSTRACT

Background seismicity, N_n , in subduction zones is found to be related to the age of the plate at the trench, T , and the relative convergence speed, V , by $N_n = a T^b V^c$ ($b, c > 0$). The number of aftershocks is correlated with the background seismicity. Since the background seismicity increases with both T and V whereas the maximum magnitude, M_w , increases with V but decreases with T , no clear relationship exists between the strength of the coupling (as measured by M_w) and the background seismicity. The data, however, suggests that truly great earthquakes occur on plate boundaries which are characterized by moderate seismicity. The regions of very high and low seismicity are, generally, not the sites of great earthquakes.

INTRODUCTION

Several studies have attempted to explain the observed characteristics of the subduction zones in terms of some key parameters. An extensive review on the subject is given by Jarrard (1986). The controlling parameters which seem to explain the morphology of the subducted plates and the maximum magnitude of earthquakes on the interface are the age (T) and the relative convergence speed (V). For example, the dependence of maximum depth of the Benioff zone on T (Vlaar and Wortel, 1976; Wortel and Vlaar, 1978), of down-dip length on V (Isacks *et al.*, 1968) and on V and T (Molnar *et al.*, 1979), of the dip of the slab on V (Luyendyk, 1970) have been suggested. Kanamori (1971) and Uyeda and Kanamori (1979) have pointed out that the maximum magnitude, M_w , along the subduction zones shows great variation, suggesting different degrees of coupling at the interface: Chilean and Mariana subduction zones are cited as the extreme cases, with the former being strongly coupled (hence characterized by great earthquakes) and the latter being weakly coupled (with relative lack of large earthquakes). Kelleher *et al.* (1974) report a correlation between the magnitude of the large earthquake with the width of the plate interface. Ruff

and Kanamori (1980), who have carried out a linear multi-variable regression between maximum M_W and V and T , find that (see also Heaton and Kanamori, 1984).

$$M_W = 7.96 + 0.134 V - 0.00889 T \quad (1)$$

where V (cm/yr) and T (m. y.). In equation 1, the multiple correlation coefficient, r , is 0.8 and the standard deviation of the observed M_W around the predicted value is 0.4.

In this paper we investigate whether the background seismicity in the subduction zones is related to T and/or V . If so, then how is this seismicity related to maximum M_W ? The study is motivated by our desire to understand the cause of observed low background seismicity NW of about $100^\circ W$ along the Mexican subduction zone, especially in the Michoacan and Jalisco regions. These areas are characterized by occurrence of large/great earthquakes (e.g., Michoacan, 1985, $M_S = 8.1$; Jalisco, 1932, $M_S = 8.2$), relatively young subducting plates (<10 m. y. old), and low convergence speeds (< 5.5 cm/yr).

DATA

For the purpose of this paper, we define background seismicity as number of events, N_B , with $m_b \geq 5$ per 1000 km^2 per yr with depth ≤ 70 km. We extracted the events for the period 1965-1988 from the National Earthquake Information Center (NEIC) tape and excluded data for one month prior and three months after any $M_S \geq 7$ event. We are assuming that if any precursory seismicity occurs before large earthquakes then it is confined to a one month period before the event and that aftershocks die out in the following three months. This assumption may be questionable. To test its validity we took a closer look at those regions where a $M_S \geq 7$ event occurred during 1965-1988 period. We computed background seismicity before and after the event after removing possible foreshocks (one month) and aftershocks (three months). We found that these two values were nearly equal suggesting that our assumption is reasonable. We are not implying that foreshock and aftershock sequences are confined to one month before and three months after a major event, respectively. The test, however, does suggest that the assumption is grossly valid for the general relationship between N_B and T and/or V that we are seeking. Furthermore, roughly equal values of N_B in adjacent regions (with T and V values nearly constant), irrespective of whether or not a large/great earthquake has occurred in one of the regions during the period of interest, give us additional confidence in the assumption.

We checked the NEIC catalog for completeness of $m_b \geq 5$ events by plotting $\log N$ versus m_b , where N is the cumulative number of events with magnitude $\geq m_b$. For some regions the catalog was found to be incomplete for $m_b \geq 5$. In such cases $\log N$ versus m_b data was fitted to Gutenberg and Richter relation, $\log N = a - bm_b$. These plots along with the b values, were used to obtain the corrected values of N for $m_b \geq 5$.

Figure 1 shows the regions where N_n values have been computed. Table 1 lists these regions. For each region the table gives the coordinate of the center and the length (along the trench) and width (perpendicular to the trench) of the rectangular area within which the seismicity has been estimated. References for the age, T , of the plate at the trench and the relative convergence speed, V , are given in Table 1. The values of T and V for the same region given by different sources some times vary. In such cases, the values listed in Table 1 are based on more recent papers dealing with these regions. In Table 1, T , V , and N_n vary by a factor of about 30 (5 to 155 m. y.), 6 (2.0 to 11.8 cm/yr), and 100 (1.5×10^{-3} to 152.0×10^{-3} event/1000 km²/yr; $m_b \geq 5$), respectively.

ANALYSIS AND RESULT

Figures 2 and 3 give $\log N_n$ versus $\log T$ and $\log N_n$ versus $\log V$ plots, respectively. These figures show that background seismicity and age, and background seismicity and convergence speed are correlated. The relations are:

$$\log N_n = (-3.133 \pm 0.242) + (0.975 \pm 0.147) \log T \quad (2)$$

with correlation coefficient $r = 0.73$ and standard deviation, $\sigma = 0.323$, and

$$\log N_n = (-2.708 \pm 0.216) + (1.410 \pm 0.256) \log V \quad (3)$$

with $r = 0.67$ and $s = 0.354$. Note that for the 40 data points the significance at 99% level corresponds to $r = 0.4$. The variables $\log N_n$ and $\log T$, and $\log N_n$ and $\log V$ are correlated above this level. Equations 2 and 3 and Figs. 2 and 3 suggest that $\log N_n$ may be better explained by a combination of $\log T$ and $\log V$. A multivariate regression analysis gives the following relation:

$$\log N_n = (-3.696 \pm 0.197) + (0.789 \pm 0.110) \log T + (1.059 \pm 0.174) \log V \quad (4)$$

with $r = 0.88$ and the standard deviation of $\log N_n$ around the predicted value of 0.308. Figure 4 shows predicted $\log N_n$ versus observed $\log N_n$.

If heterogeneities on and around the plate interface are the cause of both the background seismicity and the number of aftershocks following large ($M_s \geq 7.0$) earthquakes then it is reasonable to expect a correlation between the two. Singh and Suárez (1988) studied the regional variation in the number, N , of aftershocks ($m_b \geq 5$) of large subduction zone earthquakes ($M_w \geq 7$). In the study a 30-day interval immediately after the main shock was used to estimate N . Two reasonable scaling relations were assumed in order to estimate excess or deficiency of N : (1) N is proportional to the rupture area A (since $M_w \propto \log M_0 \propto \log A$, $N \propto A$ implies $\log N \propto M_w$) and (2) N is proportional to the seismic energy release E_s during the main shock (since $\log E_s \propto \log M_0 + 1.5 M_w$, $N \propto E_s$ implies $\log N \propto 1.5 M_w$). Let

$$\log N_r = \log (N/N_e) \quad (5)$$

where N_e is the expected number of aftershocks calculated by fitting $\log N$ versus M_w data to the scaling relations mentioned above. Note that $\log N_r$ greater than and less than zero represents excess and deficiency of aftershocks, respectively. Fig. 5 gives $\log N_r$ versus $\log N_n$ plot, where $\log N_r$ has been estimated by assuming $N \propto A$, a scaling also supported by Japanese data (Yamanaka and Shimazaki, 1990). An essentially similar plot, although with somewhat greater dispersion, results by taking $N \propto E_s$. $\log N_r$ is related to $\log N_n$ by

$$\log N_r = (1.285 \pm 0.241) + (0.936 \pm 0.171) \log N_n \quad (6)$$

with $r = 0.68$ and standard deviation $\sigma = 0.421$. As expected, the number of aftershocks is directly correlated with the background seismicity of a region.

DISCUSSION

Equations 2 to 4 and Figs. 2 to 4 strongly suggest that the background seismicity, N_n , increases with the age of the plate near the trench, T , and the relative convergence speed, V . The strength of the interface coupling, characterized by the maximum magnitude, M_w (Kanamori, 1971; Uyeda and Kanamori, 1979); Ruff and Kanamori, 1980) also increases

with V but decreases with T (equation 1). In other words, for a fixed T both background seismicity and M_W increase with V but for a fixed V , increasing T plays opposite roles, i. e., higher seismicity but smaller M_W . The results are summarized in Fig. 6 (modified from Ruff and Kanamori, 1980) which shows the dependence of background seismicity and M_W on T and V . While Ruff and Kanamori (1980) treated Mexico and Central America as one subduction zone with a maximum M_W of 8.2, we have subdivided this area into Jalisco ($M_W = 8.2$), Michoacan ($M_W = 8.1$), Guerrero + Oaxaca ($M_W = 8.4$), and Central America ($M_W = 8.2$) regions. This is justified in view of different ages of the subducting plates (5 to 40 m.y.) and varying convergence speeds (2.0 to 9.4 cm/yr) in this area. While for the Guerrero + Oaxaca region $M_W = 8.4$ is based on the estimated magnitude of the great earthquake of 1845 (G. Suárez, personal communication, 1991), all other maximum magnitudes for this area are from instrumental recordings. In Fig. 6 the lines of equal $\log N_B$ and M_W values are drawn. This figure can be qualitatively interpreted in terms of the evolutionary model of subduction proposed by Kanamori (1971, 1977), Uyeda and Kanamori (1979), and Ruff and Kanamori (1980). For a fixed T , increasing V results in greater compressive stress at the interface and, hence, in stronger coupling. Higher rate of tectonic loading for larger V also results in increasing seismicity. For a fixed V , large T involves repeated rupture and associated fracturing and gouge formation of the interface, partial decoupling of the subducted slab from the upper plate, and, perhaps, the presence of sediments with high pore pressure between the two plates. This may explain both a weaker coupling and higher seismicity on and around the interface of older subducting plates.

The dependence of the strength of coupling and the background seismicity on V and T is such that weaker seismicity of a region does not necessarily imply a stronger coupling, unless the seismicity is caused by small T and large V . If T is small and V is large, such that the background seismicity is small, can one reasonably use equation (1) to estimate maximum M_W ? We note the minimum T used in deriving equation (1) was 20 m. y. (Ruff and Kanamori, 1980). It is not clear whether this relation can be extrapolated for a very young ($T < 10$ m. y.) and, therefore, a thin underthrusting oceanic lithosphere. A case in point is the Michoacan region along the Mexican subduction zone, where V and T are about 6 cm/yr and 5 m. y., respectively. The region is characterized by a low level of background seismicity (Table 1), occurrence of great earthquakes (e. g., 1985, $M_S = 8.1$) and very small number of aftershocks (Singh and Suárez, 1988). Equation (1) predicts a maximum magnitude, M_W , of 8.7 which implies a moderate to strong coupling in the region. Historical and instrument data do not suggest an M_W much greater than 8.1 in Michoacan. The earthquake of 1985 gave rise to excellent epicentral recordings of strong motion. Peak

accelerations (<0.2 g) and velocities (<30 cm/sec), and different estimations of stress change (6 to 20 bars) during this earthquake (Anderson *et al.*, 1986) indicate a weak coupling. While the Michoacan earthquake casts some doubt on the validity of equation (1) for $T < 10$ m. y., the equation works well for the Jalisco region ($V = 2.0$ cm/yr, $T = 9$ m. y.). The standard error of 0.4 in the prediction of M_W from equation 1 and few subduction zones with $T < 10$ m. y. do not permit a definitive test on the validity of the relation for very young subducting plates. The question, however, is of great importance in estimating maximum M_W for the Juan de Fuca subduction zone ($V = 3.4$ cm/yr, $T = 8$ m. y.) which has a very weak seismicity and has no historical record of large/great earthquakes. Equation (1) yields $M_W = 8.3 \pm 0.4$ (Heaton and Kanamori, 1984). Based on an extensive comparison of this with other subduction zones, Heaton and Hartzell (1986) suggest that a $M_W = 8 \frac{1}{2}$ earthquake must be considered for the Juan de Fuca plate interface. Figure 6 suggests that truly great earthquakes occur where the background seismicity is moderate, with the exception of Nankai region in southwestern Japan ($M_W = 8.6$, $V = 3.3$ cm/yr, $T = 21$ m. y.). Heaton and Hartzell (1986) suggest that the background seismicity in southern Chile before the great 1960 earthquake ($M_W = 9.5$) may also have been very low. Table 1 and Figs. 2 to 4, on the other hand, show moderate background seismicity during the 1965-1988 period in the region. While the catalog for Chile before the 1960 event must be incomplete for $M \geq 5.0$ events, it may include aftershocks during the 1965-1988 period considered in this study. Thus, the true seismicity level in the southern Chilean region is somewhat uncertain. Only Rivera, Colima, and Michoacan regions have T and V which are similar to Juan de Fuca subduction zone. In these regions of Mexico, maximum M_W may be around 8.2. Thus, from the view point of background seismicity alone, the suggested maximum $M_W = 8 \frac{1}{2}$ for the Juan de Fuca subduction zone does not appear unreasonable.

CONCLUSIONS

1. The background seismicity, N_n , in the subduction zones is related to the age of the plate at the trench, T , and the relative convergence speed, V . This relationship can be written as

$$N_n = a T^b V^c, \quad b, c > 0.$$

Thus the seismicity increases as T and V increase.

2. The number of aftershocks following large/great earthquakes in the subduction zone is directly related to the background seismicity.
3. Ruff and Kanamori (1980) have shown that maximum magnitude, M_w , in a subduction zone, which characterizes the strength of coupling at the interface, is related to T and V by

$$M_w = a + bV - cT, \quad b, c > 0.$$

Increasing V results in higher background seismicity and greater M_w . Increasing T , however, plays opposite roles: the seismicity becomes higher but M_w becomes smaller. For this reason there is no clear relationship between M_w and N_n (Fig. 6). The data, however, suggests that truly great earthquakes, generally, do not occur in regions of very high and low background seismicity but in regions where it is moderate.

ACKNOWLEDGMENTS. We thank E. Rosenblueth for the revision of the manuscript. Fruitful discussions with J. N. Brune are acknowledged. The manuscript was completed when one of us (S. K. S.) was visiting Institut de Physique du Globe de Paris, France. The research was partly supported by DGPA, UNAM, DDF, Mexico and Fundacion Andes, Chile.

REFERENCES

- Anderson, J. G, P. Bodin, J. N. Brune, J. Prince, S. K. Singh, R. Quaas, and M. Oñate (1986). Strong ground motion and source mechanism of the Mexico earthquake of September 19, 1985, ($M_s = 8.1$), Science **233**, 1043-1049.
- Atwater, T. (1970). Implications of plate tectonics for the Cenozoic tectonic evolution of western North America, Geol. Soc. Am. Bull. **81**, 3513-3535.
- Eissler, H. and K. McNally (1982). Seismicity and tectonics of the Rivera plate and implications for the 1932 Jalisco, Mexico earthquake, J. Geophys. Res. **89**, 4520-4530.
- Heaton, T. H. and H. Kanamori (1984). Seismic potential associated with subduction in the northwestern United States, Bull. Seism. Soc. Am. **74**, 933-941.
- Heaton, T. H. and S. H. Hartzell (1986). Source characteristics of hypothetical subduction earthquakes in the northwestern United States, Bull. Seism. Soc. Am. **76**, 675-708.
- Isacks, B., J. Oliver, and L. R. Sykes (1968). Seismology and new global tectonics, J. Geophys. Res. **73**, 5855-5899.
- Jarrard, R. D. (1986). Relations among subduction parameters, Rev. Geophys. **24**, 217-284.
- Kanamori, H. (1971). Great earthquakes at island arcs and the lithosphere, Tectonophysics **12**, 187-198.
- Kanamori, H. (1977). Seismic and aseismic slip along subduction zones and their tectonic implications, in Island Arcs, Deep Sea Trenches and Back-Arc Basins, Maurice Ewing Series, M. Talwani and W. C. Pitman, Editors, American Geophysical Union, Washington, D. C. 163-174.
- Kelleher, J., J. Savino, H. Rowlett, and W. McCann (1974). Why and where great thrust earthquakes occur along island arcs, J. Geophys. Res. **79**, 4889-4899.
- Klitgord, K. D. and J. Mammerickx (1982). Northern east Pacific rise: magnetic anomaly and bathymetric framework, J. Geophys. Res. **87**, 6725-6750.
- Kobayashi, K. and M. Nakada (1978). Magnetic anomalies and tectonic evolution of the Shikoku Interarc Basin, J. Phys. Earth **26** (Supplement), 391-402.
- Luyendyk, B. P. (1970). Dips of downgoing lithospheric plates beneath island arcs, Geol. Soc. Am. Bull. **81**, 3411-3416.
- Minster, J. B. and T. H. Jordan (1978). Present day plate tectonics, J. Geophys. Res. **83**, 5331-5354.
- Molnar, P., D. Freedman, and J. Shih (1979). Lengths of intermediate and deep seismic zones and temperatures in downgoing slabs of lithosphere, Geophys. J. R. Astron. Soc. **56**, 41-54.

- Nishimura, C., D. S. Wilson, and R. N. Hey (1984). Pole of rotation analysis of present-day Juan de Fuca plate motion, J. Geophys. Res. 89, 10283-10290.
- Peterson, E. T., and Seno, T. (1984). Factors affecting seismic moment release rates in subduction zones, J. Geophys. Res. 89, 10233-10248.
- Ruff, L. and H. Kanamori (1980). Seismicity and the subduction process, Phys. Earth Planet. Interiors 23, 240-252.
- Seno, T. (1977). The instantaneous rotation vectors of the Philippine sea plate relative to the Eurassian plate, Tectonophysics 42, 209-226.
- Singh, S. K. and G. Suárez (1988). Regional variation in the number of aftershocks ($m_b > 5$) of large, subduction zone earthquakes ($M_w > 7.0$), Bull. Seism. Soc. Am. 78, 230-242.
- Uyeda, S. and H. Kanamori (1979). Back-arc opening and the mode of subduction, J. Geophys. Res. 84, 1049-1061.
- Vlaar, N. J. and M. J. R. Wortel (1976). Lithospheric aging, instability, and subduction, Tectonophysics 32, 331-351.
- Wortel, M. J. R. and N. J. Vlaar (1978). Age-dependent subduction of oceanic lithosphere beneath western South America, Phys. Earth Planet. Interiors 17, 201-208.
- Yamanaka, Y. and K. Shimazaki (1990). Scaling relations between the number of aftershocks and the size of the mainshock, J. Phys. Earth 38, 305-324.

TABLE 1. SUBDUCTION REGIONS, THEIR LOCATIONS AND DIMENSIONS, AGE OF THE PLATE AT THE TRENCH (T), RELATIVE CONVERGENCE SPEED (V), AND BACKGROUND SEISMICITY (N AND N_n)

No.	REGION	LAT	LON	LENGTH	WIDTH	T*	V*	N ⁺	N_n ⁺
			^o N	^o E	km	km	m.y.	cm/yr	(10 ⁻³)
1	JUAN DE FUCA	46.0	-125.5	400	300	10 (9)	3.4 (1)	5	1.74
2	RIVERA	21.5	-107.0	400	200	9 (2)	2.0 (3)	3	1.56
3	COLIMA	18.5	-104.8	340	200	~5 (2)	5.3 (4)	14	8.58
4	MICHOACAN	17.3	-102.7	200	200	~5 (2)	6.0 (4)	9	9.38
5	GUERRERO	16.5	-100.8	260	200	14 (2)	6.5 (4)	27	21.63
6	OAXACA	15.8	-98.3	350	200	20 (2)	7.1 (4)	45	26.79
7	C. AMERICA	14.0	-93.0	500	200	23 (2)	8.4 (4)	104	43.33
8	C. AMERICA	12.0	-88.0	580	200	23 (2)	8.2 (4)	102	36.64
9	C. AMERICA	9.0	-84.0	460	200	23 (2)	9.5 (4)	53	24.00
10	COLOMBIA	2.5	-80.0	920	200	15 (7)	7.9 (4)	46	10.44
11	N. PERU	-11.0	-79.0	920	200	45 (7)	8.9 (4)	109	24.74
12	S. PERU	-17.5	-74.0	620	200	51(10)	9.2 (4)	78	26.21
13	N. CHILE	-22.0	-71.5	660	200	51(10)	9.3 (4)	90	28.41
14	N. CHILE	-27.0	-72.0	440	200	48 (7)	9.4 (4)	140	75.76
15	N. CHILE	-30.5	-72.5	330	200	48 (7)	9.4 (4)	70	44.19
16	C. CHILE	-33.5	-73.0	330	200	43 (8)	9.3 (4)	36	25.97
17	S. CHILE	-37.5	-74.0	500	300	35 (8)	9.3 (4)	44	52.63
18	S. CHILE	-42.5	-75.0	500	300	15 (8)	9.2 (4)	21	16.75
19	S. CHILE	-46.0	-75.0	200	300	4 (8)	9.1 (4)	16	7.66
20	CARIBEAN	15.0	-59.0	500	200	68 (7)	1.9 (4)	18	7.50
21	KERMADEC	-31.0	-176.0	1220	200	113 (7)	7.0 (4)	890	152.00
22	TONGA	-22.0	-173.5	1220	200	120 (7)	8.8 (4)	632	107.90
23	N. HEBRIDES	-17.0	168.0	1000	300	52 (7)	10.0 (4)	612	91.21
24	SOLOMON	-8.0	158.5	1000	300	50 (7)	11.8 (4)	630	87.50
25	JAVA	-11.0	116.0	1000	300	138 (7)	7.7 (4)	446	69.94
26	SUMATRA	-5.0	100.5	1620	400	55 (7)	7.1 (4)	562	38.18
27	MARIANAS	16.5	147.5	700	300	155 (7)	4.7 (4)	148	29.37
28	RYUKYU	24.0	126.0	440	200	49 (7)	4.8 (4)	48	22.73
29	KYUSHU	28.5	131.0	600	200	49 (7)	3.4 (4)	160	55.56
30	BONIN TRENCH	30.5	143.0	760	200	146 (7)	5.6 (4)	210	57.57
31	HONSHU	33.0	137.5	320	200	24 (8)	2.0 (4)	17	11.07
32	NANKAI	32.0	134.0	260	200	21 (5)	~3.3 (6)	8	6.41
33	JAPAN TRENCH	38.0	144.0	670	200	130 (7)	10.6 (4)	307	95.46
34	KURILE	43.0	149.0	760	200	119 (7)	10.2 (4)	535	146.70
35	S. KAMCHATKA	48.0	157.0	580	200	90 (7)	9.7 (4)	234	84.05
36	KAMCHATKA	52.0	161.5	490	200	90 (7)	9.2 (4)	211	89.71
37	W. ALEUTIAN	51.0	174.0	510	200	60 (7)	3.2 (4)	24	9.88
38	E. ALEUTIAN	51.0	-171.0	770	200	60 (7)	8.0 (4)	153	41.40
39	ALASKA PEN.	54.0	-159.0	570	200	46 (7)	7.3 (4)	66	25.17
40	ALASKA	57.5	-150.0	650	200	46 (7)	6.6 (4)	41	21.03

* (1): Nishimura et al. (1984), (2): Klitgord and Mammerickx (1982), (3): Eissler and McNally (1982), (4): Minster and Jordan (1978), (5): Kobayashi and Nakada (1978), (6): Seno (1977), (7): Jarrad (1986), (8): Heaton and Hartzell (1986), (9): Atwater (1970), (10): Peterson and Seno (1984).

⁺ N=number of earthquakes ($m_b \geq 5$) excluding $M_S \geq 7$ events, their foreshocks (one month) and aftershocks (3 months) during the period 1965-1988. $N_n = N/1000 \text{ km}^2/\text{yr}$.

FIGURE CAPTIONS

Fig.1. Location of the subduction regions. Background seismicity has been estimated in a rectangular area (whose dimensions are given in Table 1) with the circle as its center. Numbers are keyed to Table 1.

Fig.2. Log N_n versus log T plot. N_n = Background seismicity, T = age of the plate at the trench in m. y. Numbers associated with the data points in this and the following three figures are keyed to Table 1.

Fig.3. Log N_n versus log V plot where V = relative convergence speed in cm/yr.

Fig.4. Predicted log N_n versus observed log N_n plot. Predicted values are from multivariate regression analysis.

Fig.5. Log N_r versus log N_n plot where N_r is the excess (>0) or deficiency (<0) in the number of aftershocks (see text). Note that N_r is not available for all regions listed in Table 1.

Fig.6. The dependence of background seismicity and maximum magnitude on age of the plate at the trench and relative convergence speed. Continuous lines: equal background seismicity contours, dashed lines: equal M_w contours. Observed M_w values (modified from Ruff and Kanamori, 1980) are shown near circles and dots. Circles and dots refer to regions with and without active back-arc basins, respectively.

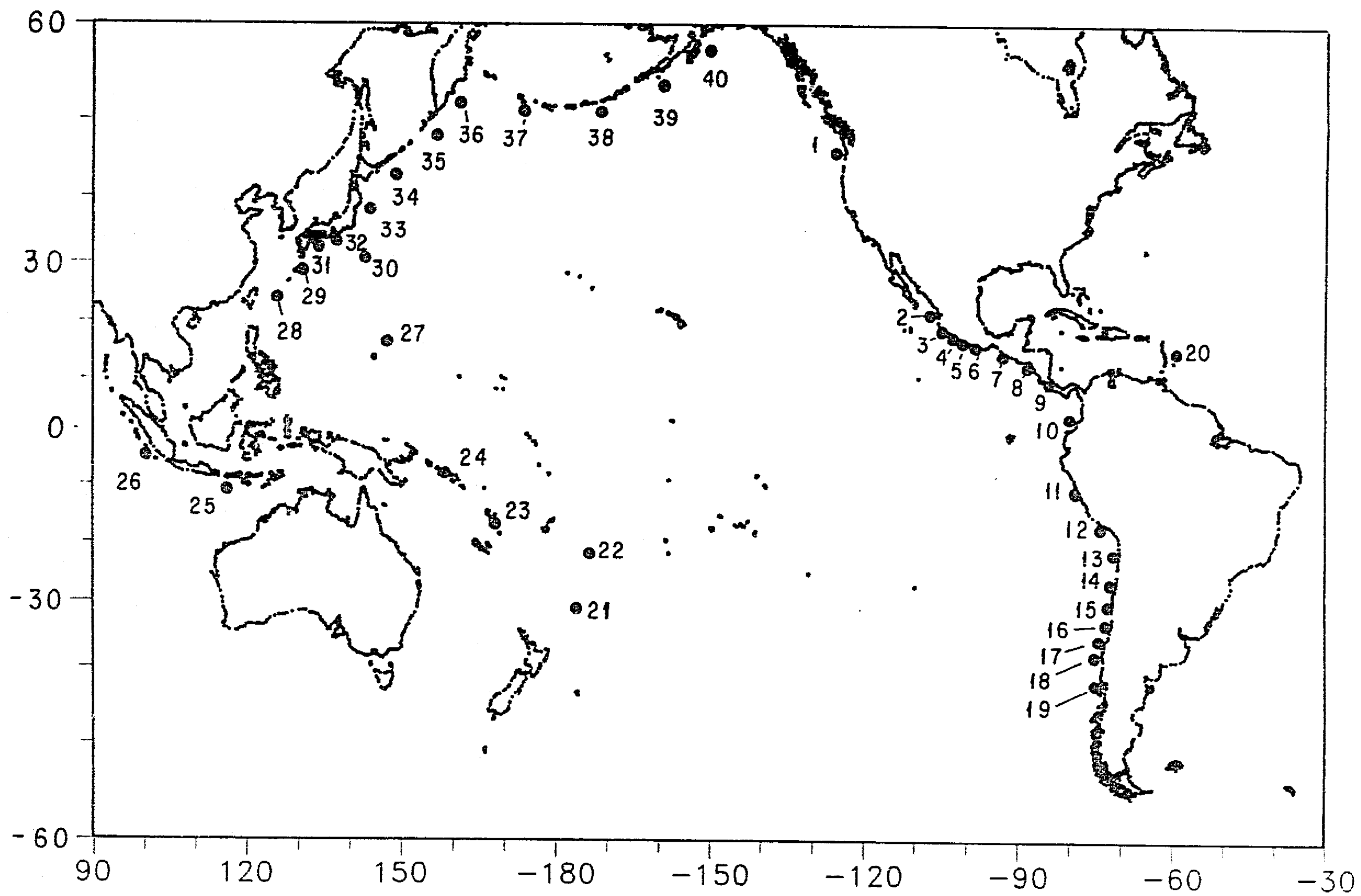


Fig. 1

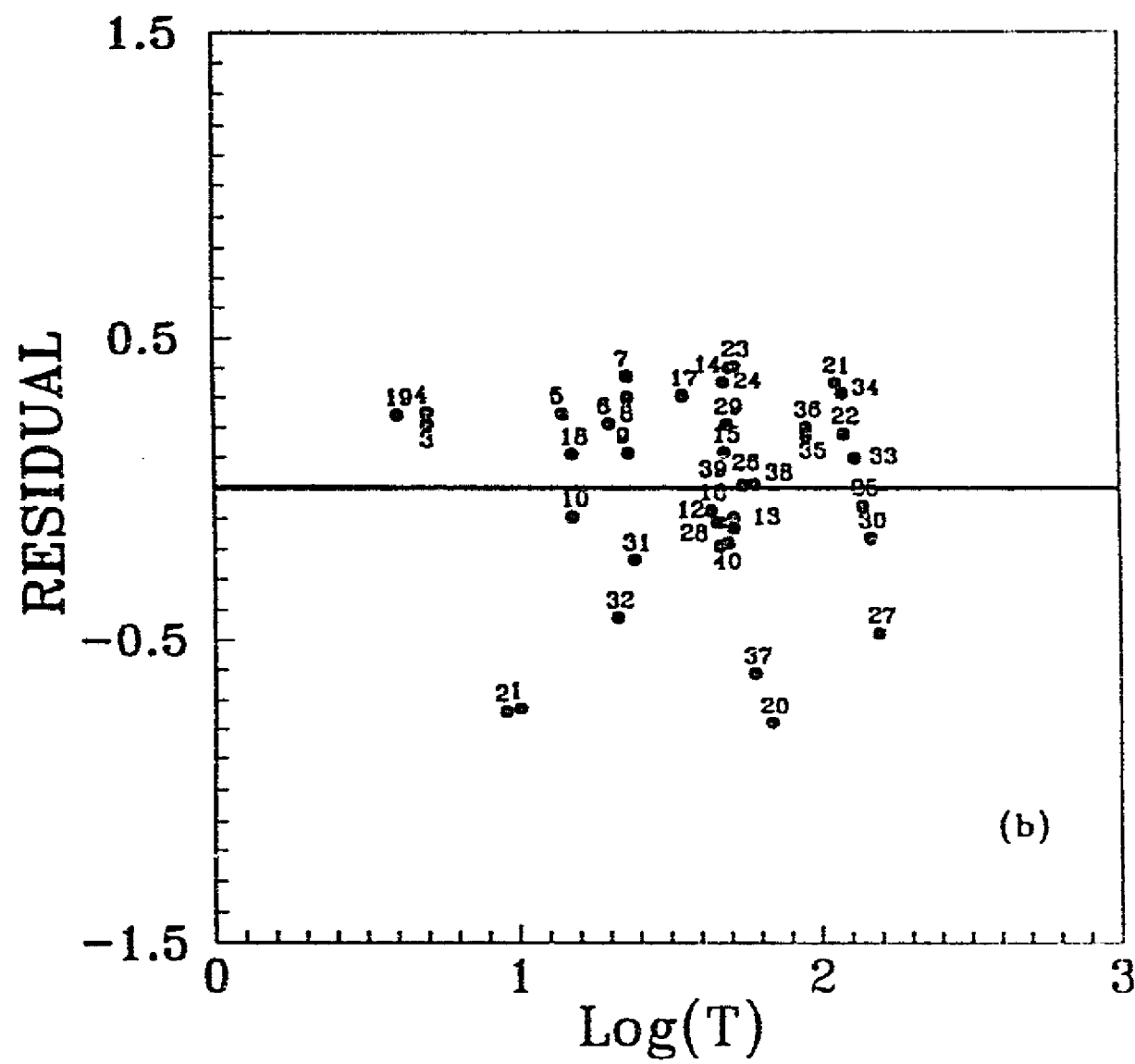
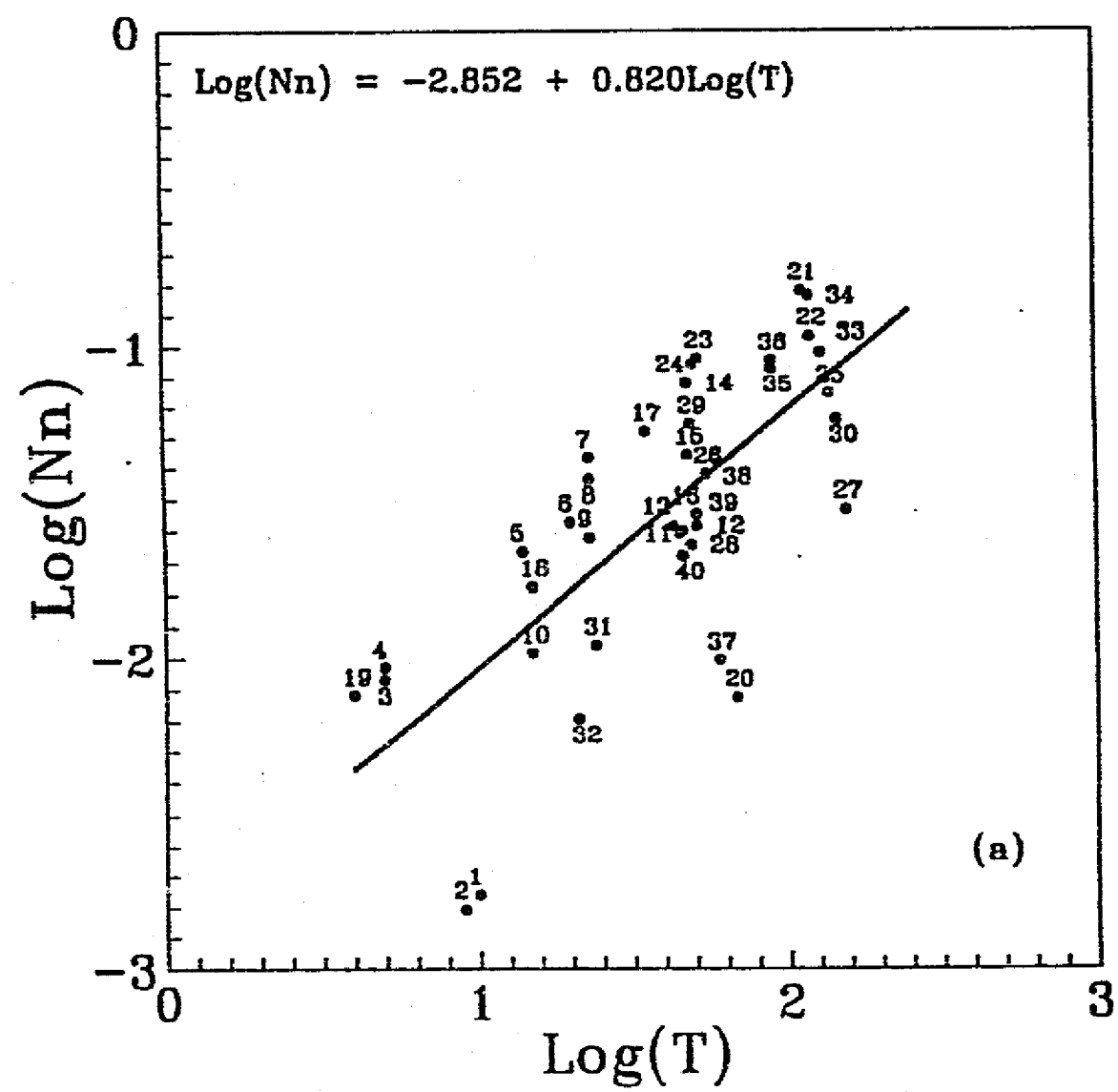


Fig. 2

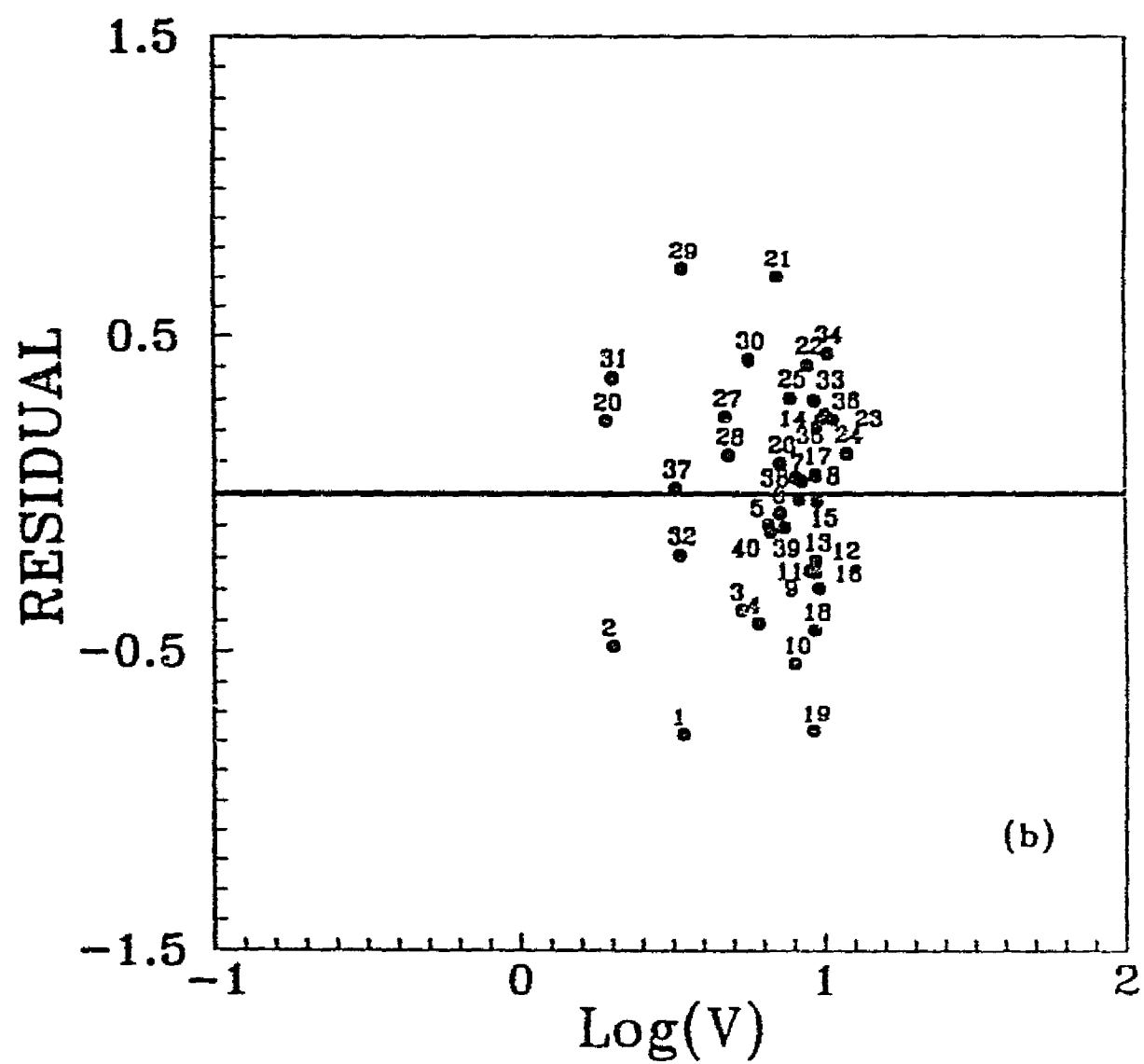
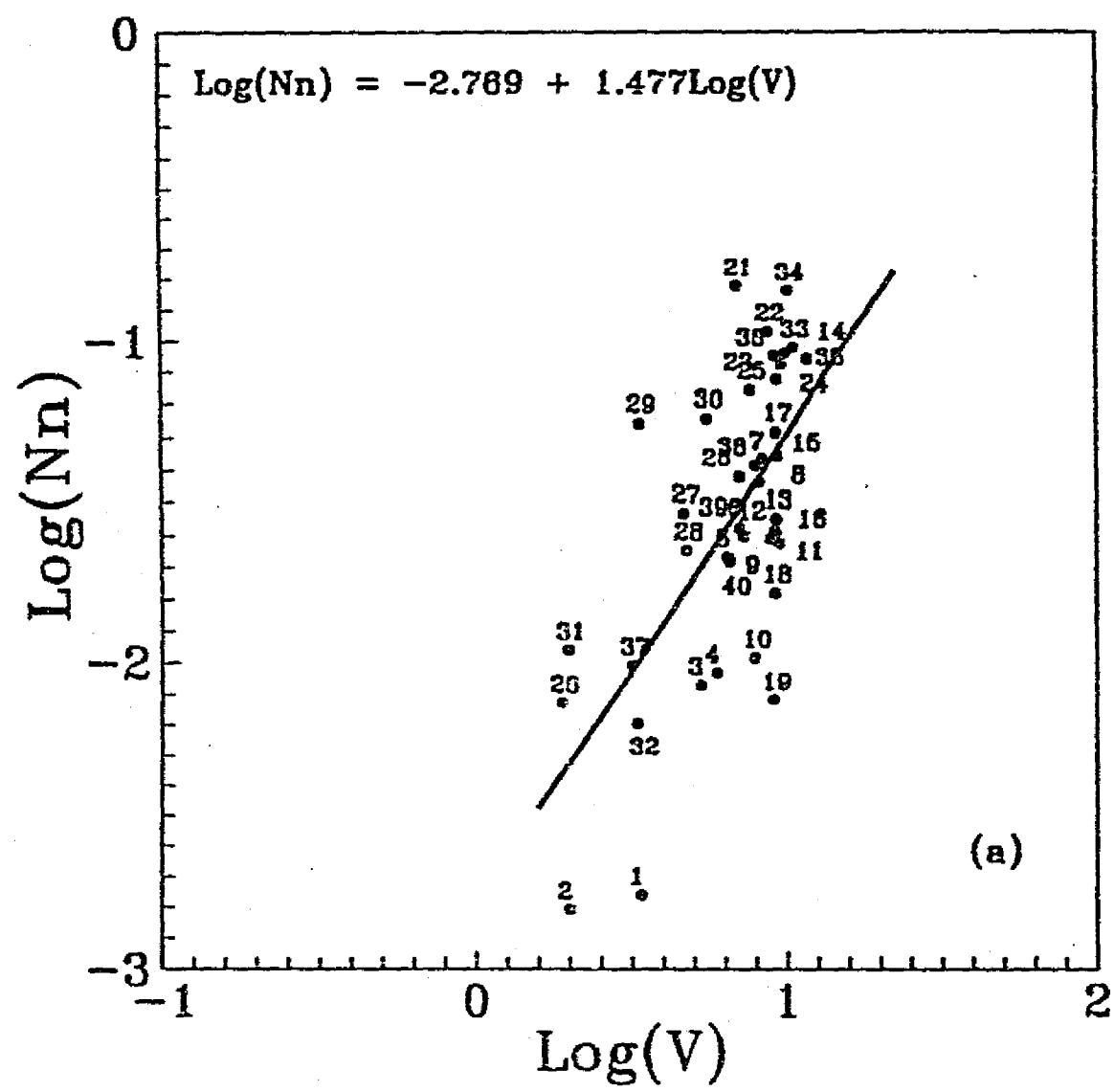


Fig. 3

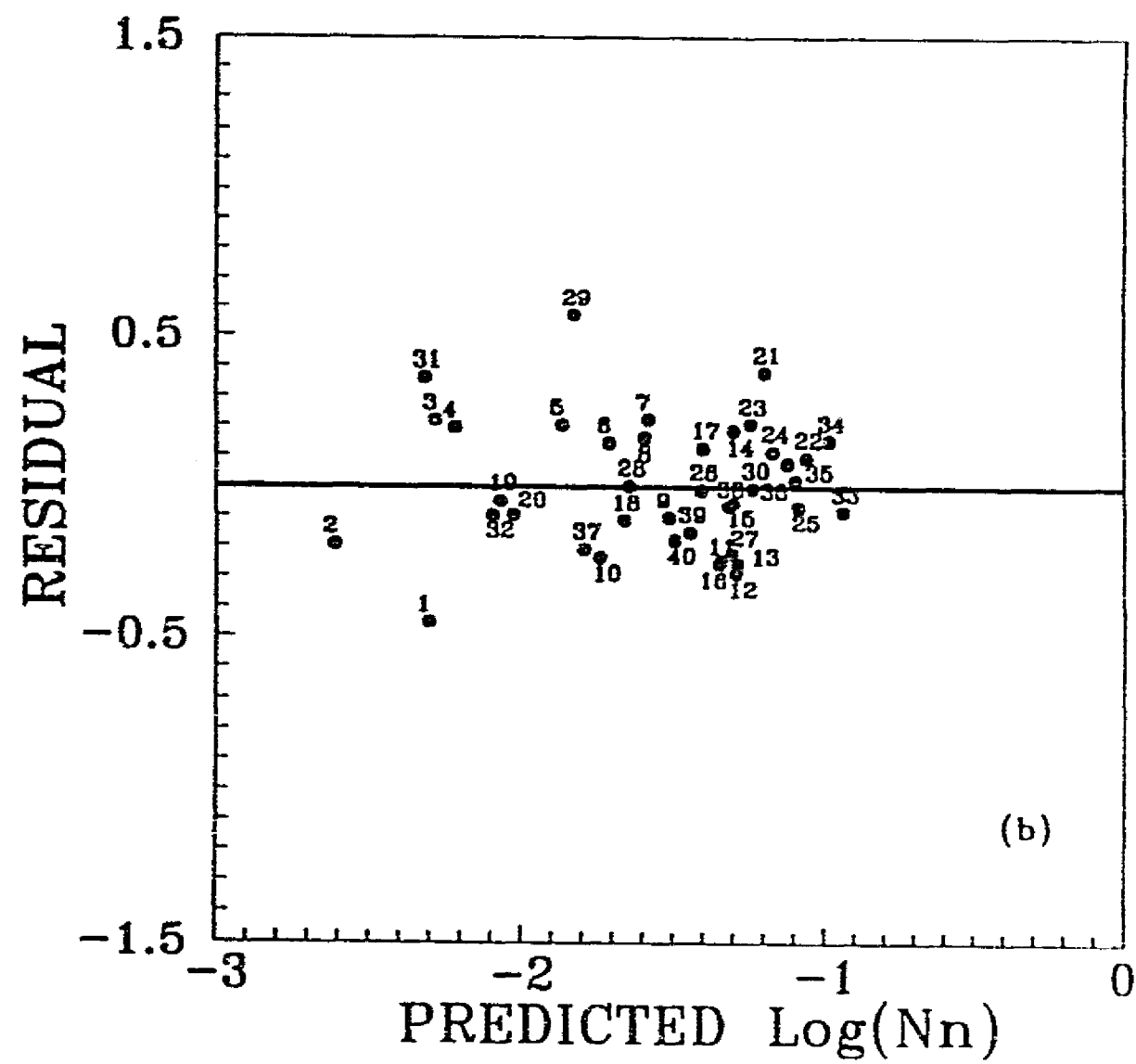
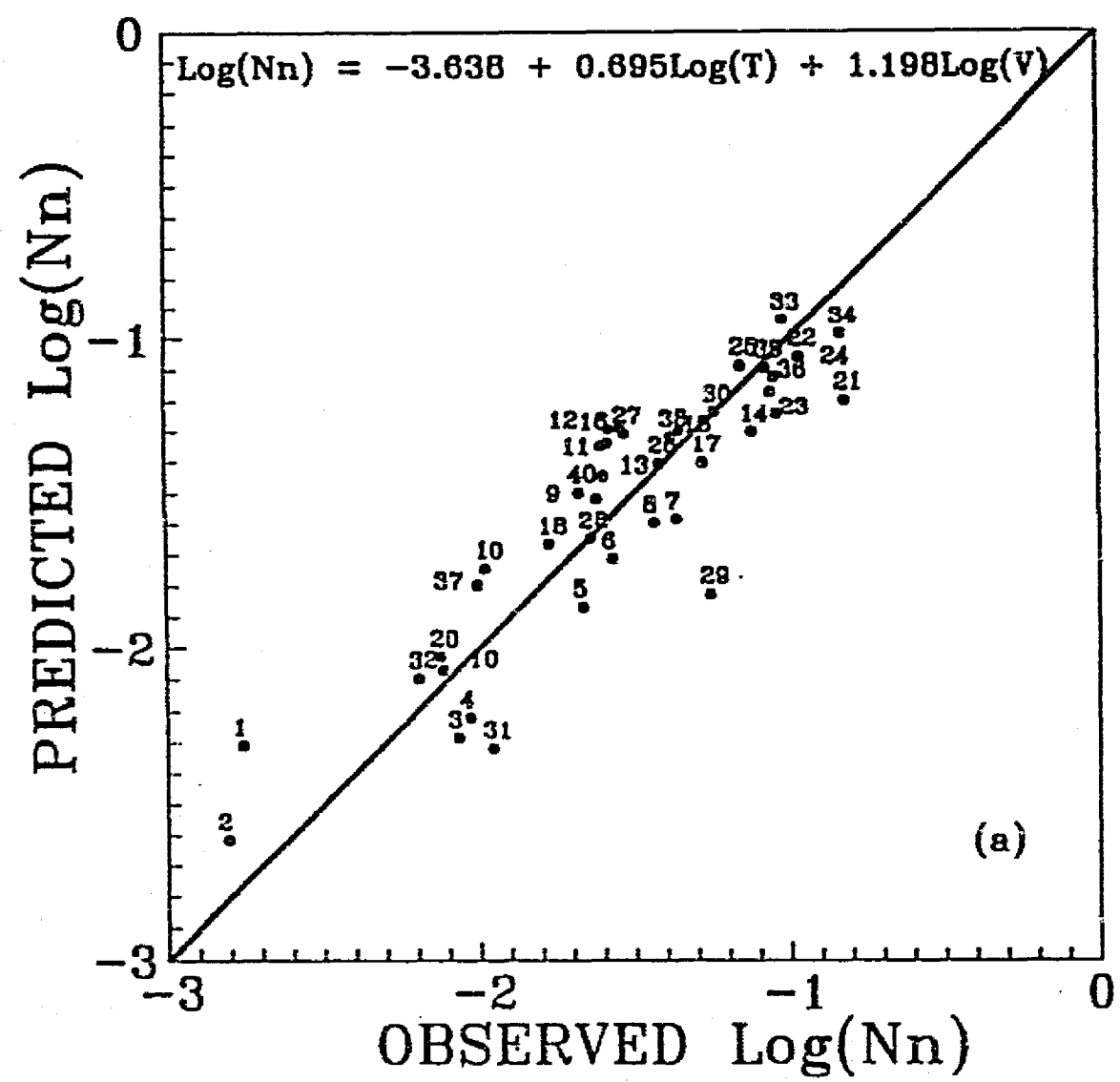


Fig. 4

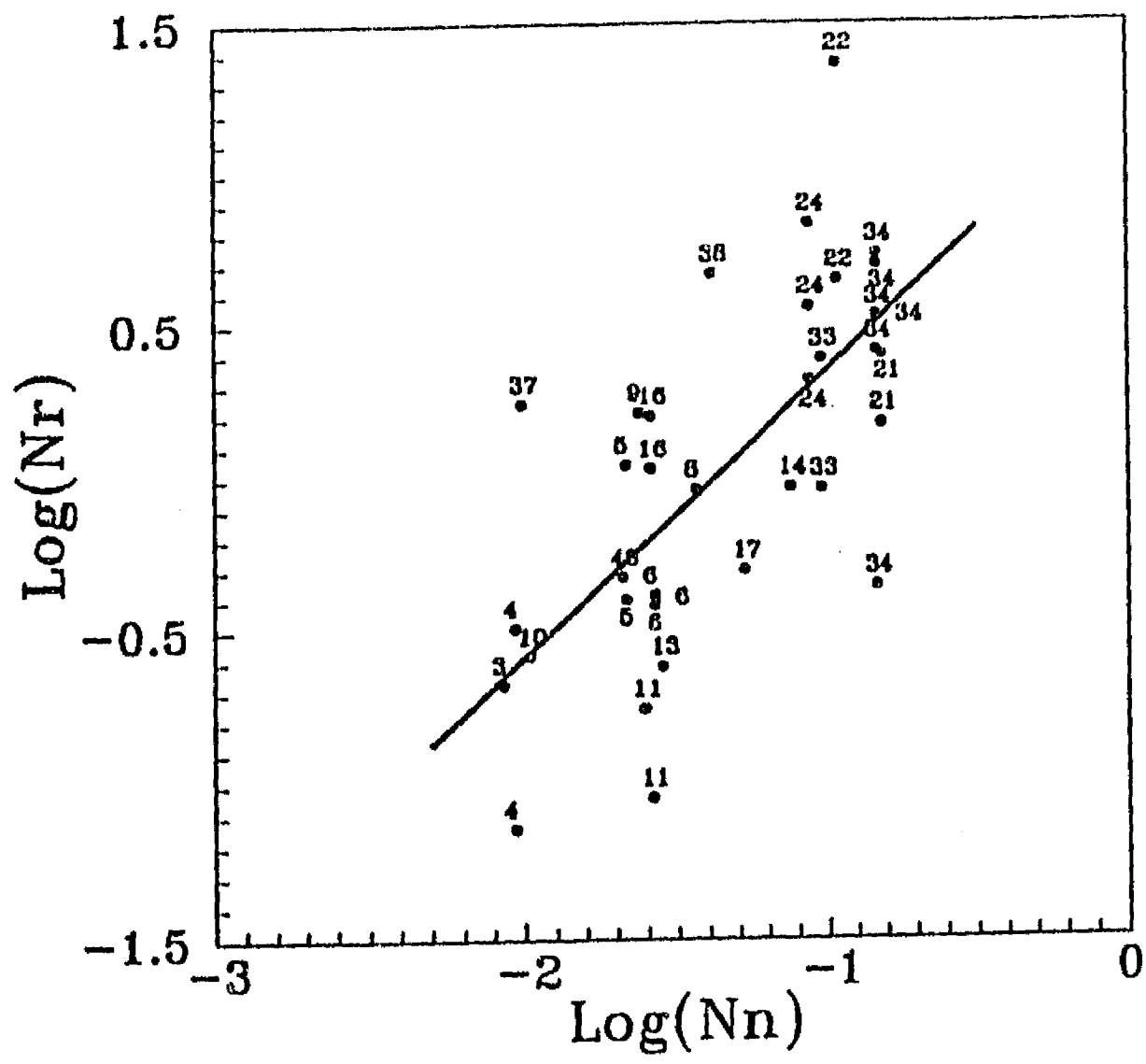


Fig. 5

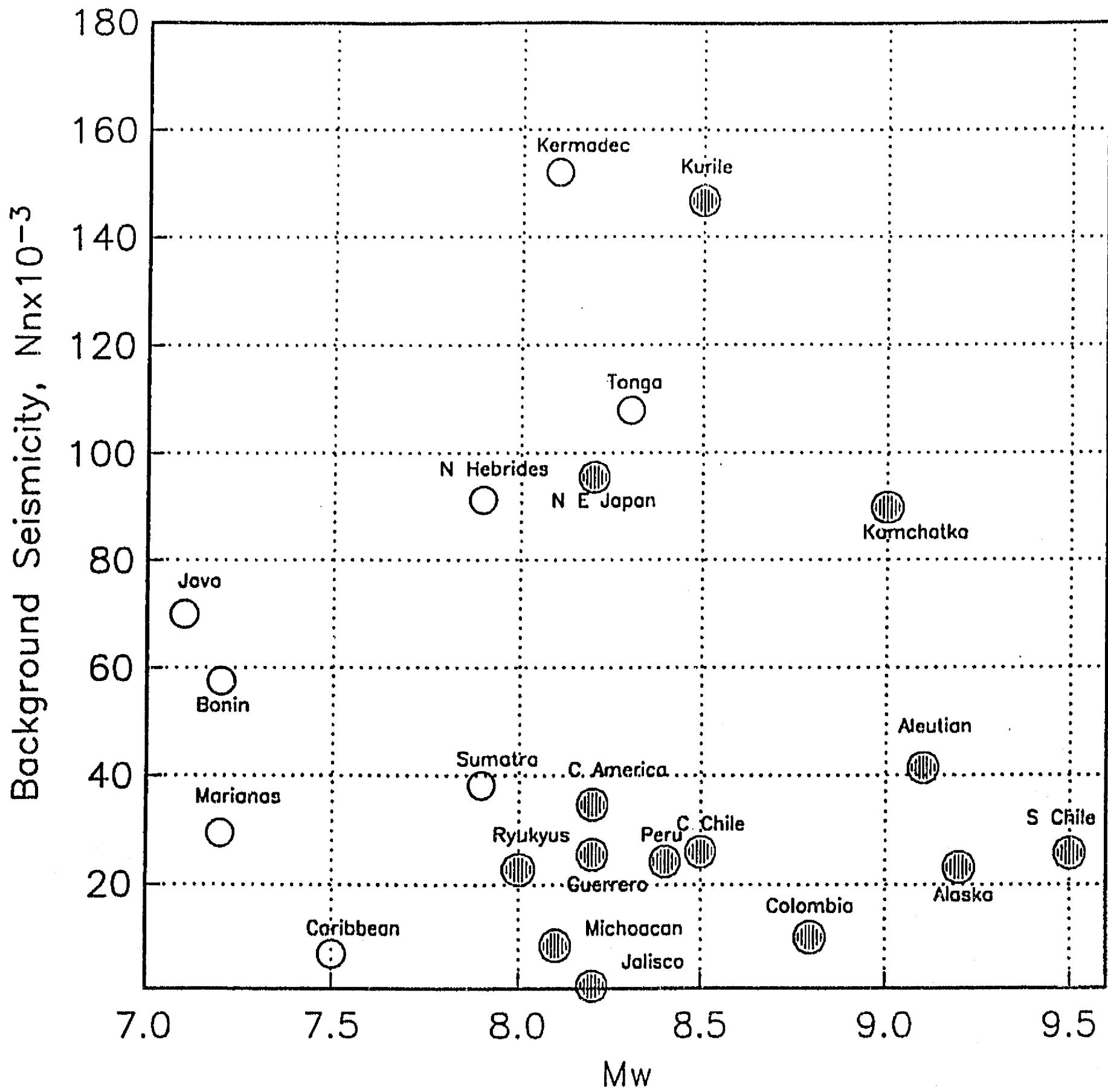


Fig. 6

III. Geometría de la Zona de Benioff y Estado de Esfuerzos en la Placa Continental en México Central

(Publicado en: *Geophys Res. Lett.*, 20, 1483-1486, 1993)

GEOMETRY OF THE BENIOFF ZONE AND STATE OF STRESS IN THE OVERRIDING PLATE IN CENTRAL MEXICO

S. K. Singh¹ and M. Pardo^{1,2}

¹Instituto de Geofísica, Universidad Nacional Autónoma de México, Mexico D.F. 045510

²Departamento de Geofísica, Universidad de Chile, Casilla 2777, Santiago, Chile

Abstract. Analysis of depths and focal mechanisms of 16 small earthquakes in Central Mexico, along with previous data, shows that (a) the subducted Cocos plate becomes subhorizontal between 110 and 260 km from the trench reaching a depth of about 50 km and (b) the bottom part of the overriding continental plate is in tensional stress regime. Neotectonic structures in Central Mexico and stress orientations (estimated from borehole elongations, cinder cone alignments, and fault-slip analysis) in the Trans Mexican Volcanic Belt, which lies in the northeastern portion of the area under study, also indicate the same stress regime. Absolute motion of the North American plate in the region has a component normal to the trench of 20 mm/yr which, if true, would result in compressional stress regime if the trench position is fixed in an absolute frame of reference. If we allow for seaward retreat of the trench then the tensional stress in the overriding plate and the observed geometry of the Benioff zone can be explained. This, however, implies that seaward retreat of a trench is possible even for a young (~15 m.y. old) subducting slab. Alternatively, tectonic erosion of the leading edge of the continent which has been proposed to explain truncated igneous and metamorphic continental terrane could give rise to the tensional stress but would not explain the geometry of the Benioff zone.

Introduction

Morphology of the Benioff zone below Mexico NW of 99°W is poorly known because of lack of intermediate-depth, moderate and large earthquakes in this region of the continent and a poor seismic network [e.g., Burbach et al., 1984; Singh and Mortera., 1991]. Since 1986 there has been an increase in the number of seismic and strong motion stations in the region. A fairly dense network of seismic stations is in place along the coast of Guerrero between ~100° to 101.5° W [Suárez et al., 1990]. Several digital accelerographs, which form part of the attenuation arm of the Guerrero Accelerograph Array [Anderson et al., 1986], are also in operation since mid-1985 in the region, as are a few seismic stations operated by the University of Puebla and the Federal Power Commission. As a

consequence, the detection capability of smaller events in Central Mexico, shown by an inclined rectangular box in Figure 1, has improved.

From these records we have selected 16 well-recorded events which may shed light on the geometry of the Benioff zone. Of these events 11 are normal faulting earthquakes. These events, along with previous data and published results, provide (1) a firm support for a subhorizontal Benioff zone below Central Mexico, previously pointed out by Suárez et al. [1990], and (2) suggest a tensional stress regime in a broad area of the overriding plate. We first present the evidence from the events and then show that none of the existing models explain satisfactorily both the geometry of the Benioff zone and the tensional stress regime in the upper plate.

Data and Analysis

Table 1 lists events, including their locations, depths, and focal mechanisms, which were used in the analysis. From the table we have excluded some shallow events near the coast since this part of the Benioff zone is well defined [Suárez et al., 1990]. Locations of the older events (before 1985), if available from the use of master event technique by G. Malavé (personal communication, 1992), were considered more reliable and are given in Table 1.

The 16 events, located for this study, had a minimum of eleven readings (at least six P and two S, and some S-P times). We were especially careful in searching for events with probable inland location. We use the crustal model given by Campillo et al. [1989] to locate these events. Changing initial depth and starting crustal model did not change the epicenters by more than ± 2 km and depths by more than ± 2.5 km. To determine the focal mechanisms we checked the polarity of the stations by using deep, teleseismic earthquakes with known focal mechanisms. While P polarity data was often sufficient to suggest the type of faulting, especially from direct P wave recorded near the epicenter, the fault planes were poorly constrained. For seven out of the 16 events, we modeled P and/or S displacement records (obtained by double integration of rotated digital accelerograms) from close stations, using synthetics generated in an infinite space. The focal mechanism was varied until both first motions and waveforms were reasonably well fit. An example for event 38 is given in Figure 2. While we are reasonably confident about the type of faulting associated with these events, the strike and dip of the fault planes are probably uncertain by 15° or more.

The epicenters of the events are given in Figure 1. The focal mechanisms of the normal faulting events, determined in this study, are shown along the margin of the figure. Figure 3 illustrates the projection of the hypocenters along a vertical plane oriented $N35^\circ E$ which is

the direction of relative convergence between Cocos and North American plates [DeMets et al., 1990]. The inclined rectangle in Figure 1 is also oriented in this direction. The continuous line in Figure 3 shows our delineation of the plate interface which is similar to the one inferred by Suárez et al. (1990). Suárez et al. had limited data beyond 150 km from the trench, so the new data provide a firm support to the inferred plate interface geometry and, likewise, suggest that the oceanic plate penetrates below this part of Mexico with a shallow dip and becomes subhorizontal beyond about 110 km from the trench (at a depth of about 50 km). The subducted plate remains subhorizontal up to about 250 km from trench. Beyond this distance it can not be traced due to lack of seismic events. In Figure 3 the dashed line indicates the geometry of the subducted slab beyond 275 km assuming that the active volcanos are located ~100 km above the plate interface. There is a surprising lack of seismicity in the continental wedge from the coast up to 180 km inland, although the seismic network is especially dense in this region.

Note that a few normal faulting events lie above the subducted slab (Figure 3). For these events the T axes are shown in Figure 1 by arrows through the epicenters. Although the T axis determined from focal mechanism may not represent the minimum horizontal principal stress, S_{hmin} , in the region because of pre-existing faults [see e.g., Zoback et al., 1989], in this study we shall assume that it does. We are mainly interested in the general trend of S_{hmin} (the quality and quantity of data on T axes does not permit otherwise).

Discussion and Conclusions

As seen in Figure 3, the seismicity suggests extensional regime in the deeper part of the overriding plate beginning about 180 km from the trench. There is surface evidence showing similar stress regime in Central Mexico. Figure 1 shows neotectonic structures inferred from Landsat Thematic Mapper imagery by Johnson and Harrison [1989]. Suter [1991] has compiled stress orientation data for the region in Figure 1 from drillhole elongations, alignment of Quarternary cinder cones, and striation analysis of active faults. A more detailed analysis of active faults and stress orientations has been given by Suter et al. [1992a,b] for the two small rectangular areas near 19.9°N, 100.2°W and 20.6°N, 99.5°W shown in Figure 1. These areas are characterized by E-W trending normal faults with slight left-lateral strike-slip component, with S_{hmin} roughly in the N-S direction. In Figure 1 we show by dashed lines the S_{hmin} orientations for the area of interest in this study and by thick (diverging) arrows the stress provinces for the entire region, taken from Suter [1991]. We note that the S_{hmin} orientations with respect to the direction of relative convergence vary from subparallel to nearly orthogonal; the subparallel orientations are reminiscent of

back-arc basins [Zoback and Zoback, 1991]. This tensional stress regime is rather surprising since, generally, strike-slip faulting is found landward of the trench, near active volcanos. Normal faulting is expected beyond the volcanos especially in regions where back-arc spreading may be occurring [e.g., Nakamura and Uyeda, 1980]. Suter [1991] and Suter et al. [1992a] have suggested that this stress regime is caused by topographic high of the altiplano since such relief will give rise to extension. However, other areas of high elevation, e.g. Himalayas and South America, generally have (unlike Central Mexico) Shmin orthogonal to the direction of plate convergence [Zoback et al., 1989]. Furthermore the entire overriding plate in Central Mexico appears to be in extension. Thus the stress regime in Central Mexico is somewhat unique and suggests that factors other than high elevation may also be playing a role in creating wide-spread extension.

We now consider possible models which may explain these observations. We first note that the convective flow in the upper mantle wedge between the subducting and the overriding lithosphere as the cause of tension in the upper plate [e.g. Sleep and Toksöz, 1973] is not very appealing in our case since such a mechanism would give rise to tensional stress beyond the volcanos.

The absolute motion of the North American plate in the region of our interest, calculated from model AM1-2 of Minster and Jordan [1978], is 28 mm/yr in the direction N243°E (Figure 1), its component normal to the trench is 20 mm/yr. Absolute motions inferred from hot spot data, however, are not well constrained [e.g. Minster and Jordan, 1978; Molnar and Atwater, 1978]. If the trench is fixed in an absolute frame of reference and the continent is indeed advancing normal to the trench, then this should give rise to compression and crustal shortening in the upper plate. What is observed in Mexico is just the opposite. Since depth of the subducted plate in the region is less than about 100 km, the assumption that the slab is anchored in the mantle is not reasonable. Assuming that the continent is advancing towards the trench, it is possible that the trench itself is not fixed but is retracting towards the ocean, not in response to the advance of the continent but on its own. Thus a seaward retreat of the middle America trench (along with the tensional stress caused by high elevation) is a possible mechanism to explain the observed extension and geometry of the Benioff zone in the area of our study. This would also explain the lack of truly great subduction earthquakes ($M_w > 8.4$), and a poorly developed outer gravity high. This retreat of the trench may be roughly equal to the advance of the continent, i.e., 20 mm/yr. Seaward migration of a trench has been discussed by several authors [e.g., Molnar and Atwater, 1978; Uyeda and Kanamori, 1979; Nakamura and Uyeda, 1980]. Generally, however, such retreat has been proposed for old (> 50 m.y.) subducted slabs [e.g. Kanamori, 1971; Molnar and Atwater, 1978]. Back-arc spreading is often associated with

the subduction of such older slabs whereas cordilleran tectonics generally prevails where the subducted ocean plate is less than 50 m.y. old [Molnar and Atwater, 1978]. As pointed out by these authors there are exceptions such as the Caribbean and Cascade regions.

An alternative model, which can explain the tensional stress regime (but not the subhorizontal Benioff zone), is related to the tectonic erosion of the continent due to subduction [Murauchi, 1971]. Rather prominent truncated igneous and metamorphic continental terrane and narrow inner trench slope along the Pacific coast of Mexico (from Jalisco to Tehuantepec) may be explained by this mechanism. This explanation is controversial: Karig et al. [1978] and Beck [1990] prefer a right-lateral translation of the continental margin between 7 and 80 m.y.b.p. whereas Böhnel et al. [1992] provide data which does not support this displacement. On the other hand, based on a detailed marine geophysical survey of the trench and the continental slope in the area of this study, Karig et al. [1978] report accretion of trench turbidites and development of a small but typical accretionary prism probably since Miocene. If tectonic erosion between 7 and 80 m.y.b.p. is the cause of the truncated margin, then the presence of a recent accretion prism may imply that this process has stopped since the Miocene. More generally, the presence of the accretionary prism may argue against both seaward retreat of the trench as well as tectonic erosion at present.

Acknowledgments. We thank G. Suárez, J. Dominguez, G. Gonzales Pomposo, and E. Lomas for facilitating data. We are grateful to W. Bandy, D. Morán, E. Rosenblueth, G. Suárez and M. Suter for helpful discussions and revision of the manuscript. The Guerrero Accelerograph Array is jointly operated by Instituto de Ingeniería, U.N.A.M. and University of Nevada-Reno. This research was partially supported by DGAPA and PADEP, U.N.A.M. (Projects No. IN109961 and DCCH9231).

REFERENCES

- Anderson, J. G., P. Bodin, J. N. Brune, S.K. Singh, R. Quass and M. Oñate, Strong ground motion and source mechanism of the Mexico earthquake of September 19, 1985 ($M_S = 8.1$) *Science*, 233, 1043-1049, 1986.
- Astiz, L. M., Sismicidad en Acambay, Estado de México. El temblor del 22 de febrero de 1979, B. S. thesis, 130 pp., Univ. Nac. Autón. Méx., Mexico City, 1980.
- Beck, M. E., Case for northward transport of Baja and coastal southern California. Palomagnetic data, analysis and alternatives, *Geology*, 19, 506-509, 1991.
- Böhm, H., D. Morán-Zenteno, P. Schaaf, and J. Urrutia-Fucugauchi, Paleomagnetic and isotope geochronology data from southwestern Mexico and the controversy concernin the pre-neogene position of Baja California, *Geofís. Int*, 3, 253-261, 1992.
- Burbach, G. V., C. Frohlich, W. D. Pennington, and T. Matumoto, Seismicity and tectonics of the subducted Cocos plate, *J. Geophys. Res.*, 89, 7719-7735, 1984.
- Campillo, M., J. C. Gariel, K. Aki and F. J. Sánchez-Sesma, Destructive ground motion in Mexico city: Sorce, path, and site effects during the great 1985 Michoacán earthquake, *Bull. Seismol. Soc. Am.*, 79, 1718-1735, 1989.
- Chael, E. P. and G. S. Stewart, Recent large earthquakes along the middle American trench and their implications for the subduction process, *J. Geophys. Res.*, 87, 329-338, 1982.
- Dean, B. W. and C. L. Drake, Focal mechanism solutions and tectonics of the Middle American Arc, *J. Geol.*, 86, 111-128, 1978.
- DeMets, C., R. G. Gordon, D. F. Argus, and S. Stein, Current plate motions, *Geophys. J. Int.*, 101, 425-478, 1990.
- Gonzalez-Ruiz, J., Earthquakes source mechanics and tectonophysics of the Middle America subduction zone in Mexico, *Ph.D. thesis, Univ. of Calif., Santa Cruz*, 1986.
- Johnson, C. A. and C. G. A. Harrison, Tectonics and volcanism in central Mexico: A Landsat Thematic Mapper perspective, *Remote Sens. Envir.*, 28, 273-286, 1989.
- Karig, D. E., R. K. Cardwell, G. F. Moore, and D. G. Moore, Late Cenozoic subduction and continental margin truncation along the northern Middle America Trench, *Geol. Soc. Am. Bull.*, 89, 265-279, 1978.
- Kanamori, H., Great earthquakes at island arcs and lithosphere, *Tectonophysics*, 12, 187-198, 1971.
- LeFevre, L. V. and K. C. McNally, Stress distribution and subduction of aseismic ridges in the middle America subduction zone, *J. Geophys. Res.*, 90, 4495-4510, 1985.
- Minster, J. B. and T. H. Jordan, Present-day plate motions, *J Geophys. Res.*, 83, 5331-5353, 1978.

- Molnar, P. and T. Atwater, Interarc spreading and cordilleran tectonics as alternates related to the age of subducted oceanic lithosphere, *Earth Planet. Sci. Lett.*, 41, 330-340, 1978.
- Molnar, P. and L. R. Sykes, Tectonics of the Caribbean and Middle American region from focal mechanisms and seismicity, *Geol. Soc. Am. Bull.* 80, 1639-1684, 1969.
- Murauchi, S., The renewal of island arcs and the tectonics of marginal seas, in *Island Arcs and Marginal Seas*, pp. 39-56, Tokai University Press, Tokyo, 1971.
- Nakamura, K. and S. Uyeda, Stress gradient in arc-back arc regions and plate subduction, *J. Geophys. Res.*, 85, 6419-6428, 1980.
- Sleep, N. and M. N. Toksöz, Evolution of marginal basins, *Nature*, 233, 548-550, 1973.
- Singh, S. K. and F. Mortera, Source-time function of large Mexican subduction earthquakes, morphology of the Benioff zone, age of the plate, and their tectonic implications, *J. Geophys. Res.*, 96, 21487-21502, 1991.
- Suárez, G. and L. Ponce, Intraplate seismicity and crustal deformation in central Mexico [abs.]: *EOS Transactions of the American Geophysical Union*, 67, 1114, 1986.
- Suárez, G., T. Monfret, G. Wittlinger, and C. David, Geometry of subduction and depth of the seismogenic zone in the Guerrero gap, Mexico, *Nature*, 345, 336-338, 1990.
- Suter, M., State of stress and active deformation in Mexico and western Central America, *The Geology of North America*, vol. DMV001, *Neotectonics of North America*, edited by D. B. Slemmons et al., Geological Society of America, 401-421, 1991.
- Suter, M., O. Quintero, and C. A. Johnson, Active faults and state of stress in the central part of the Trans-Mexican Volcanic Belt, Mexico. 1. The Venta de Bravo fault, *J. Geophys. Res.*, 97, 11983-11993, 1992a.
- Suter, M., M. Carrillo, and M. López, Active faults in Trans-Mexican Volcanic Belt - The Aljibes half-graben; structure, kinematics and seismic hazard estimate, *GEOS UGM* [abs.], 12, 12, 1992b.
- Uyeda, S. and H. Kanamori, Back arc opening and the mode of subduction, *J. Geophys. Res.*, 84, 1049-1061, 1979.
- Zoback, M. D., and M. L. Zoback, Tectonic stress field in North America and relative plate motions, *The Geology of North America*, vol. DMV001, *Neotectonics of North America*, edited by D. B., Slemmons et al., Geological Society of America, 339-366, 1991.
- Zoback, M. L., et al., Global patterns of tectonic stress, *Nature*, 343, 291-298, 1989.

TABLE 1. Events Used in This Study and Their Source Parameters

N	Date	Epicenter		Depth Km	mb	Mo N-m	Focal Mechanism		
		Lat °N	Lon °W				ϕ	δ	λ
1	640706	18.31	100.50 ¹	55 ²	6.3 ¹	1.15E20 ²	292	38	-63 ²
2	651209	16.99	100.21 ³	29 ³	5.9 ¹		314	14	90 ⁴
3	660925	18.10	100.98 ³	49 ³	5.7 ¹		275	56	-71 ⁴
4	670414	17.20	100.43 ³	35 ³	5.0 ¹		160	48	-106 ⁵
5	680702	17.29	100.45 ³	38 ³	5.7 ¹		328	21	-73 ⁶
6	730716	17.09	100.85 ³	13 ³	5.6 ¹		303	10	90 ⁵
7	760201	16.88	100.33 ³	19 ³	5.8 ¹		280	62	90 ⁷
8	760607	17.13	100.83 ³	16 ³	6.0 ¹		325	21	76 ⁷
9	760919	17.95	100.67 ³	50 ³	5.5 ¹		292	50	-90 ⁵
10	761004	20.48	99.15 ¹	9 ⁸	5.3 ¹		290	75	-66 ⁸
11	780319	16.80	99.83 ³	34 ³	5.7 ¹		310	20	90 ⁷
12	780705	18.24	100.18 ³	55 ³	5.4 ¹	2.68E17 ⁹	292	44	-77 ⁹
13	790126	17.21	100.97 ³	16 ³	5.8 ¹	8.96E18 ⁹	302	24	110 ⁹
14	790126	17.24	101.21 ³	12 ³	5.4 ¹	5.74E17 ⁹	302	22	99 ⁹
15	790126	17.19	101.20 ³	10 ³	5.4 ¹	2.39E17 ⁹	319	21	117 ⁹
16	790222	19.89	100.18 ¹⁰	8 ¹⁰	5.3 ¹		240	51	-44 ¹⁰
17	790228	17.30	101.22 ³	13 ³	5.2 ¹	4.93E17 ⁹	303	22	101 ⁹
18	790314	17.46	101.47 ³	14 ³	6.3 ¹	2.70E20 ¹¹	293	14	87 ¹¹
19	790318	17.34	101.13 ³	17 ³	5.3 ¹	3.32E17 ⁹	316	27	116 ⁹
20	820102	16.49	100.17 ³	7 ³	5.3 ¹	2.02E17 ⁹	275	18	68 ⁹
21	820102	16.58	100.26 ³	8 ³	5.4 ¹	7.43E16 ⁹	271	24	26 ⁹
22	840714	17.18	99.80 ³	46 ³	5.2 ¹	1.90E17 ⁹	129	74	-158 ⁹
23	860611	18.28	100.28 ¹²	38 ¹²	5.1 ¹	2.00E16 ¹²	201	54	-66 ¹²
24	880205	18.18	98.92 ¹²	45 ¹²	3.9 ¹		24	71	-63 ¹²
25	880208	17.50	101.14 ¹²	19 ¹²	5.5 ¹	7.37E17 ⁹	261	38	63 ⁹
26	880616	18.06	99.93 ¹²	59 ¹²	4.1 ¹³	3.70E15 ¹²	92	80	-133 ¹²
27	880802	17.95	99.44 ¹²	49 ¹²	3.2 ¹³	1.50E14 ¹²	119	26	-65 ¹²
28	890224	17.86	99.64 ¹²	50 ¹²	3.4 ¹³	8.50E14 ¹²	165	55	-25 ¹²
29	890310	17.45	101.19 ¹²	20 ¹²	5.2 ¹	1.35E17 ⁹	251	35	47 ⁹
30	890403	17.99	99.43 ¹²	45 ¹²	3.9 ¹³	1.70E14 ¹²	170	80	-50 ¹²
31	890421	18.48	100.44 ¹²	29 ¹²	4.0 ¹³		118	61	-126 ¹²
32	890812	18.06	101.13 ¹²	47 ¹²	5.2 ¹	8.50E16 ¹²	270	71	-90 ¹²
33	891008	17.19	100.21 ¹²	37 ¹²	5.0 ¹	4.74E16 ⁹	252	50	106 ⁹
34	900309	18.64	99.64 ¹²	27 ¹²	3.3 ¹³		165	10	-65 ¹²
35	900511	17.12	100.81 ¹²	21 ¹²	5.3 ¹⁴	8.80E16 ¹²	317	39	100 ¹²
36	900531	17.16	100.82 ¹²	23 ¹²	5.8 ¹⁴	6.00E17 ¹²	317	39	100 ¹²
37	901124	18.05	100.40 ¹²	46 ¹²	4.0 ¹⁴		128	17	-119 ¹²
38	911027	18.28	99.22 ¹²	53 ¹²	3.9 ¹⁴	8.00E14 ¹²	241	71	-83 ¹²

- 1 International Seismological Centre Bulletins
- 2 Gonzalez-Ruiz [1986]
- 3 G. Malavé (personal communication, 1992)
- 4 Molnar and Sykes [1969]
- 5 LeFevre and McNally [1985]
- 6 Dean and Drake [1978]
- 7 Burbach et al. [1984]
- 8 Suárez and Ponce [1986]
- 9 From Harvard Centroid Moment Tensor Solution Catalog
- 10 G. Suárez (personal communication, 1992)
- 11 Chael and Stewart [1982]
- 12 This study, local data
- 13 Local duration magnitude
- 14 PDE, USGS

FIGURE CAPTION

Fig. 1. Plate tectonic map of Mexico. Area of study is shown by a shaded rectangle, inclined N35°E which is the direction of relative plate convergence. Stress provinces in the region and stress orientations (S_{hmin}) are shown by thick diverging arrows and dashed lines, respectively. Dots: thrust faulting events, open circles: normal faulting events. Numbers of events are keyed to Table 1. T axes of normal faulting events in the overriding plate are shown by straight lines. Solid triangles: recent, active volcanos; thin arrows: absolute motion vectors. Small boxes in the Trans-Mexican Volcanic Belt and near 17°N, 100.8°W delineate areas of detailed studies by Suter et al. [1992a,b] and Karig et al. [1978], respectively. EPR: East Pacific Rise; OFZ: Orozco Fracture Zone; OGFZ: O'Gorman Fracture Zone; TZG: Tepi-Zacoalco Graben; CG: Colima Graben; C-O FZ: Chapala-Oaxaca Fracture zone; TMVB: Trans Mexican Volcanic Belt.

Fig. 2. Focal mechanism of event 38 (lower hemisphere equal area projection). Open circle: dilatation, dot: compression. Plus and minus denote less reliable compression and dilatation. Dashed fault planes fit first motion data (with some exceptions) but not the U_{sv} and U_{sh} waveforms (shown in boxes) at TEAC and TNLP, which require fault planes shown by lines. The waveforms were obtained by integrating digital accelerograms which triggered after the arrival of P wave. Synthetics (dashed lines in the boxes) were generated in an infinite space.

Fig. 3. Top: Elevation profile along the middle of the shaded inclined rectangle in Figure 1. Bottom: Projection of hypocenters along a vertical plane oriented N35°E. Solid dots: thrust events; open circles: normal faulting events. Continuous line shows geometry of the Benioff zone; its extension as dashed line indicates inferred geometry assuming that the slab reaches ~100 km below the active volcanos. Stippled region depicts surface manifestation of tensional stress regime.

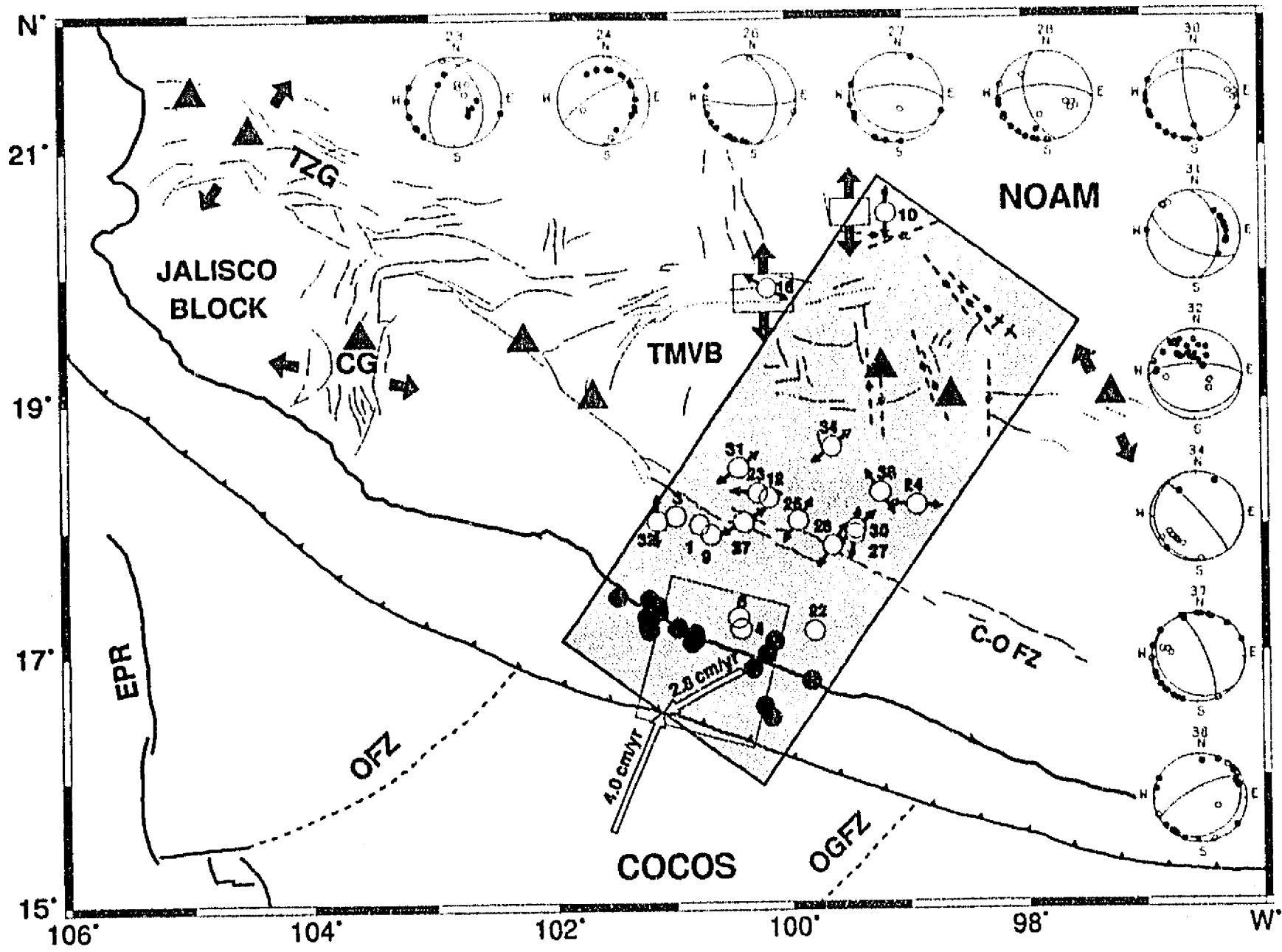


Fig. 1

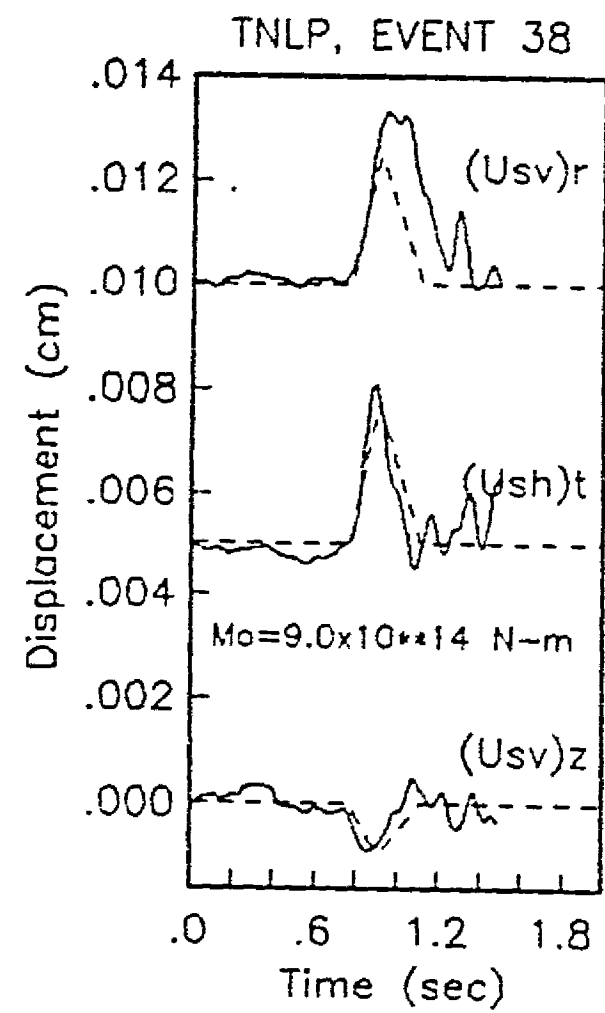
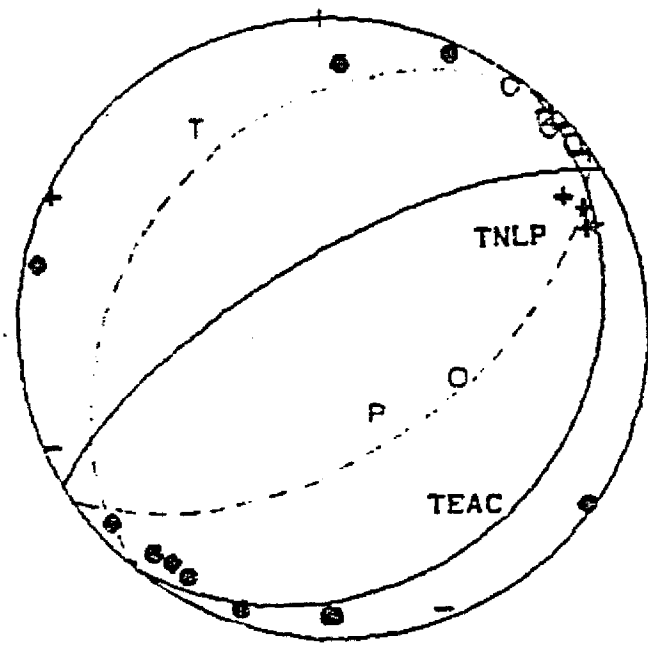
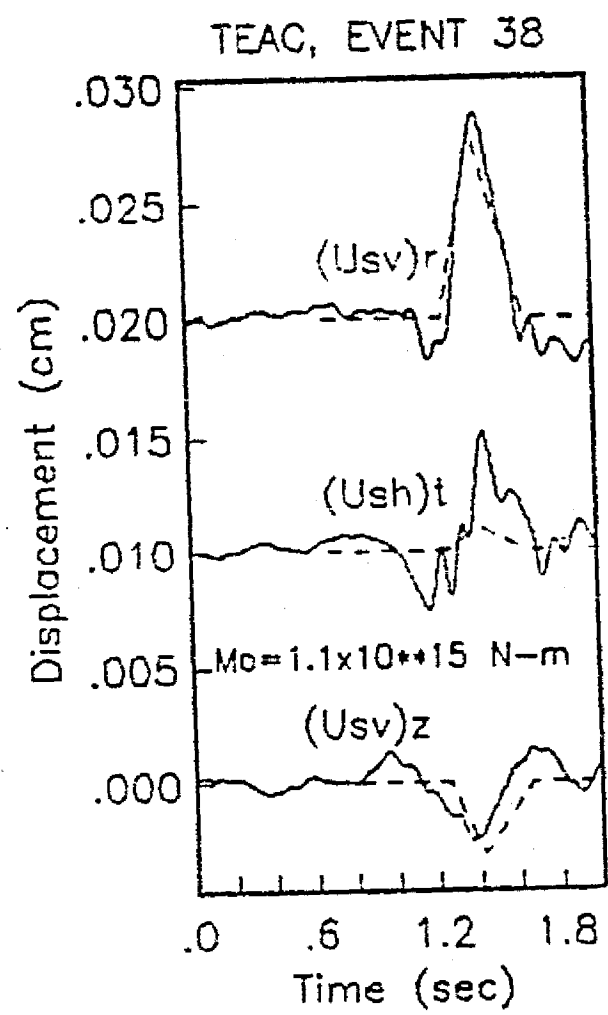


Fig. 2

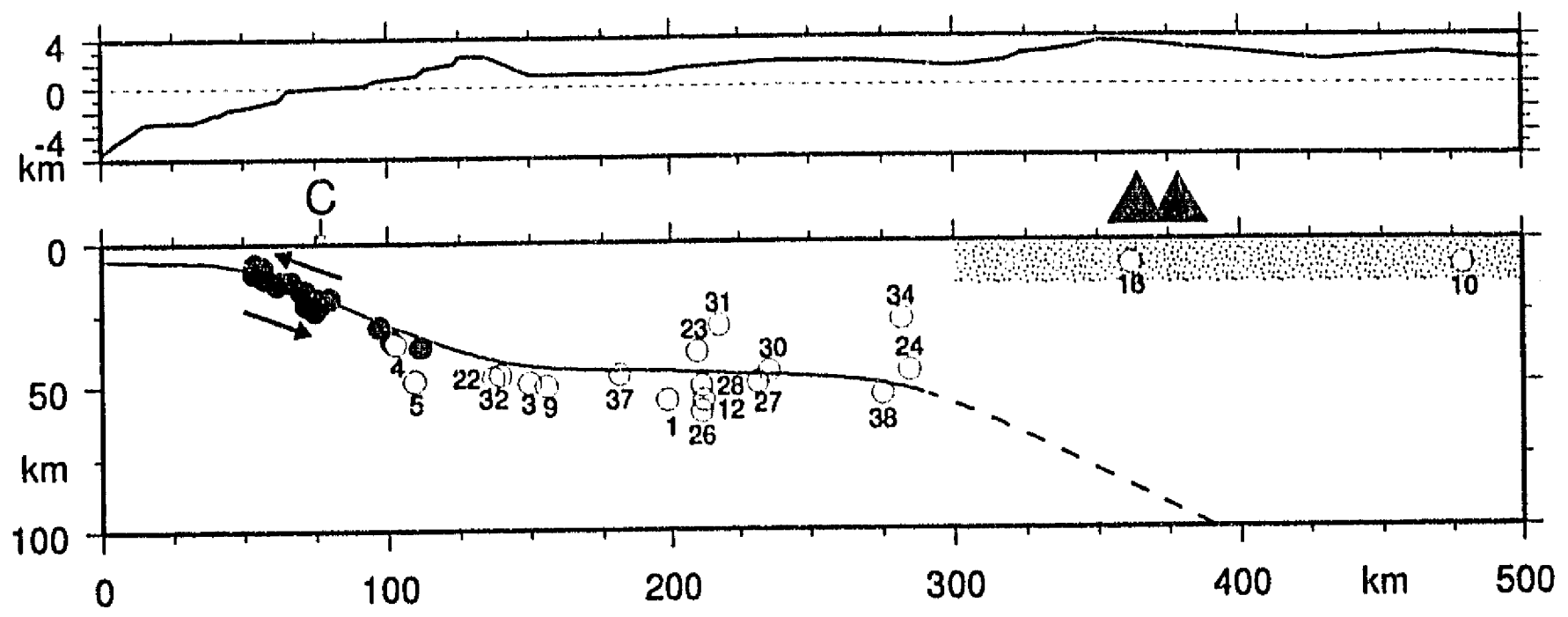


Fig. 3

**IV. Geometría Inclinada de la Subducción de la Placa de Rivera Bajo el
Bloque de Jalisco en el Oeste de México**

(Publicado en: *Geophys. Res. Lett.*, 20, 2391-2394, 1993)

**STEEP SUBDUCTION GEOMETRY OF THE RIVERA PLATE BENEATH THE
JALISCO BLOCK IN WESTERN MEXICO**

Mario Pardo^{1,2} and Gerardo Suárez¹

¹Instituto de Geofísica, Univ. Nacional Autónoma de México, México, D.F., 04510

²Departamento de Geofísica, U. de Chile, Casilla 2777, Santiago, Chile.

Abstract. The morphology of the Rivera plate subducted beneath the Jalisco block in western Mexico is determined from accurately located hypocenters of locally recorded microearthquakes, and from earthquakes with magnitude $m_b \geq 4.5$ recorded at teleseismic distances. The hypocenters of these latter earthquakes are relocated, and for five of them the focal depth is constrained by the inversion of long-period body waves. The Wadati-Benioff zone inferred from these data indicates a steep subduction of the Rivera plate that resembles the geometry of subduction of the Cocos plate beneath Central America. It is, however, very different from the shallower and almost subhorizontal subduction of the Cocos plate observed in southern Mexico, southeast of this region. The Rivera plate is comparable to the Juan de Fuca plate in terms of the small areal extent, young seafloor age, low relative velocity, and low teleseismic activity in the subduction zone. This study shows that the dip of both the Juan de Fuca and Rivera plates are similar once they are decoupled from the overriding continental crust. The downgoing Rivera plate initially starts with a dip of $\sim 10^\circ$ down to a depth of 20 km and then increases gradually to a constant dip of $\sim 50^\circ$ below a depth of 40 km. Intermediate-depth seismicity is low in this zone associated with the subduction of the slow (2 cm/yr) and young (9 m.y.) Rivera plate. The maximum depth extent of earthquakes observed in the Rivera subduction zone is about 130 km. The andesitic, calc-alkaline Colima volcano appears to be directly related to the subduction of the Rivera plate. To the NW of this volcano, the observed Quaternary volcanism in the Jalisco block, which is parallel to the trench, may also be explained by the subduction of the Rivera plate.

Introduction

The shape of the Wadati-Benioff zone of the Rivera plate beneath western Mexico is poorly known. This is due to the low rate of teleseismically recorded earthquake activity and

to the poor local seismic coverage. However, the Jalisco-Rivera plate boundary is far from being aseismic, for it was the site, in 1932, of the largest instrumentally recorded earthquake in Mexico ($M_w=8.2$) [Singh et al., 1985; Eissler and McNally, 1984].

Because of the lack of teleseismically located seismic activity, Nixon [1982] suggested that the Rivera plate subducts aseismically. Few focal mechanisms of shallow earthquakes and only one intermediate-depth earthquake associated apparently to the Rivera plate subduction have been reported [Dean and Drake, 1978; LeFevre and McNally, 1985]. In order to study the subduction regime of this small plate, Eissler and McNally [1984] relocated earthquakes on and near the boundaries of the Rivera plate. They were unable, however, to discern the geometry of the downgoing slab.

The pole of relative motion for the last 3.0 m.y. of the Rivera plate with respect to North America is located very close to the Rivera plate (22.8°N , 109.4°W , $1.883^\circ/\text{m.y.}$) [DeMets and Stein, 1990] (Figure 1). The rotation vector of DeMets and Stein [1990] predicts a relative velocity of 2.15 cm/yr offshore Colima (18.6°N , 105°W). The plate consumed at the trench is of late Miocene age (9 m.y.) and is therefore one of the youngest lithospheres being subducted [Klitgord and Mammerrickx, 1982]. The slow rate of convergence and the high temperatures of this young oceanic plate may be responsible for the low rate of observed seismicity.

The purpose of this study is to determine the geometry of the subducted Rivera plate from reliable hypocentral locations of microearthquakes and from the relocated hypocenters and focal mechanisms of earthquakes recorded at teleseismic distances. Understanding the geometry of subduction of this young plate is of fundamental importance to unravel the complex tectonic structure of this region.

Data Analysis

The data used to infer the morphology of the subducted Rivera plate beneath the Jalisco block are accurately determined hypocenters obtained from several datasets: 1) Local microearthquakes recorded by five temporary seismological stations deployed for one month in 1989 around the Colima graben. These data are complemented with the permanent seismic stations operated by the University of Colima, Mexico and by the National Seismological Service, UNAM (Figure 2); 2) Twenty teleseismic events, relocated using the method of Joint Hypocenter Determination (JHD) [Dewey, 1971]; and 3) Five events ($m_b \geq 5.0$) for which the depth and focal mechanism are constrained using a long-period body wave inversion scheme [Nábelek, 1984].

Local microearthquake data. The microearthquake data were located using HYPO71 [Lee and Valdes, 1985] and the velocity model reported by Suárez et al. [1992], with a ratio $V_p/V_s = 1.76$ determined for this zone. Hypocentral locations were considered reliable and included in the dataset when they met the following criteria: 1) A minimum of seven phases were read with at least one S-wave reading; 2) A root mean square error of less than 0.25 s; 3) Estimated hypocentral errors of less than 10 km; and 4) A hypocentral variation of less than 10 km when the initial trial depth was varied from 10 to 150 km. A final subset of 100 reliable hypocenters were obtained from a total of 162 microearthquakes.

Relocated earthquakes. The largest aftershock of the 1973 Colima earthquake ($M_s=7.5$) was used as the calibration event in a JHD scheme [Dewey, 1971]. This aftershock ($m_b=5.6$, $M_s=6.2$) was located with a temporary seismic network deployed after the mainshock [Reyes et al., 1979]. The time adjustments of the seismological stations were obtained from the variance of the different phase arrival times, read from the ISC catalog, of the calibration event and of five other events reported in this study for which the focal depth was constrained using a body wave inversion. These calibration station-phases were then used in a single-event location method to obtain the relocated hypocenters of twenty earthquakes ($m_b \geq 4.5$) reported by the ISC between 1964 and 1986 (Table 1).

The precision of each relocated hypocenter relative to the calibration event is estimated by computing error ellipsoids for each pair of hypocentral coordinates at a 90% confidence level. The estimated errors of the epicentral coordinates and focal depth average 15.5, 8.8 and 7.6 km respectively. An independent test on the accuracy of the focal depth computed from the relocation scheme was done for earthquake number 19 (Table 1). A pP-P time of ~6 sec was read from the stacked records of the Yellow Knife Array in Canada, which is in good agreement with the depth of 21 km computed by the JHD method. In contrast, the ISC reported a focal depth of 87 km for this event.

Long-Period Body Wave Inversion. Application of the body wave inversion technique [Nábelek, 1984] to P, SV and SH waveforms constrains the focal mechanism and the centroidal depth. Long-period seismograms from the Global Digital Seismograph Network (GDSN) were used for one event that occurred in 1981, and from the World Wide Standardized Seismograph Network (WWSSN) for four events that occurred prior to 1980.

Discussion and Conclusions

The resulting data (Figure 2) show that the seismicity is concentrated southwest of the Colima volcano. To the north of this volcano, the seismicity is scarce along the Colima and Tepic-Zacoalco grabens, although the seismic coverage was better here than towards the

south. To the NW, there is a dearth of teleseismic earthquakes ($m_b \geq 4.5$) and no microearthquake data is available. The crustal seismicity within the Jalisco block is high in and around the southern part of the Colima graben (Figure 3).

The focal depth and mechanism of the deepest event in Figure 3a (event 1 on Table 1) are constrained by the body wave inversion scheme [Nábelek, 1984]. This event was reported as a compressional event with a similar focal depth (130 km) by LeFevre and McNally [1985] using only first motions of P waves. However, based on the long-period inversion of P, SV, and SH waveforms, short-period P waveforms and the reported first motions of P waves from the ISC, this earthquake is clearly a tensional event (Figure 4).

The inferred slab shows a relatively steep dip, reaching a maximum depth of 130 km (Figure 3). The initial dip is 10° down to a depth of 20 km and then gradually increases to a relatively constant dip of $\sim 50^\circ$ below a depth of 40 km. The focal mechanisms indicate compression down to a depth of 40 km (Figure 3a and 3b) and down-dip tension below this depth. The orientation of the T-axes agrees with the dip inferred for the Wadati-Benioff zone (Figure 3a).

Although the location of the Rivera-Cocos plate boundary is still controversial [e.g., Bourgois and Michaud, 1991], we assume that this boundary is close to the dashed line shown on Figure 2. This line represents the trajectory, according to the Rivera-North America pole [DeMets and Stein, 1990], of a point on the trench which was extrapolated from the offshore strike of the Rivera fracture zone and from the focal mechanisms reported in the Harvard CMT catalog (Figure 1). Cross-section BB' is clearly located in the Rivera plate (Figure 3). Although the depth extent of the earthquakes on BB' is shallower than on AA', the geometry of both seismic zones is very similar (Figure 3). This suggests that the steep Wadati-Benioff zone on cross section AA' also corresponds to the subduction of the Rivera plate beneath the Jalisco block.

This plate geometry is very different from the shallow dip angle of the slab observed to the east of Jalisco, in Central Mexico [Pardo and Suárez, 1993], which becomes almost subhorizontal at a depth of about 50 km [Suárez et al., 1991]. The inferred geometry of the Rivera plate resembles the subduction of the Cocos plate under Central America, where the Wadati-Benioff zone dips steeply [e.g., Burbach et al., 1984; Ponce et al., 1992].

The Rivera plate is comparable to the Juan de Fuca plate in terms of the size, young seafloor age, slow relative plate velocity, and low seismic activity. The dip of these two slabs are similar once they are decoupled from the overriding continental crust (~ 40 km). Below this depth, the Cascadia subduction zone dips at an angle of $\sim 50^\circ$ [Crosson, 1992; Taber and Smith, 1985]. The subhorizontal subduction observed in other subduction zones of the world has been attributed to the young age and presumably bouyant nature of these

slabs. This assertion is not confirmed by the geometry of the Cascadian, Central American, and Jalisco block subduction zones.

The andesitic, calc-alkaline Colima volcano is located where the downgoing Rivera plate reaches a depth of ~100 km (Figure 3a), suggesting a link between this volcano and the subduction of the downgoing slab. Thus, the Colima volcano may be the easternmost volcano associated with the subducted Rivera plate. To the NW of the Colima volcano, Lange and Carmichael [1991] and Wallace et al. [1992] reported the existence of three volcanic fields parallel to the trench: Los Volcanes, Mascota and San Sebastián (Figure 2). From their chemical composition, they conclude that they are characteristic of lavas erupted at convergent plate margins. Although the locations of the microearthquakes on cross section CC' are not as reliable as those in the other cross sections, if we assume that the shape of the subducted slab continues at depth in a manner similar to AA' and BB', it is possible that these volcanic fields may also be related to the subduction of the Rivera plate.

The Quaternary volcanic arc parallel to the trench (Figures 1 and 2), may be extended to the northwest as far as the Tepic-Zacoalco graben (TZG), and those volcanoes could also be related to the subduction of the small Rivera plate if the dip here is similar to that observed on cross sections AA' and BB'. However, the presence of the Tequila volcano, located in the TZG and far from the coast (Figure 2), would not be explained by a Rivera plate dipping steeply throughout the Jalisco Block. Therefore, we can not rule out a change in dip beneath a depth of 40 km to the NW of cross section BB'.

In summary, the resulting morphology of the subducted Rivera plate below the Jalisco block explains the presence of the Colima volcano and perhaps of other Quaternary calc-alkaline volcanoes found in the region parallel to the trench. In order to refine the geometry of the Wadati-Benioff zone and its relation to the complex volcanism of the area, local seismic networks must be installed in the zone due to the low magnitude and rate of seismicity.

Acknowledgments. We thank I. Galindo, Z. Jimenez and R. North for data from the Colima network and the Yellow Knife Array. The paper was improved by the reviews of J. Bourgois and an anonymous reviewer. We thank C. Mendoza and S. Nishenko for their thoughtful reviews. The local temporary stations were installed in 1989 as part of a joint project between UNAM and Institut de Physique du Globe, France; we thank R. Gaulon and T. Monfret for their participation during the experiment and G. Patau for reading seismograms. This research was partially supported by PADEP, UNAM (DCCH9231) and grants from DDF and CENAPRED. One of us (MP) acknowledges support by the Secretaría de Relaciones Exteriores, México.

References

- Bourgois, J., et al., La jonction orientale de la dorsal Est-Pacifique avec la zone de fracture de Rivera au large du Mexique, C. R. Acad. Sci. Paris, t. 307, Serie II, 617-626, 1988.
- Bourgois, J. and F. Michaud, Active fragmentation of the North American plate at the Mexican triple junction area off Manzanillo, Geo-marine Lett., 11, 59-65, 1991.
- Burbach, G. V., C. Frohlich, W. D. Pennington, and T. Matumoto, Seismicity and tectonics of the subducted Cocos plate, J. Geophys. Res., 89, 7719-7735, 1984.
- Crosson, R. S., Cascadia subduction zone: Large scale structure from receiver function analysis, seismicity, and teleseismic arrival time tomography, [abs.], Wadati Conference on Great Subduction Earthquakes, Alaska, Sep. 16-19, pp. 35, 1992.
- Dean, B. W. and C. L. Drake, Focal mechanism solutions and tectonics of the Middle America arc, J. Geol., 86, 111-128, 1978.
- DeMets, C. and S. Stein, Present-day kinematics of the Rivera plate and implications for tectonics in southwestern Mexico, J. Geophys. Res., 95, 21931-21948, 1990.
- Dewey, J. W., Seismicity studies with the method of joint hypocenter determination, Ph.D. Thesis, University of California, Berkeley, 1971.
- Eissler, H. and K.C. McNally, Seismicity and tectonics of the Rivera plate and implications for the 1932 Jalisco, Mexico earthquake, J. Geophys. Res., 89, 4520-4530, 1984.
- Klitgord, K. D. and J. Mammerickx, Northern East Pacific Rise: Magnetic anomaly and bathymetric framework, J. Geophys. Res., 87, 6725-6750, 1982.
- Lange, R. and I. Charmichael, A potassic volcanic front in western Mexico: The lamprophyric and related lavas of San Sebastian, Geol. Soc. Am. Bull., 103, 928-940, 1991.
- Lee, W. H. K. and C. M. Valdés, HYPO71PC: A personal computer version of the HYPO71 earthquake location program, Open-File Report 85-749, United States Department of the Interior, Geological Survey, 1985.
- LeFevre, L. V. and K. C. McNally, Stress distribution and subduction of aseismic ridges in the middle America subduction zone, J. Geophys. Res., 90, 4495-4510, 1985.
- Nábelek, J. L., Determination of earthquake source parameters from body waves, Ph. D. thesis, MIT, Cambridge, 1984.
- Nixon, G. T., The relationship between Quaternary volcanism in central Mexico and the seismicity and structure of subducted ocean lithosphere, Geol. Soc. Am. Bull., 93, 514-523, 1982.

- Pardo, M. and G. Suárez, Morphology of the Rivera and Cocos plate subduction beneath southern Mexico: Implications on the location of the Trans Mexican Volcanic Belt, [abs.], Seism. Res. Lett., 64, pp. 15, 1993.
- Ponce, L., R. Gaulon, G. Suárez, and E. Lomas, Geometry and the state of stress of the downgoing Cocos plate in the Isthmus of Tehuantepec, Mexico, Geophys. Res. Lett., 19, 773-776, 1992.
- Reyes, A., J. Brune, and C. Lomnitz, Source mechanism and aftershock study of the Colima, Mexico earthquake of January 30, 1973, Bull. Seismol. Soc. Am., 69, 1819-1840, 1979.
- Singh, S. K., L. Ponce, and S. Nishenko, The great Jalisco, Mexico, earthquake of 1932: Subduction of the Rivera Plate, Bull. Seismol. Soc. Am., 75, 1301-1313, 1985.
- Suárez, G., T. Monfret, G. Wittlinger, and C. David, Geometry of subduction and depth of the seismogenic zone in the Guerrero gap, Mexico, Nature, 345, 336-338, 1990.
- Suárez, G., J. P. Ligorria, and L. Ponce, Preliminary crustal structure of the coast of Guerrero, Mexico, using the minimum apparent velocity of refracted waves, Geoffs. Int., 31, 247-252, 1991.
- Taber, J. and S. Smith, Seismicity and focal mechanisms associated with the subduction of the Juan de Fuca plate beneath the Olympic peninsula, Washington, Bull. Seismol. Soc. Am., 75, 237-249, 1985.
- Wallace, P., I. Carmichael, K. Richter, and T. Becker, Volcanism and tectonism in western Mexico: A contrast of style and substance, Geology, 20, 625-628, 1992.

Table 1. Focal parameters of relocated earthquakes along the Rivera plate subduction zone

N	Date Y M D	O.Time GMT	Lat °N	Lon °W	Depth km	mb ISC	ϕ °	δ °	λ °
*	730210	115328.	18.41	103.6	11.0	5.6			
1	730729	161633.	19.56	103.4	127.4 ¹	5.0	352	71	-119 ¹
2	731018	104939.	19.34	104.9		6.0	296	33	86 ¹
3	760717	090212.	19.28	104.7		5.2	311	12	115 ¹
4	780425	125610.	19.22	104.1		5.3	282	34	105 ¹
5	810309	223853.	18.76	103.9		5.9	260	28	60 ¹
6	640227	113535.	18.86	103.9	24.6	4.7			
7	650924	171354.	20.15	105.7	14.0	4.6			
8	690430	150437.	18.93	104.2	18.5	4.8			
9	690623	070829.	18.30	104.5	11.0	5.5			
10	700907	180832.	19.52	105.0	19.5	5.1			
11	710205	052905.	18.91	105.0	10.0	4.7			
12	730510	175055.	18.86	104.6	18.6	5.1			
13	731019	004953.	19.28	105.0	14.1	4.9			
14	740126	053546.	19.00	103.8	50.8	5.2	355	65	-145 ²
15	750625	055914.	19.69	104.8	22.2	4.8			
16	760307	214841.	18.80	103.9	29.6	4.9			
17	760413	201748.	18.54	104.8	5.0	5.3			
18	810207	053715.	20.64	105.7	25.5	4.6			
19	810522	143007.	19.59	105.2	21.0	4.8			
20	830311	030549.	19.01	104.4	21.4	4.8			

* Calibration event [Reyes et al., 1979].

¹ Focal depth and mechanism from the long-period body wave inversion.

² Focal mechanism from P waves first motion.

Figure Captions

Fig. 1. Tectonic sketch map of the Rivera plate and the Jalisco block. Focal mechanisms are from Harvard CMT catalog. Numbered focal mechanisms are listed on Table 1. Black triangles indicate Quaternary andesitic volcanoes and shaded triangles are Quaternary rhyolitic eruptive centers. Solid diamond is the location of Rivera-N. America rotation pole [DeMets and Stein, 1990]. CG: Colima graben. EPR: East Pacific Rise. MAT: Middle American trench. PRR: Pacific Rivera Rise. RFZ: Rivera Fracture Zone. TFZ: Tamayo fracture zone. TZG: Tepic-Zacoalco graben.

Fig. 2. Locations of the selected epicenters related to the Rivera subduction. Solid squares are the relocated epicenters where the depth was fixed by long period body-wave inversion. Solid diamonds are relocated epicenters (Joint Hypocenter Determination), and the solid circles are epicenters of locally recorded microearthquakes. Seismological stations are shown as open diamonds. Andesitic volcanoes are shown as solid triangles and numbered: 1) Colima, 2) Los Volcanes, 3) Mascota, 4) San Sebastián, and 5) Tequila. The location of the three cross sections on Figure 3 are also shown. The dashed line to the east indicates the motion of a point on the trench as predicted from the Rivera-North America pole [DeMets and Stein, 1990].

Fig. 3. Cross sections plotted in the direction of relative plate convergence ($N46^{\circ}E$). Symbols are the same as on Figure 2. Side-looking, lower-hemispheric focal mechanisms are from the body-wave inversion (black) and P-wave first motions (shaded). The projected location of Colima volcano and Los Volcanes volcanic field are shown as solid triangles on cross sections (a) and (c) respectively. Local microearthquakes shown as shaded circles indicates less reliable locations.

Fig. 4. (a) Lower-hemispheric projection of the focal mechanism from long-period body wave inversion for the deepest event ($h=127$ km) located under the Colima volcano (event 1 on Table 1). The observed seismograms are shown as solid lines and the synthetics with dashed lines. (b) Observed (solid line) and synthetic (dashed) short-period P waveforms computed for the same mechanism and depth obtained using long-period data, and P-wave focal mechanism from the inversion showing all the ISC reported first motion polarities.

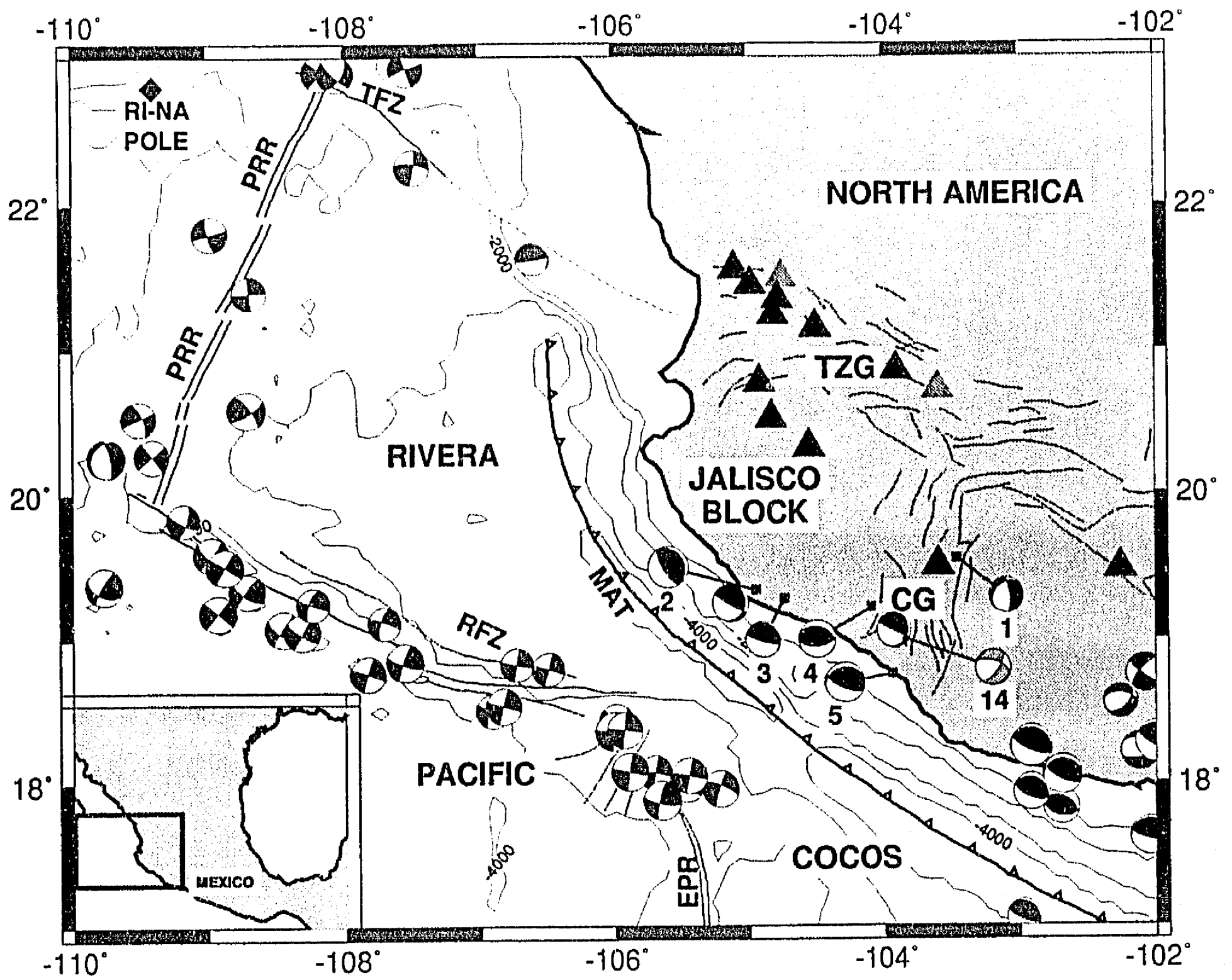


Fig. 1

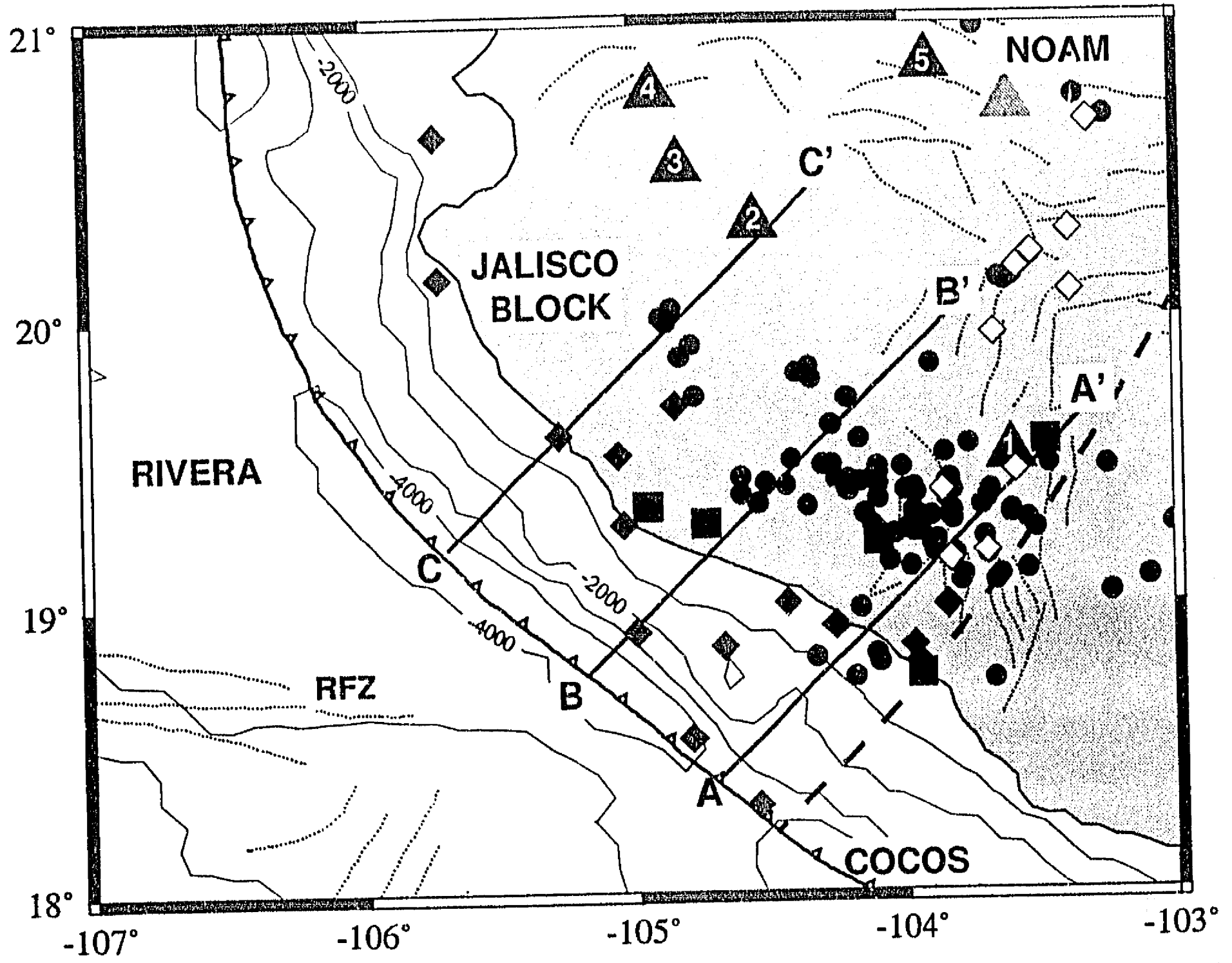


Fig. 2

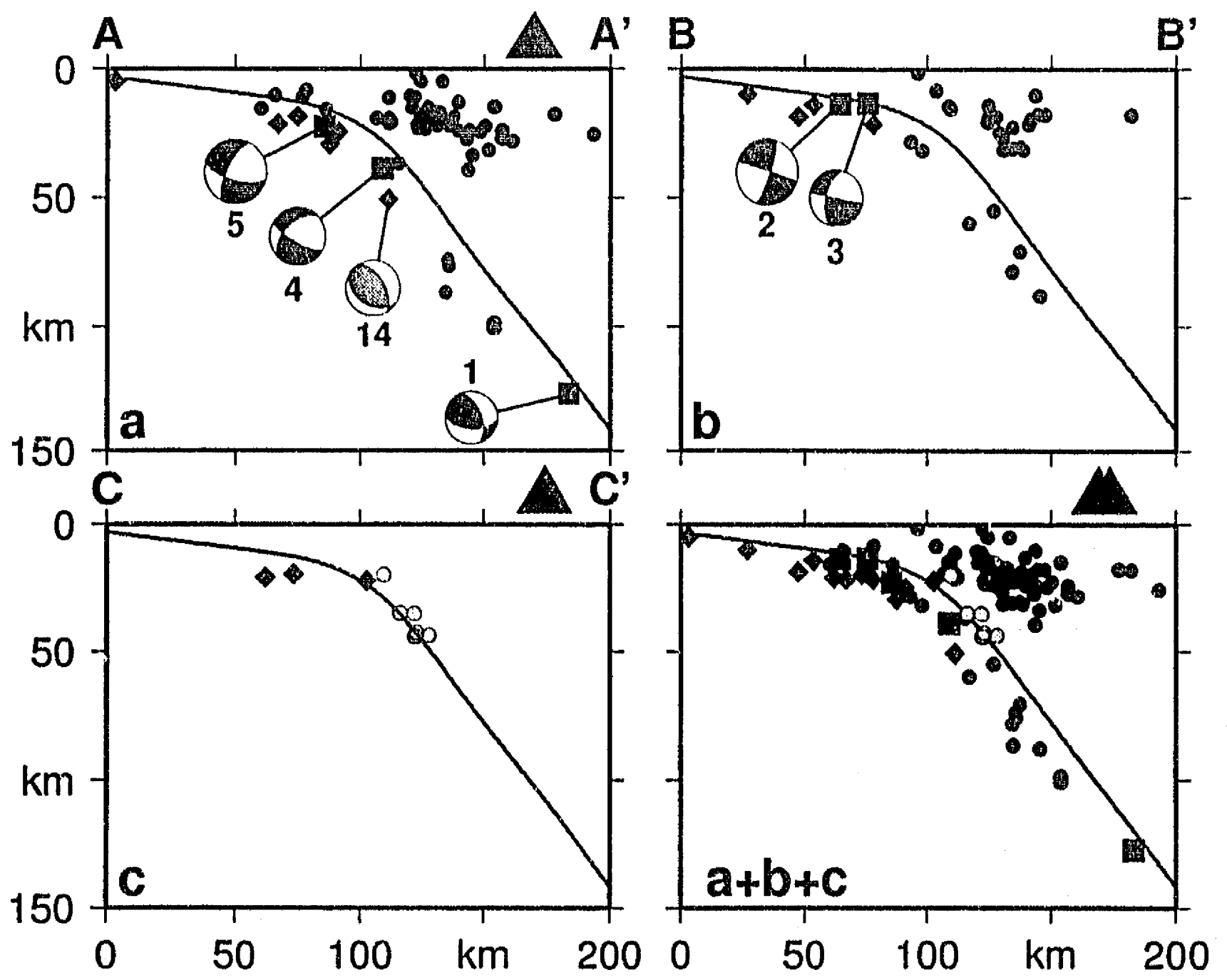


Fig. 3

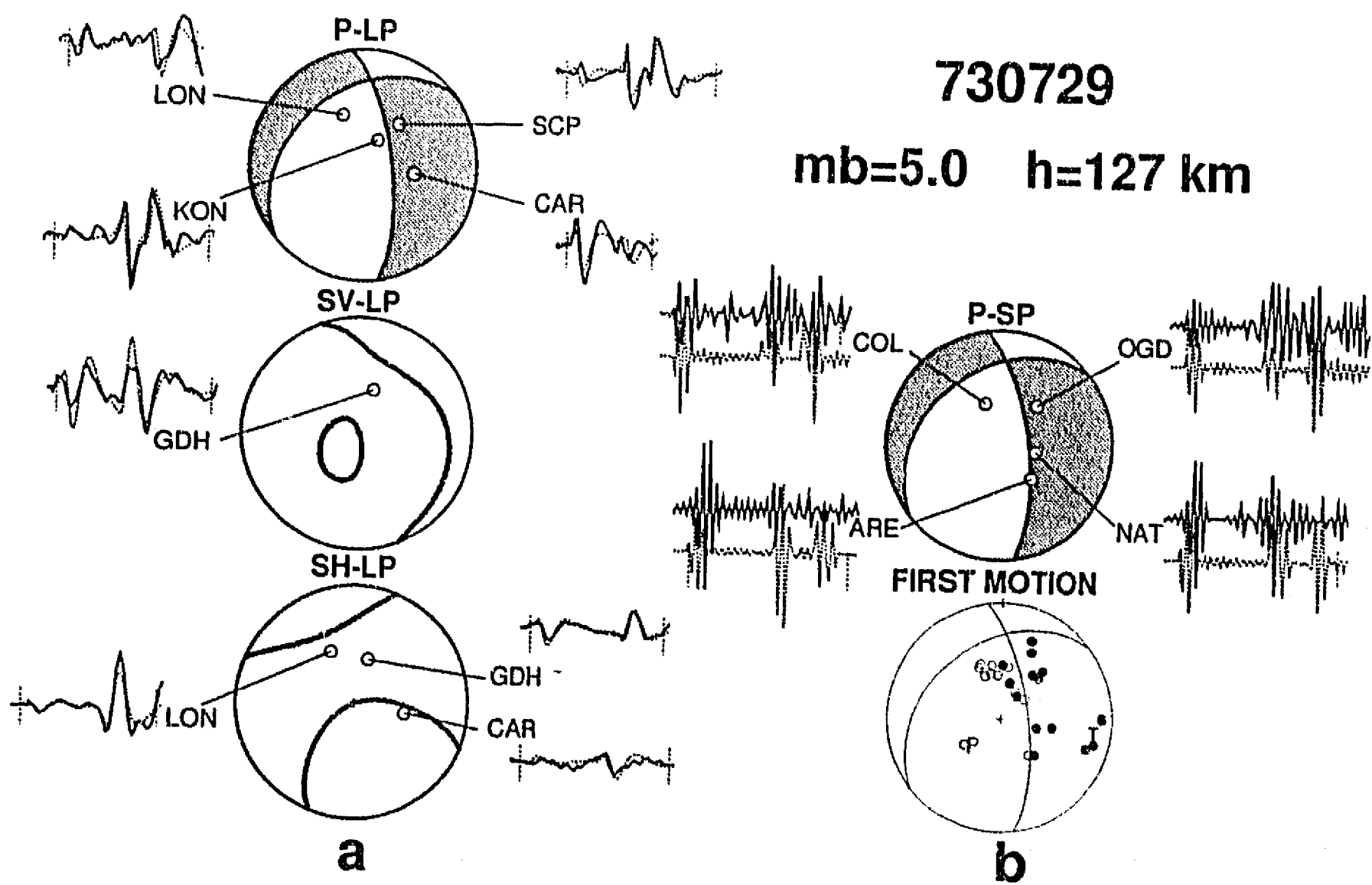


Fig. 4

V. Forma de la Subducción de las Placas de Rivera y Cocos en el Sur de México: Implicaciones Sísmicas y Tectónicas
(En Preparación para: *J. Geophys. Res.*, 1993)

SHAPE OF THE SUBDUCTED RIVERA AND COCOS PLATES IN SOUTHERN MEXICO: SEISMIC AND TECTONIC IMPLICATIONS

Mario Pardo^{1,2} and Gerardo Suárez¹

¹Instituto de Geofísica, Univ. Nacional Autónoma de México, México, D.F., 04510

²Departamento de Geofísica, U. de Chile, Casilla 2777, Santiago, Chile.

Abstract. The shape of the subducted Rivera and Cocos plates beneath the North American plate in southern Mexico is determined, based on accurately located hypocenters of local and teleseismic earthquakes. The hypocenters of the teleseisms were relocated, and for a subset of 21 events, the focal depth was constrained using a body-wave inversion. The subduction in southern Mexico may be approximated as a subhorizontal slab bounded at the edges by the steep subduction geometry of the Cocos plate beneath the Caribbean plate to the east, and of the Rivera plate beneath North America to the west. Lateral changes on the dip of the subducted plate are observed only once it decouples from the overriding plate, with a constant interplate contact geometry at least down to 30 km depth. The maximum depth of the seismogenic interplate zone is ~30 km for the Cocos plate and ~40 km for the Rivera plate. Based on the seismicity, focal mechanisms and the geometry of the downgoing slab, southern Mexico can be segmented in four regions: (1) The Jalisco region to the west, where the Rivera plate shows a steep subduction that resembles the geometry of the Cocos plate beneath the Caribbean plate in Central America; (2) The Michoacan region, where the dip angle of the Cocos plate decreases gradually towards the east. This region is bounded to the east by the subduction of the Orozco fracture zone and to the west by the projection of the Rivera fracture zone and the El Gordo graben at the trench; (3) The Guerrero region, bounded by the Orozco and the O'Gorman fracture zones, where the subducted slab is almost subhorizontal; and (4) The Oaxaca region, between the O'Gorman fracture zone and the Tehuantepec ridge, where the dip of the subduction gradually increases to a steeper subduction in Central America. The drastic changes in dip do not appear to take place on tear faults, suggesting that smooth contortions accommodate these dip changes. The Rivera-Cocos boundary shows a rapid change in dip. However, the available data is not sufficient to resolve whether a tear fault or a contortion may be the cause. The inferred 80-100 km depth contours of the subducted slab appear to be beneath the front of the Trans Mexican Volcanic Belt. This volcanic belt is directly related to the subduction, and the observed non-parallelism with the trench is mainly due to the geometry of the Rivera and Cocos plates beneath the North American plate in southern Mexico.

INTRODUCTION

The seismicity and tectonics of southern Mexico are characterized by the subduction of the oceanic Cocos and Rivera plates beneath the North American plate along the Middle America Trench (MAT). One of the main characteristics of this subduction zone is the lateral variation in the dip of the subducted oceanic lithosphere (*Molnar and Sykes, 1969; Stoiber and Carr, 1973; Dean and Drake, 1978; Nixon, 1982; Bevis and Isacks, 1984; Burbach et al., 1984*).

The most prominent surface tectonic feature in the upper-plate is the Trans Mexican Volcanic Belt (TMVB), a broad chain of Plio-Quaternary volcanoes. This volcanic arc exhibits variations in structure and chemical composition, and a general orientation that is oblique ($\sim 16^\circ$) with respect to the strike of the MAT (Figure 1).

There have been several studies of Wadati-Benioff zone seismicity along parts of the Middle America Trench in southern Mexico in recent years [*Stoiber and Carr, 1973; Hanus and Vanek, 1978; Havskov et al., 1982; Burbach et al., 1984; Bevis and Isacks, 1984; Suárez et al., 1990; Singh and Mortera, 1991; Ponce et al., 1992; Singh and Pardo, 1993; Pardo and Suárez, 1993; Cruz and Suárez, 1993*]. Based on teleseismic data, *Burbach et al.* [1984] concluded that in the region the subducted Cocos plate can be divided in three major segments, bounded by contortions of the slab. Also, *Bevis and Isacks* [1984], using hypocentral trend surface analysis find no evidence for tears in the subducted Cocos plate, and they suggested a probable flexure between the flat slab-steep slab transition observed near 96°W , which may be related to differences in age of oceanic lithosphere on either side of the Tehuantepec ridge.

The regional stress distribution associated with the subduction of the Cocos plate have been studied from focal mechanisms of large and intermediate size earthquakes that occurred within the region [*Molnar and Sykes, 1969; Dean and Drake, 1978; LeFevre and McNally, 1985; Suárez et al., 1990*]. However, in almost all these studies the geometry of the subducted Rivera and Cocos plate beneath the North American plate (NW of 94°W), and the associated stress distribution is poorly defined due to the low intermediate-depth earthquake activity (depth > 40 km) and to the scarcity of local seismic stations in southern Mexico.

Various studies show that the subduction of bathymetric features, like ridges or fracture zones, affect the characteristics and geometry of the subduction (*e.g., Kelleher and McCann, 1976; Vogt et al., 1976, Isacks and Barazangi, 1977; Cross and Pilger, 1982*). In southern Mexico there are four of these major features subducting along the MAT: The El Gordo graben (EG), the Orozco fracture zone (OFZ), the O'Gorman fracture Zone

(OGFZ), and the Tehuantepec Ridge (TR). These features are oriented nearly parallel to the direction of plate convergence and are subducted almost perpendicular to the trench (Figure 1).

The purpose of this study is to determine the geometry of the subducted Cocos and Rivera plate, based on reliable hypocenter locations of earthquakes recorded with local and teleseismic networks, and to study the regional distribution of stresses with reported and new determined focal mechanisms. Together, this data are analyzed to determine its implications on the seismicity and tectonics in southern Mexico.

TECTONIC SETTING

The zone of study includes the subduction of the Rivera and Cocos plates in southern Mexico beneath the North American plate, west of the intersection of the Tehuantepec ridge with the MAT (Figure 1). According to *Mammerickx and Klitgord* [1982], the tectonic history of the zone for the last 25 m.y. has suffered at least three major plate reorganizations. The old Farallon plate evolved first to the Guadalupe plate, which was later segmented into the actual Rivera and Cocos plates. The position of the spreading centers moved east, from 12.5 to 11 m.y.b.p., to the Mathematician seamounts and later, between 6.3 to 3.5 m.y.b.p., to the actual position of the East Pacific Rise (EPR).

Rivera Plate

The existence of the small Rivera plate was first suggested by *Atwater* [1970] with boundaries defined by the RFZ, EPR, the Tamayo fracture zone (TFZ) and the MAT (Figure 1). *Bandy and Yan* [1989] presented data that supporting the that Rivera and Cocos are separate plates. *Eissler and McNally*, [1984] and *DeMets and Stein* [1990] also concluded that the Rivera plate is kinematically distinct from the North American and Cocos plates.

The eastern junction between EPR and RFZ is located 165 km west of the MAT [*Bourgeois and Michaud*, 1991]. The Rivera-Cocos boundary is still controversial, with apparently no clear bathymetric features that can be associated to a discrete boundary [*Eissler and McNally*, 1984; *Mammerickx*, 1984; *Bourgeois and Michaud*, 1991]. However, *Bandy* [1992] suggests that the El Gordo graben may be the eastern margin of the Rivera-Cocos plate boundary (Figure 1).

The seismicity is caused primarily by the subduction of the Rivera plate beneath the Jalisco block (Figure 1), where at least six large earthquakes ($M_s > 7.0$) since 1837 have

been documented, including the great 1932 Jalisco earthquake ($M_s=8.2$) [Eissler and McNally, 1984; Singh *et al.*, 1985]. This evidence contradicts Nixon's [1982] suggestion that the Rivera plate subducts aseismically. Based on locally recorded microearthquake hypocenters and relocated hypocenters from teleseismic data, concluded that the subduction of the Rivera plate takes place with a steep angle ($\sim 50^\circ$) below depths of 40 km, that resembles the dip observed in Central America beneath the Caribbean plate [Pardo and Suárez, 1993].

The Rivera lithosphere consumed at the trench is of late Miocene age (~ 9 m.y.) [Klitgord and Mammerickx, 1982]. The slow rate of convergence (~ 2 cm/yr) [DeMets and Stein, 1990] and the relatively high temperature of this young oceanic plate are probably responsible for the sparse subduction macroseismicity observed associated to the Rivera plate. The alleged Jalisco block would have an insignificant motion (< 5 mm/yr) relative to North America [Bandy and Pardo, 1993]. Thus, in this study we assume that it is part of the North American plate.

Cocos Plate

The Cocos plate is formed at the EPR and subducts beneath the North American plate with relative velocity that increases eastward from 4.8 cm/yr at 104.5°W to 7.5 cm/yr at 94°W [DeMets *et al.*, 1990]. The age of the Cocos plate also varies along the MAT, with jumps associated to fracture zones that follow arcuate trajectories, concave to north and away from the EPR (Figure 1). The more prominent fracture zones in the eastern flank of the EPR are the Orozco and O'Gorman fracture zones. The OFZ is a broad topographic structure consisting of several parallel deep troughs and large ridges. The OGFZ is the largest of the fracture zones in the region that does not offset the EPR, consists of a deep trough [Klitgord and Mammerickx, 1982].

In the eastern part of the study area, the Tehuantepec ridge intersects the MAT at $\sim 95^\circ\text{W}$. This ridge is the largest linear bathymetric feature on the east flank of the EPR, and has a large relief because it is the morphological expression of a fracture zone that presumably separates crust of significantly different ages. A younger and shallower crust to the northwest differs in age to that southeast of the TR by approximately 10 to 25 m.y. [Couch and Woodcock, 1981].

South of the TMVB, the continental margin has characteristics of a truncated composite margin. It is apparently composed by accreted allochthonous terranes [e.g. Karig *et al.*, 1978; Beck, 1991]. Paleomagnetic data from southern Mexico indicate a relative stability since mid-Cretaceous with no evidence of latitudinal displacements, implying that the terrane transport process has stopped since that time [Bönhel *et al.*, 1992].

Trans Mexican Volcanic Belt

The TMVB is a geological province that crosses southern Mexico from east to west at about 19°N. The distribution of the volcanic arc is oblique (~16°) relative to the MAT (Figure 1), in an unusual geometry which is not parallel to the subduction zones. The TMVB is ~100 km wide and is cut by a sequence of grabens that are oblique relative to the general trend of the arc [Nixon, 1982].

It is mainly composed of andesitic rocks erupted since the Miocene, mostly during the Pliocene-Quaternary. A diversity of volcanic structures, such as great strato-volcanoes, monogenetic cinderic cones, shield volcanoes, and several calderas, are found on the volcanic belt. The chemical and petrological characteristics of the TMVB indicate that, in general, the volcanic sequences that form this belt are calc-alkaline, although some localized zones of alkaline volcanism exist along the TMVB, especially in western Mexico [Luhr *et al.*, 1985; Allan *et al.*, 1991].

A number of contrasting hypotheses have been proposed to account for the non-parallelism of the TMVB relative to the MAT and its relation with the subducted oceanic plate. These hypotheses can be divided in two groups: (1) those which favor a direct association between subduction and volcanism [e.g., Molnar and Sykes, 1969; Demant and Robin, 1975; Nixon, 1982; Burbach *et al.*, 1984; Suárez and Singh, 1986; Singh and Mortera, 1991], and (2) those who suggest that the TMVB bears no direct tectonic relation with the subduction along the MAT and explain its origin as resulting from zones of weakness within the crust of southern México, inherited from earlier episodes of deformation [e.g., Mooser, 1972, Gastil and Jensky, 1973, Shurbet and Cebull, 1984; Johnson and Harrison, 1989].

DATA

The data used to infer the morphology of the subducted Rivera and Cocos plates beneath southern Mexico are accurately determined hypocenters obtained from local microearthquake data recorded by permanent and temporary seismological stations, and from events recorded at teleseismic distances, relocated using the method of Joint Hypocenter Determination (JHD) [Dewey, 1971]. For some of the larger events ($m_b \geq 5.0$) the focal depth was constrained from the inversion of long-period body waves [Nábelek, 1984].

Local Microearthquakes Data

All the available local data from the permanent and temporary seismic networks installed in southern Mexico was used in order to accurately locate the hypocenters of microearthquakes within the zone [Nava, 1984; UNAM Seismology Group, 1986; Sansores, 1990; Pardo and Suárez, 1993; Ponce et al., 1993; Zuñiga et al., 1993].

The hypocenters were located using HYPO71 [Lee and Valdes, 1985] with the velocity model reported by Suárez et al. [1992], and a velocity ratio ($V_p/V_s = 1.76$) determined for the Guerrero zone. Hypocentral locations were considered reliable and included in the final dataset when they met the following criteria: 1) A minimum of seven phase readings with at least one S-wave reading; 2) A root mean square error of less than 0.25 s; 3) Estimated hypocentral errors of less than 10 km; and 4) A hypocentral variation of less than 10 km when the initial trial depth was varied from 10 to 150 km. From over 3000 events, a final subset of only 1101 reliable hypocenters satisfied these criteria (Figure 2).

Relocated earthquakes

We relocate earthquakes with magnitude $m_b > 4.5$ in southern Mexico, using the JHD method [Dewey, 1971] and the phase readings reported by the International Seismological Centre (ISC) between 1964 and January 1990. Different calibration events were used along the region: (a) The largest aftershock of the 1973 Colima earthquake ($M_s=7.5$) for the zone between 103° - 105° W. This aftershock ($M_s=6.2$) was located with a temporary seismic network deployed after the mainshock [Reyes et al., 1979]. (b) For the zone between 100° - 103° W, the 1979 Petatlan earthquake ($M_s=7.8$) recorded with portable stations [Valdés et al., 1982], and (c) The 1981 Ometepepec earthquake ($M_s=7.2$) [Nava, 1984] for the easternmost region.

The JHD method [Dewey, 1971] determines relocated hypocenters relative to the hypocenter of the calibration event, applying time adjustments to the phase readings of P, pP, and S. These time adjustments of the reporting seismological stations were obtained from the variance of the different phase arrival times of the calibration event and from the events reported in this study for which the focal depth was constrained using a long-period body wave inversion. These calibration station-phases were then used in a single-event location method [Dewey, 1971] to determine the relocated hypocenters within the zones of each calibration event. For the eastern part of the region, we used the relocated hypocenters obtained by Cruz and Suárez [1993], who applied the same procedure. The precision of each relocated hypocenter relative to the calibration event is estimated by computing error ellipsoids for the hypocentral coordinates at a 90% confidence level. A hypocentral location was considered reliable when the ellipsoid semi-axes were less than 20 km; all events

which did not comply this criteria were discarded from the final dataset. A final subset of 207 reliable hypocenters were obtained from an initial set of over 300 events (Appendix A and Figure 2).

Long -Period Body Wave Inversion

Application of a body wave inversion technique [Nábelek, 1984] to P, SV and SH waveforms constrains the focal mechanism and the centroidal depth. Long-period seismograms of teleseismic earthquakes ($25^\circ \leq \Delta \leq 90^\circ$) from the Global Digital Seismograph Network (GDSN) were used for the events that occurred between 1980 and 1987, and from the World Wide Standardized Seismograph Network (WWSSN) for the events that occurred prior to 1980. The analog seismograms were hand-digitized and filtered with a high-pass filter with cutoff frequency of 0.017 Hz (60 s) to eliminate long-period noise. The events modeled are in the magnitude range $5.0 \leq m_b \leq 6.1$, therefore, a point source was assumed (Appendix B).

ANALYSIS OF HYPOCENTRAL DATA

In plain view, the seismicity in southern Mexico shows a distribution in bands parallel to the trench (Figure 2). The band along the coast is apparently related to the interplate contact. North of it lies an almost aseismic zone, which becomes broader between 96°W and 101°W . Farther inland, a second band of deeper intraplate events (depths > 50 km) in the oceanic downgoing slab lies at distance (Dt) of 150-250 km from the trench. Beyond this last band, which is immediately to the south of the TMVB, shows a surprising absence of local and teleseismic seismicity in the downgoing plate.

In order to map the geometry of the subducted slab, twelve cross-sections of the seismicity were drawn (Figures 2 and 3). The origin of all the cross-sections is at the trench and they are oriented in the direction of convergence predicted between Rivera-North America [DeMets and Stein, 1990] and Cocos-North America [DeMets et al., 1990] (Figure 2).

The shallow part of the subduction zone ($h < 30$ km), indicates an interplate geometry that initially dips at $\sim 10^\circ$ and gradually increases to $\sim 25^\circ$ at a depth of 30 km (Figure 3). This geometry is observed throughout the subduction zone in southern Mexico, and appears to be independent of the age and the relative convergence velocity of the subducted oceanic plate; no lateral changes of the interplate geometry are observed where major bathymetric features are subducted.

Geometry of the Subducted Plate

The subducted Rivera and Cocos plates shows a geometry with lateral variation in the dip at depths greater than 30 km (Figure 3). The dip of the Cocos plate decreases from the TR towards the west, becoming subhorizontal, and then increasing to a steep subduction geometry of the Rivera plate.

In the isthmus of Tehuantepec (cross section AA' on Figure 2, Figure 3a), the seismicity defines a Wadati-Benioff zone dipping with 30° below the depth of 40 km. Towards the west (Figure 3b), the shape of the downgoing slab is shallower and the Wadati-Benioff zone dips with $\sim 25^\circ$. The seismicity on Figures 3c to 3g shows that the geometry of the downgoing slab is almost subhorizontal at Dt between 110 km to 275 km and at depths of about 50 km. The same results have been inferred for Guerrero (Figures 3f and 3g) by *Suárez et al.* [1990] and *Singh and Pardo* [1993]. There is a remarkable lack of seismic events beyond Dt > 300 km and depths > 70 km, north of 18°N . At the westernmost region of the Cocos plate (Figures 3h and 3i), the dip of the subducted slab increases to $\sim 30^\circ$ at depth greater than 40 km, from the almost subhorizontal geometry observed in the region of Guerrero (Figures 3c to 3g) to a similar dip as that observed on Figure 3a, near the TR.

On the Rivera plate subduction zone (Figures 3j-3k), the top of the Wadati-Benioff zone inferred from the hypocenters on Figure 3j also fits the seismicity to the west (Figures 3k and 3l). The dip of the downgoing slab changes rapidly from a dip of $\sim 30^\circ$ (Figure 3i) to one of $\sim 50^\circ$ at depths below 40 km in the Rivera plate.

A cross-section almost parallel to the trench, from (19°N , 106°W) to (15°N , 95°W), shows the variation in depth of the hypocenters within southern Mexico (Figure 4). For the Rivera plate, the maximum focal depth is 130 km below the Jalisco region. Towards the east, the maximum depth observed for earthquakes in the Cocos plate between the EG and the OFZ is 100 km. To the southeast, from the OFZ to the OGFZ, where a good coverage of local stations exists on the western part, the maximum observed focal depth is 70 km. From the OGFZ to the TR the maximum depth of earthquakes increases continuously down to 180 km.

Although there is no deep seismicity beneath and to the north of the volcanic belt, the geometry of the subducted slab may be inferred from the general trend of the subduction zone. Smooth contours to depth of the top of the Wadati-Benioff zone were obtained, using 2-D splines interpolation [*Smith and Wessel*, 1990], from the contours controlled by the hypocenters (Figure 5). To the west of 96°W , the 100 km depth contour of the slab is drastically shifted towards the west, beneath the volcanic belt. The interpolation of this

depth contour to that near 103°W, shows that the slab beneath the front of the TMVB would lie at depths of 80 to 100 km (Figure 5). This suggests that the TMVB is directly related with the subduction of the oceanic slab beneath the North American plate, and that the observed non-parallelism of the volcanic belt with the trench is mainly due to the geometry of the subducted plate.

FOCAL MECHANISMS AND STATE OF STRESS

In this study, we report 21 new focal mechanisms of earthquakes in southern Mexico occurring within the subducting Cocos plate (Appendix A and B). The lower hemispheric projection of the focal mechanisms obtained from the waveform inversion, reported in this study and in previous works in the area, are shown on Figure 6 and Appendix A. These focal mechanisms are also shown on lateral projection on the cross-sections (Figure 3). Due to the absence of seismic stations to the south and west and, to lesser extent, to the east of southern Mexico, the focal mechanisms reported from first motion P-waves are poorly constrained [e.g., *Burbaich et al.*, 1984]. Therefore, only one mechanism from first motion of P waves was used (event 67 on Appendix A; from *Pardo and Suárez*, 1993).

Analogous to the seismicity, the stress pattern observed along the subduction zone may be divided in zones parallel to the trench. (Figures 3 and 6) A shallow-depth zone close to the trench shows interplate thrust events followed by down-dip normal faulting events. Down-dip, a zone of low seismic activity is observed followed farther inland by an area of intraplate events showing normal faulting at distances from the trench of 150-250 km and depths greater than 50 km.

The thrust earthquakes are observed down to a maximum depth of ~30 km along the Cocos plate (events 50 and 172 on Appendix A, Figures 3d and 3i), and down to a maximum depth of ~40 km at the Rivera plate (event 92 on Appendix A, Figure 3j). Down-dip normal faulting events are observed near the coast beneath a sheet of compressional events, with depths ranging from 40 km to 50 km (events 47, 70, 158, 28, 152 and 67 on Appendix A, Figures 3b, 3d, 3e, 3f, 3h and 3j). This double zone in stress is probably associated to flexural stresses associated to the slab bending upward [*Suárez et al.*, 1990].

Intraplate normal faulting events, is observed farther inland in the deeper seismic zone (Figure 6). A lower intraplate seismicity is observed close to the Rivera-Cocos plate boundary (Figure 3i). The deepest intraplate earthquake is event 61 (Appendix A), located

under the Colima volcano (Figure 2 and 3j). This normal faulting event shows a lateral component of tension to the west [*Pardo and Suárez*, 1993].

Practically no crustal seismicity is observed in the overriding plate over the subducted Cocos plate (Figure 3). The few crustal microearthquakes on Figures 3e, 3f, and 3g, correspond to tensional events that suggest the overriding plate is under tensional stress regime in these regions, at Dt over than 150 km [*Singh and Pardo*, 1993]. In contrast, there is a relatively high crustal seismicity within the Jalisco region in western Mexico (Figures 2 and 3j-3l), suggesting that the deformation of the Jalisco block is greater than that observed in the North American plate over the Cocos plate [*Pardo and Suárez*, 1993].

The normal faulting events in the downgoing slab (Figure 6), show, in general, T-axes direction parallel to the gradient of the subducted oceanic plate (Figure 5). Only where the slab shows a rapid change in the dip the stress distribution is more complex (Figure 7).

DISCUSSION

Although the conditions controlling the geometry of subduction zones are still controversial, several authors have suggested that the principal factors affecting the geometry are the relative convergence rate in the subduction zone, the age of the slab, the absolute motion of the overriding plate, and the subduction of aseismic bathymetric features, like ridges or intraplate sea-mounts [*e.g.*, *Cross and Pilger*, 1982; *Jarrard*, 1986]. Except for the age of the slab, all of these parameters correlate negatively with the dip of the downgoing plate. Thus, young lithosphere is relatively more buoyant than old plates and subducts at lower dip angle.

Therefore, the general shape of the subducted plate in the case of southern Mexico should show a low dip angle because of its young age, moderate convergence rate, and rapid upper plate absolute motion toward the trench (Figure 1). The Cocos plate, east of TR, subducts beneath the Caribbean plate with a steep dip angle [*e.g.*, *Burbach et al.*, 1984], being 10 to 25 m.y. older than to the west of TR [*Couch and Woodcock*, 1981], and with relative low motion of the upper Caribbean plate towards the trench compared to the North American plate [*Gripp and Gordon*, 1990; Figure 1]. At the westernmost part of southern Mexico, the small Rivera plate also subducts with a steep dip angle that resembles the subduction observed beneath Central America [*Pardo and Suárez*, 1993, this study]. The parameters that affect the shape of the downgoing slab are similar between the Rivera and the Cocos subduction zone in southern Mexico, except for the slow convergence rate between the Rivera and North American plates (~ 2 cm/yr) [*DeMets and Stein*, 1990], relative to a

greater Cocos-North America convergence rate (~6 cm/yr) [DeMets *et al.*, 1990] (Figures 1 and 4), suggesting that this low rate possible become an important parameter affecting the steep geometry of the subducted Rivera plate.

Seismic and Tectonic Implications

No lateral changes are observed in the dip of the shallow interplate contact, at least down to depths of about 30 km (Figures 3 and 5). The depth extent and dip of the interplate contact does not exhibit any clear correlation with the age of the subducted plate and/or with the convergence velocity, or with the subduction of bathymetric features along the trench (Figures 3 and 5). Thus the different rupture modes and complexity of the seismic sources of large thrust earthquakes along the coupled interplate contact in southern Mexico [Singh and Mortera, 1991], is probably related to the variation in the strength of coupling along the plates interface due to other factors than the geometry of the subduction at the coupled interplate zone.

The maximum depth of the seismogenic zone can be estimated from the deepest depth of the underthrusting earthquakes [Suárez and Comte, 1993]. For the subduction of the Cocos plate in southern Mexico, this depth is about 30 km. A value similar to that reported by Suárez *et al.* [1990] and Pacheco *et al.* [1993]. This depth yields a seismogenic zone width of ~60 km. For the subduction of the Rivera plate, this maximum depth appears to be about 40 km based on the depth of the deepest thrust event, which has a rather high dip (34°) related to the steep subduction of the Rivera plate (Figure 3j; event 92 on Appendix A). Therefore, the width of the seismogenic zone of the Rivera plate is larger (~75 km) than that at the Cocos plate. Potentially, earthquakes of greater magnitude could be generated in the Rivera plate than in the Cocos plate interface with similar rupture length. Interestingly, the largest earthquake this century on the MAT, the 1932, Jalisco earthquake (Ms=8.2) [Eissler and McNally, 1984; Singh *et al.*, 1985] occurred in the Rivera plate interface.

The lateral variation in the dip angle of the subducted plate at depths greater than 40 km, and the seismicity pattern observed in the zone (Figure 3, 4 and 5), suggest that southern Mexico can be divided into four regions with different seismotectonic characteristics and bounded by the major bathymetric features subducted along the trench (Figures 5 and 8): 1) The Jalisco region, shows a steep subduction of the Rivera plate beneath North America and is bounded to the east by the subduction of the El Gordo graben. 2) The Michoacan region, is a transition zone between the steep subduction of the Rivera plate and the almost subhorizontal subduction to the east. It is bounded by the El Gordo graben to the west and by the Orozco fracture zone to the east. 3) The Guerrero region, shows an almost

subhorizontal geometry of the subducted Cocos plate, and is bounded by the Orozco and O'Gorman fracture zones. 4) The Oaxaca region, is a transition zone between the flat subduction geometry beneath Guerrero and the steep subduction geometry of the Cocos plate beneath the Caribbean plate towards the east. It is bounded by the O'Gorman fracture zone and the Tehuantepec ridge.

The remarkable absence of seismic events with depths greater than 70 km, north of $\sim 18^{\circ}\text{N}$ and of the TMVB, suggests that if the downgoing plate continues to subduct it loses its brittle characteristic and sinks aseismically into the mantle. Otherwise, it is possible that small events exist of magnitude that are too low to be detected by the poor seismic network coverage of the area that exists today.

The inferred 80-100 km depth contours of the downgoing slab appear to be beneath the front of the TMVB (Figure 5), confirming the association of this volcanic belt with the subduction of the oceanic plate beneath the North American plate. The broad zone of the TMVB and the actual position of the 100 km depth contour (Figure 5) support a proposed last migration of the volcanism toward the trench, since 5.3 m.y.b.p., based on radiometric ages of volcanic rocks [Delgado *et al.*, 1993]. Thus the observed non-parallelism of the TMVB with the trench is mainly due to the geometry of the subducted Rivera and Cocos plates in southern Mexico.

SUMMARY AND CONCLUSIONS

The shape of the subducted Rivera and Cocos plates beneath the North American plate in southern Mexico was determined using accurately located hypocenters of earthquakes within the zone. A total of 1101 microearthquake hypocenters from local networks and 207 relocated hypocenters of earthquakes recorded at teleseismic distances were used as the database. For 21 teleseismic events ($m_b > 5.0$), the source parameters were determined using a formal long-period body wave inversion [Nábelek, 1984]. In the relocation procedure [Dewey, 1971], the focal depth of these latter events was constrained by the inversion and used within the initial subset of events to generate the variance of the residuals at each teleseismic station, which were then applied to all the events in the relocalization scheme.

The subduction in southern Mexico may be approximated as a subhorizontal slab subducting beneath the North American plate, which is bounded at its edges by the steep subduction geometry of the Cocos plate beneath the Caribbean plate to the east, and the Rivera plate beneath the North American plate to the west. No lateral changes in the dip of

the coupled interplate zone are observed at depths of less than 30 km. The changes in dip of the downgoing slab geometry are observed once it is decoupled from the overriding plate. The maximum depth of the seismogenic interplate zone is ~30 km for the Cocos plate and ~40 km for the Rivera plate. Therefore, the width of the seismogenic zone of the Rivera plate is larger (~75 km) than that of the Cocos plate (~60 km).

Based on the observed seismicity, focal mechanisms, and the variations in dip of the subducted plate, southern Mexico can be divided into four regions with different seismotectonic characteristics. The boundaries of these regions appear to be correlated with the subduction of major bathymetric features. The changes in dip of the downgoing slab do not appear to take place on tear faults, suggesting that smooth contortions accommodate these dip changes. In the Rivera-Cocos boundary zone where a rapid change of the dip is observed, the available data is not sufficient to resolve whether a tear fault or a contortion may be the cause.

The inferred 80-100 km depth contours of the subducted plate appear to be beneath the front of the TMVB, suggesting there is a direct association of this volcanic belt with the complex subduction geometry of the subducted Rivera and Cocos plates beneath the North American plate in southern Mexico.

Acknowledgements. We thank the Servicio Sismológico-UNAM, the Instituto de Geofísica, Instituto de Ingeniería at UNAM, and Colima University for facilitating data. We are grateful to S.K. Singh and J. Pacheco for helpful discussions and revision of the manuscript. This research was partially supported by project UACPyP-UNAM 30309. One of us (MP) acknowledges support by the Secretaría de Relaciones Exteriores, México.

REFERENCES

- Allan, J.F., S.A. Nelson, J.F. Luhr, I.S.E. Charnichael, M. Wopat, and P.J. Wallace, Pliocene-Holocene rifting and associated volcanism in southwest Mexico, In: The Gulf and Peninsular provinces of the Californias, *Am. Ass. Petrol. Geol., Memoir 47*, Dauphin J. and Simoneit, Editors, 1991.
- Atwater, T., Implications of plate tectonics for the Cenozoic tectonic evolution of western North America, *Geol. Soc. Am. Bull.*, 81, 3513-3536, 1970.
- Bandy, W.L., Geological and Geophysical investigation of the Rivera-Cocos plate boundary: Implications of plate fragmentation, *Ph.D. Thesis, Texas A&M University, Colege Station, Texas*, 1992.
- Bandy, W.L. and C-Y. Yan, Present-day Rivera-Pacific and Rivera-Cocos relative plate motions, [abs.] *EOS, Trans. AGU*, 70, 1342, 1989.
- Bandy, W.L. and M. Pardo, Statistical examination of the existence and relative motions of the Jalisco and southern Mexico blocks, Submitted to *Tectonics*, 1993.
- Beck, M.E., Case for northward transport of Baja and coastal southern California. Palomagnetic data, analysis and alternatives, *Geology*, 19, 506-509, 1991.
- Bevis, M. and B.L. Isacks, Hypocentral trend surface analysis: Probing the geometry of Benioff zones, *J. Geophys. Res.*, 89, 6153-6170, 1984.
- Böhnel, H., D. Morán-Zenteno, P. Schaaf, and J. Urrutia-Fucugauchi, Paleomagnetic and isotope data from southern Mexico and the controversy over the pre-neogene position of Baja California, *Geofis. Intern.*, 31, 253-261, 1992.
- Bourgois, J. and F. Michaud, Active fragmentation of the North American plate at the Mexican triple-junction area off Manzanillo, *Geo-Marine Lett.*, 11, 59-65, 1991.
- Burbach, G., C. Frolich, W. Pennington and T. Matumoto, Seismicity and tectonics of the subducted Cocos plate, *J. Geophys. Res.*, 89, 7719-7735, 1984.
- Chael, E. P. and G.S. Stewart, Recent large earthquakes along the middle American trench and their implications for the subduction process, *J. Geophys. Res.*, 87, 329-338, 1982.
- Couch, R. and S Woodcock, Gravity and structure of the continental margins of southwestern Mexico and northwestern Guatemala, *J. Geophys. Res.*, 86, 1829-1840, 1981.
- Cross, R.H. and T.A. Pilger, Controls of subduction geometry, location of magmatic arcs, and tectonics of arc and back-arc regions, *Geol. Soc. Am. Bull.*, 93, 545-562, 1982.

- Cruz, M. and G. Suárez, Seismicity and tectonics in Oaxaca, Mexico, In Preparation, 1993.
- Dean, B.W. and C.L. Drake, Focal mechanism solutions and tectonics of the Middle America arc, *J. Geol.*, 86, 111-128, 1978.
- Demant, A. and C. Robin, Las fases del volcanismo en México; una síntesis en relación con la evolución geodinámica desde el Cretácico, *Rev. Inst. Geol., UNAM*, 75, 70-82, 1975.
- Delgado, H., P. Cervantes, and R. Molinero, Origen de la faja volcánica trans-mexicana hace 8.3 Ma y sus migraciones hacia el W, SW y SSW desde 5.3 Ma, [abs.] *GEOS, Unión Geofísica Mexicana*, 13, 31-32, 1993.
- DeMets, C. and S. Stein, Present-day kinematics of the Rivera plate and implications for tectonics in southwestern Mexico, *J. Geophys. Res.*, 95, 21, 931-21, 948, 1990.
- DeMets, C., R.G. Gordon, D.F. Argus, and S. Stein, Current plate motions, *Geophys. Res. J. Int.*, 101, 425-478, 1990.
- Dewey, J.W., Seismicity studies with the method of Joint Hypocenter Determination, *Ph.D. Thesis, University of California, Berkeley*, 1971.
- Eissler, H. and K.C. McNally, Seismicity and tectonics of the Rivera plate and implications for the 1932 Jalisco, Mexico, earthquake, *J. Geophys. Res.*, 89, 4520-4530, 1984.
- Gastil, R.G. and W. Jensky, Evidence for strike-slip displacement beneath the Trans-Mexican volcanic belt, *Stanford Univ. Publ. Geol. Sci.*, 13, 171-180, 1973.
- Gonzalez-Ruiz, J., Earthquake source mechanics and tectonophysics of the middle America subduction zone in Mexico, *Ph.D. Thesis, U. of California, Santa Cruz*, 1986.
- Gripp, A. and R. Gordon, Current velocities relative to the hotspots incorporating the NUVEL-1 global plate motion model, *Geophys. Res. Lett.*, 17, 1109-1112, 1990.
- Hanus, V. and J. Vanek, Subduction of the Cocos plate and deep active fracture zones of Mexico, *Geofís. Inter.*, 17, 14-53, 1978.
- Havskov, J., S.K. Singh and D. Novelo, Geometry of the Benioff zone in the Tehuantepec area in southern Mexico, *Geofís. Int.*, 21, 325-330, 1982.
- Isacks, B.L. and M. Barazangi, Geometry of Benioff zones: Lateral segmentation and downward bending of the subducted lithosphere, In: *Island arcs, Deep sea trenches, and back-arcs basins, Maurice Ewing Ser., vol. 1*, edited by M. Talwani and W. C. Pitmann III, pp. 99-114, AGU, Washington, D. C., 1977.
- Jarrard, R.D., Relations among subduction parameters, *Rev. of Geophys.*, 24, 217-284, 1986.

- Johnson, C.A. and C.G.A. Harrison, Tectonics and volcanism in central Mexico: A Landsat Thematic Mapper perspective, *Remote Sens. Envir.*, 28, 273-286, 1989.
- Karig, D.E., R.K. Cardwell, G.F. Moore, and D.G. Moore, Late Cenozoic subduction and continental margin truncation along the northern Middle America Trench, *Geol. Soc. Am. Bull.*, 89, 265-279, 1978.
- Kelleher, J. and W. McCann, Bouyant zones, great earthquakes, and unstable boundaries of subduction, *J. Geophys. Res.*, 81, 4885-4896, 1976.
- Klitgord, K. and J. Mammerickx, Northern East Pacific Rise: Magnetic anomaly and bathymetric framework, *J. Geophys. Res.*, 87, 6725-6750, 1982.
- Lee, W.H.K. and C. Valdes, HYPO71PC: A personal computer version of the HYPO71 earthquake location program, *Open-file Report 85-749, USGS*, 1985.
- LeFevre, L.V. and K.C. McNally, Stress distribution and subduction on aseismic ridges in the middle America subduction zone, *J. Geophys. Res.*, 90, 4495-4510, 1985.
- Luhr, J., S. Nelson, J. Allan, and I.S.E Charmichael, Active rifting in southwestern Mexico: Manifestations of an incipient east-ward spreading-ridge jump, *Geology*, 13, 54-57, 1985.
- Mammerickx, J., The morphology of propagating spreading centers: New and old, *J. Geophys. Res.*, 89, 1817-1828, 1984.
- Mammerickx, J. and K. Klitgord, Northern East Pacific Rise: Evolution from 25 m.y.B.P. to the present, *J. Geophys. Res.*, 87, 6751-6759, 1982.
- Molnar, P., Fault plane solutions of earthquakes and direction of motion in the Gulf of California and on the Rivera Fracture zone, *Geol. Soc. Am. Bull.*, 84, 1651-1658, 1973.
- Molnar, P. and L. R. Sykes, Tectonics of the Caribbean and Middle American region from focal mechanisms and seismicity, *Geol. Soc. Am. Bull.* 80, 1639-1684, 1969.
- Mooser, F., The Mexican volcanic belt: Structure and tectonics, *Geofis. Int.*, 12, 55-70, 1972.
- Nábelek, J.L., Determination of earthquake source parameters from inversion of body waves, *Ph.D. thesis, 346 pp., Mass. Inst. of Technol., Cambridge*, 1984.
- Nava, E., Estudio de los temblores de Ometepe del 7 de Junio de 1982 y sus replicas, *Thesis, Univ. Nacional Autónoma de México, México D.F.*, 1984.
- Nixon, G. T., The relationship between Quaternary volcanism in central México and the seismicity and structure of subducted oceanic lithosphere, *Geol. Soc. Am. Bull.*, 93, 514-523, 1982.
- Pacheco, J.F., L.R. Sykes, and C. H. Scholz, Nature of seismic coupling along simple plate boundaries of the subduction type, *J. Geophys. Res.*, 98, 14133-14159, 1993.

- Pardo, M. and G. Suárez, Steep subduction geometry of the Rivera plate beneath the Jalisco block in western Mexico, *Geophys. Res. Lett.*, 1993.
- Ponce, L., Gaulon, G. Suárez, and E. Lomas, Geometry and state of stress of the downgoing Cocos plate in the Isthmus of Tehuantepec, Mexico, *Geophys. Res. Lett.*, 19, 773-776, 1992.
- Reyes, A., J. Brune, and C. Lomnitz, Source mechanism and aftershock study of the Colima, Mexico earthquake of January 30, 1973, *Bull. Seismol. Soc. Am.*, 69, 1819-1840, 1979.
- Sansores, L., Sismicidad, esfuerzos y atenuación previos y posteriores al terremoto del 29-XI-1978, Oaxaca (Ms=7.8), *Thesis, Univ. Nacional Autónoma de México, Mexico D.F.*, 1990.
- Shurbet, D.H. and S.E. Cebull, Tectonic interpretation of the Trans-Mexican volcanic belt, *Tectonophys.*, 101, 159-165, 1973.
- Singh, S.K., L. Ponce, and S.P. Nishenko, The great Jalisco, Mexico, earthquake of 1932: Subduction of the Rivera Plate, *Bull. Seismol. Soc. Am.*, 75, 1301-1313, 1985.
- Singh, S.K., and F. Mortera, Source time functions of large Mexican subduction earthquakes, morphology of the Benioff zone, age of the plate, and their tectonic implications, *J. Geophys. Res.*, 96, 21487-21502, 1991.
- Singh, S.K. and M. Pardo, Geometry of the Benioff zone and state of stress in the overriding plate in Central Mexico, *Geophys. Res. Lett.*, 20, 1483-1486, 1993.
- Smith, W.H.F and P. Wessel, Gridding with continuous curvature splines in tension, *Geophysics*, 55, 293-305, 1990.
- Stoiber R.E. and M.J. Carr, Quaternary volcanic and tectonic segmentation of Central America, *Bull. Volcanol.*, 37, 304-325, 1973.
- Suárez, G. and S.K. Singh, Tectonic interpretation of the Trans-Mexican Volcanic Belt-Discussion, *Tectonophys.*, 127, 155-160, 1986.
- Suárez, G., T. Monfret, G. Wittlinger, and C. David, Geometry of subduction and depth of the seismogenic zone in the Guerrero gap, Mexico, *Nature*, 345, 336-338, 1990.
- Suárez, G., J.P. Ligorría, and L. Ponce, Preliminary crustal structure of the coast of Guerrero, Mexico, using the minimum apparent velocity of refracted waves, *Geofís. Int.*, 31, 247-252, 1992.
- Suárez, G. and D. Comte, Comment on "Seismic coupling along the Chilean subduction zone" by B.W. Tichelaar and L.R Ruff, *J. Geophys. Res.*, 98, 15825-15828, 1993.
- UNAM Seismology Group, The September 1985 Michoacan earthquakes: Aftershock distribution and history of rupture, *Geophys. Res. Lett.*, 13, 573-576, 1986.

- Valdés, C., R. Meyer, R. Zuñiga, J. Havskov, S.K. Singh, Analysis of the Petatlan aftershocks: Numbers, energy release and asperities, *J. Geophys. Res.*, 87, 8519-8529, 1982.
- Vogt, P.R., A. Lowrie, D. Bracey and R. Hey, Subduction of aseismic oceanic ridges: Effects on shape, seismicity, and other characteristics of consuming plate boundaries, *Geol. Soc. Am., Special Paper 172*, 1976.
- Zuñiga, F.R., C. Gutierrez, E. Nava, J. Lermo, M. Rodríguez and R. Coyoli, Aftershocks of the san Marcos earthquake of April 25, 1989 ($M_s=6.9$) and some implications for the Acapulco-San Marcos seismic potential, *Pure and Applied Geophys.*, 140, 287-300, 1993.

FIGURE CAPTIONS

Fig. 1. General tectonic setting of the studied zone, Rivera and Cocos plate subducted beneath the North American plate in southern Mexico. Five lithospheric plates are shown: Pacific, Rivera, Cocos, North America and Caribe. Relative convergence rates (cm/yr) between the oceanic and continental plates are indicated by open arrows, and absolute motion of the upper plates, North America and Caribe, relative to hotspots are shown by dashed arrows. EPR: East Pacific Rise; TFZ: Tamayo Fracture Zone; RFZ: Rivera Fracture Zone; OFZ: Orozco Fracture Zone; OGFZ: O'Gorman Fracture Zone; TR: Tehuantepec Ridge; MAT: Middle American Trench; JB: Jalisco Block; CG: Colima Graben; EG: El Gordo Graben. Solid triangles indicate Quaternary volcanism and the pattern region indicates the Trans Mexican Volcanic Belt zone (TMVB).

Fig. 2. Epicenters of the reliable located earthquakes in southern Mexico used in this study. Black dots indicate located from local data. Black squares indicate relocated with focal depth constrained by body-wave inversion [Nábelek, 1984]. Diamonds indicate relocated epicenter, with report of focal mechanism from wave-form modeling (large and dark diamonds), with focal mechanism from first motion P-waves (grey intermediate size diamonds), and without focal mechanism (open small diamonds). Relocated hypocenters were obtained from Joint Hypocenter Determination method [Dewey, 1971]. The position of the cross-sections, A-L, of Figure 3 are shown oriented on the relative convergence direction of Rivera and Cocos plates [DeMets and Stein, 1990, DeMets et al., 1990]. Volcanoes and labels as in Figure 1.

Fig. 3.- Hypocenters cross sections with origin at the trench and oriented in the convergence direction of Rivera and Cocos plates [DeMets and Stein, 1990, DeMets et al., 1990]. Hypocenter symbols as the epicenters on Figure 1. Focal mechanisms on lateral projection, blacks are from body-wave inversion (this study), dark grey are from wave-form modeling (reported) and the gray one on cross-section 3j is from first motion of P-waves. Numbers of the mechanisms are keyed to Appendix A. The downgoing plate interface, top of the Wadati-benioff zone, is shown on each cross-section with continuous line and dashed line where it is interpolated. At the top of cross-sections are projected the location of the Quaternary andesitic volcanoes, and the pattern indicate the TMVB zone.

Fig.4. (Top) Hypocenters cross-section almost parallel to the trench, from (19°N, 106°W) to (15°N, 95°W). Hypocenters symbols as on Figure 1. Jalisco, Michoacan, Guerrero and Oaxaca are the names of the segments along which southern Mexico can be separated based on the seismicity and the location at the trench of the bathymetric features: RFZ-EG, Rivera Fracture Zone-El Gordo Graben; OFZ, Orozco Fracture Zone; OGFZ, O'Gorman Fracture zone; TR, Tehuantepec Ridge. (Bottom) Solid circles: Age of the subducted slab at the trench in m.y.b.p. [Klitgord and Mammerrickx, 1982]. Solid squares: Convergence rate (cm/yr) at the trench [DeMets and Stein, 1990, DeMets *et al.*, 1990]. Also shown the projected location of the cross-sections, A-L, of Figures 2 and 3.

Fig. 5. Isodepth contours, each 20 km, to the top of the Wadati-Benioff zone of the subducted oceanic slab beneath the North American plate in southern Mexico. Dashed lines indicate interpolation of the contours where no hypocentral data were available. Hypocenter symbols, volcanoes and bathymetric features as in Figure 1. Along the MAT are shown the age (m.y.b.p.) of the oceanic slab, and in parentheses the convergence rate (cm/yr) .

Fig. 6. Focal mechanisms on lower hemispheric projection. Blacks are from body-wave inversion (this study) and greys are reported from wave-form modeling. P and T axes are shown as black and white dots respectively. Numbers are keyed to Appendix A.

Fig. 7. T-axes direction from the tensional earthquakes obtained from wave-form modeling; blacks arrows are from focal mechanisms of this study and dark greys arrows are from reported focal mechanisms. Only one mechanism from first motion of P-wave is shown with grey at the Rivera subduction zone. The Middle American Trench (MAT) and the depth contours of Figure 5 are shown.

Fig. 8. Cross-sections within the proposed regions of southern Mexico. The regions are as in Figure 4. The seismicity and the plate interface geometry are superposition of the cross-sections of Figure 3 and labeled with the same letters. At the bottom is shown the shape of the subduction, top of the Wadati-Benioff zone, of each region in southern Mexico.

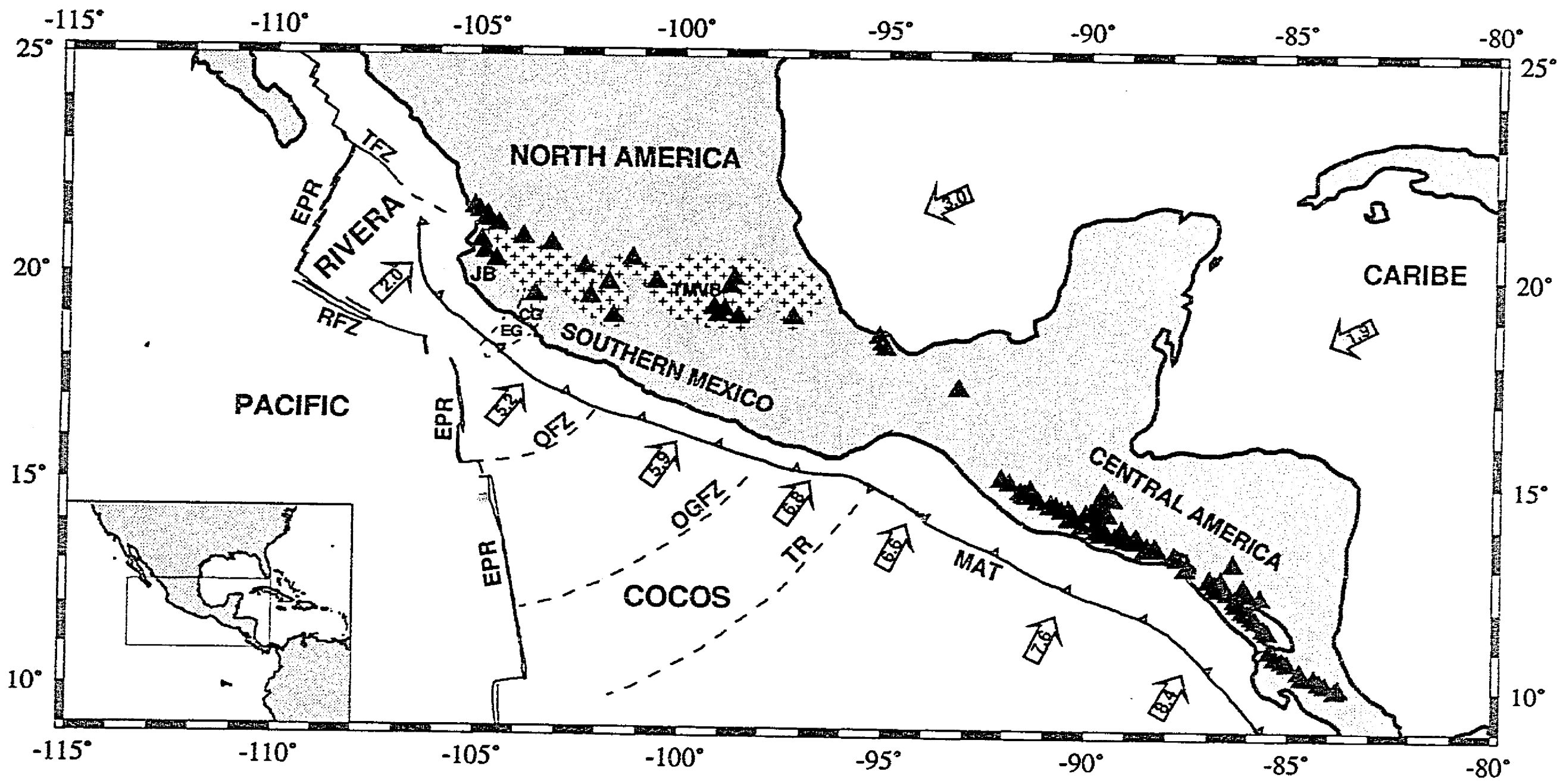


Fig. 1

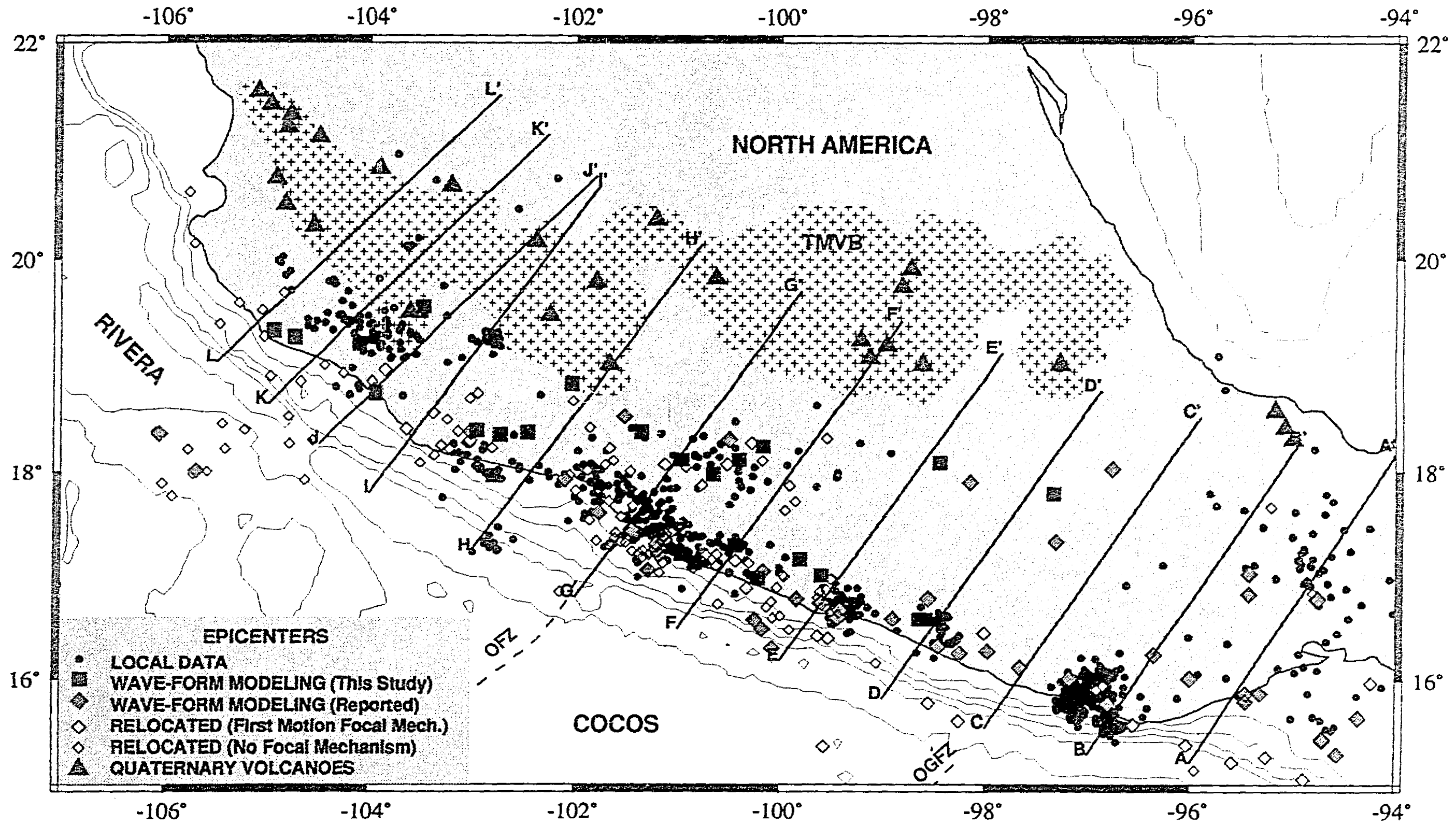


Fig. 2

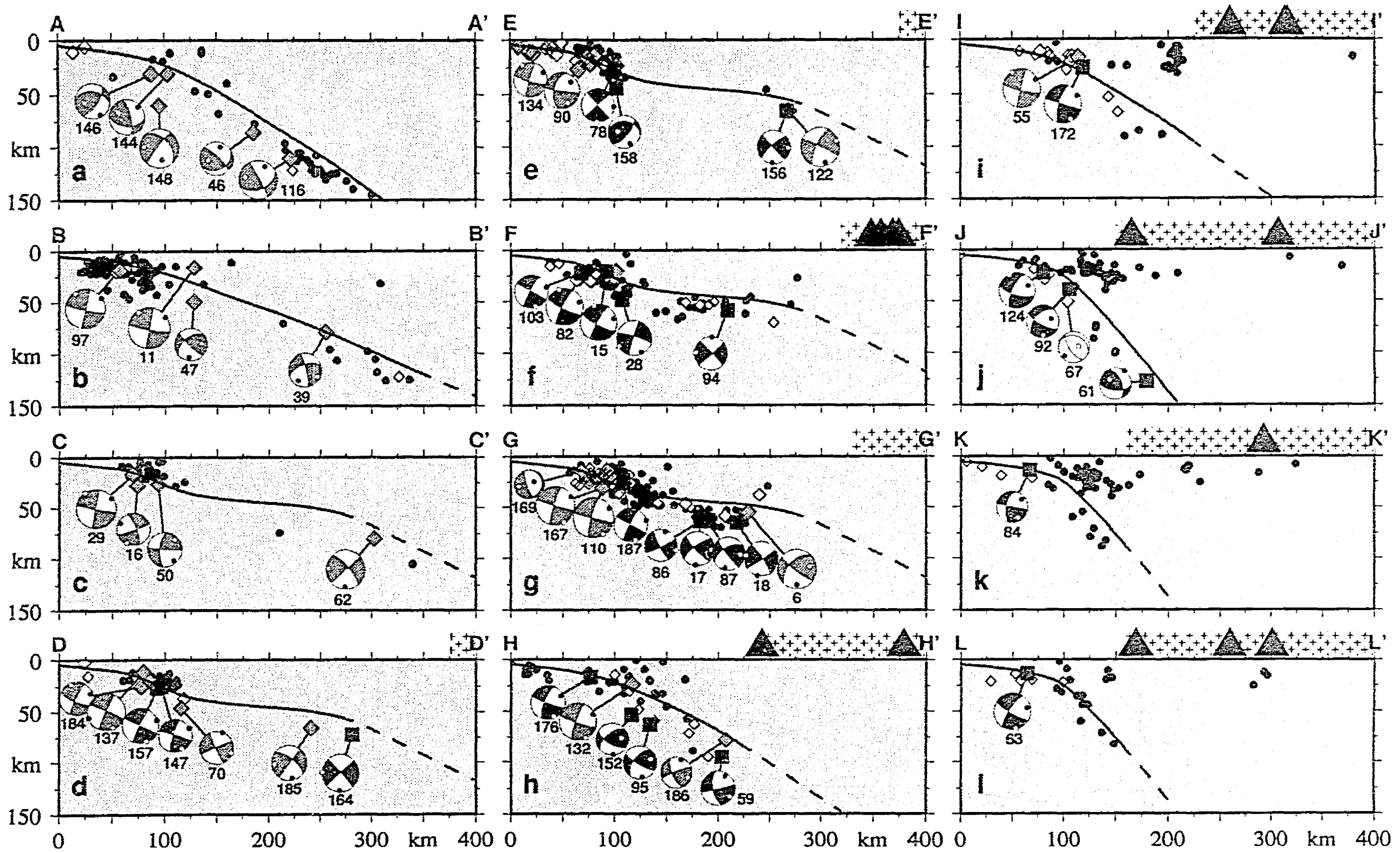


Fig. 3

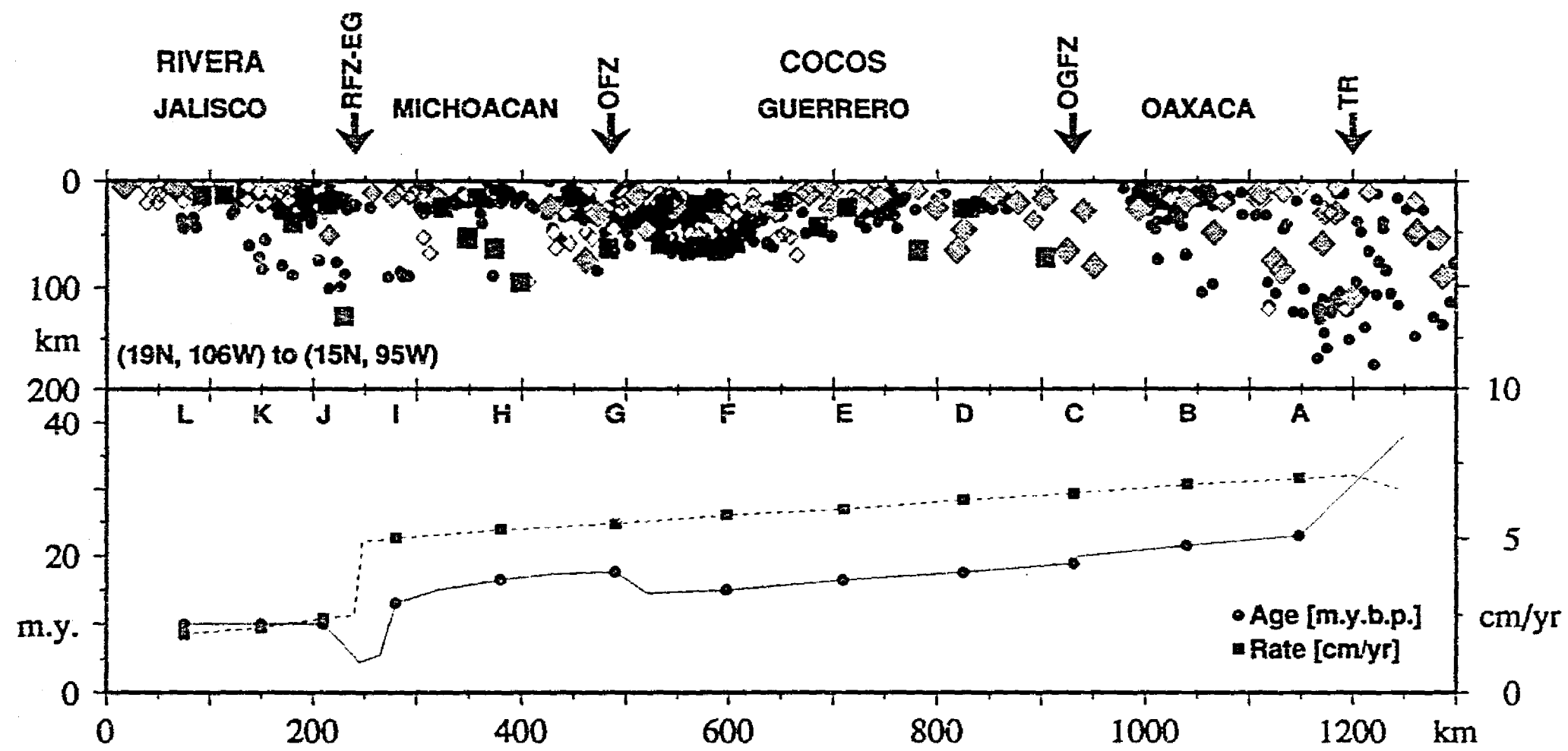


Fig. 4

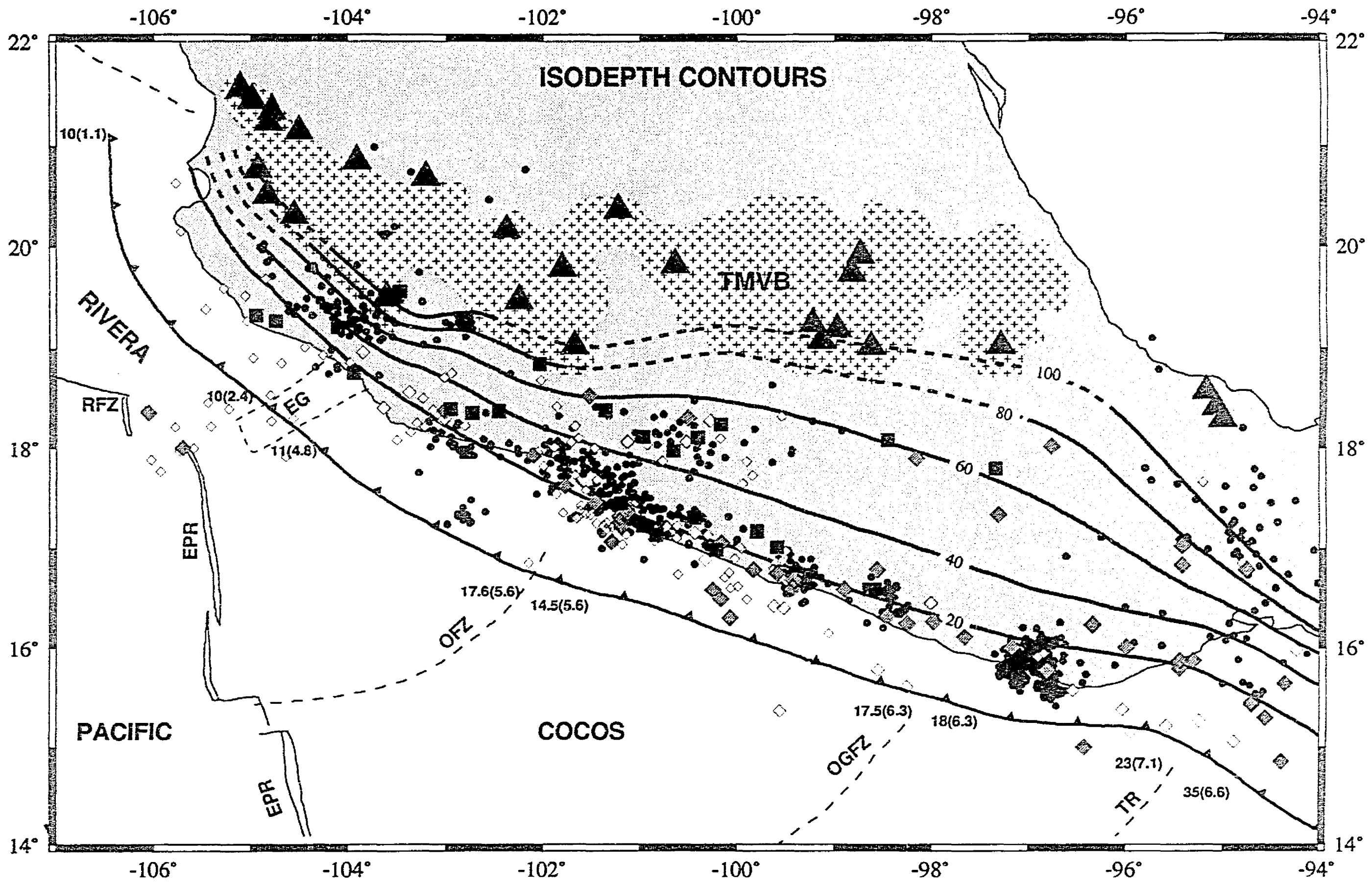


Fig. 5

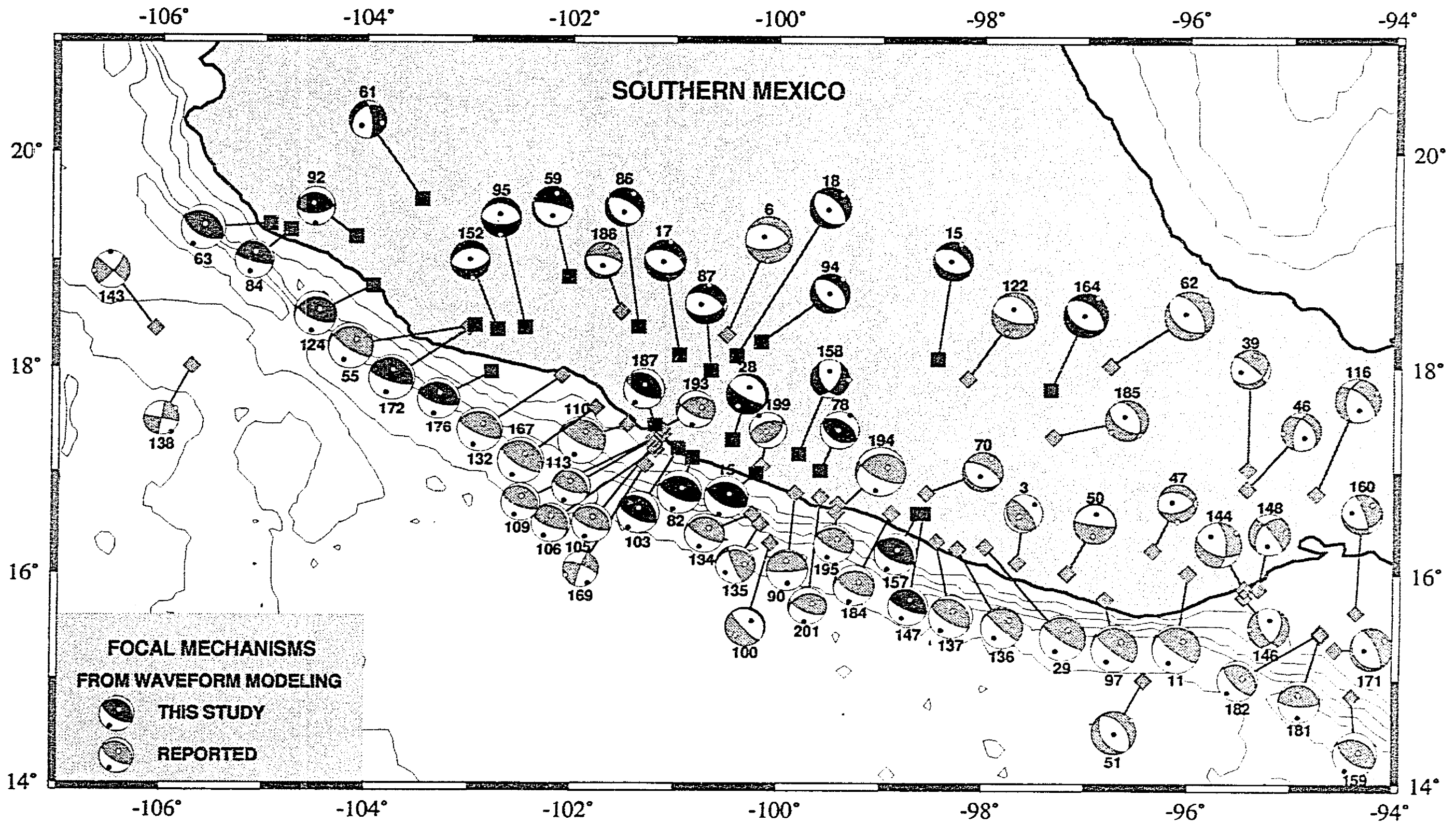


Fig. 6

EVERY TIME TO BE
 FROM THE RELATION

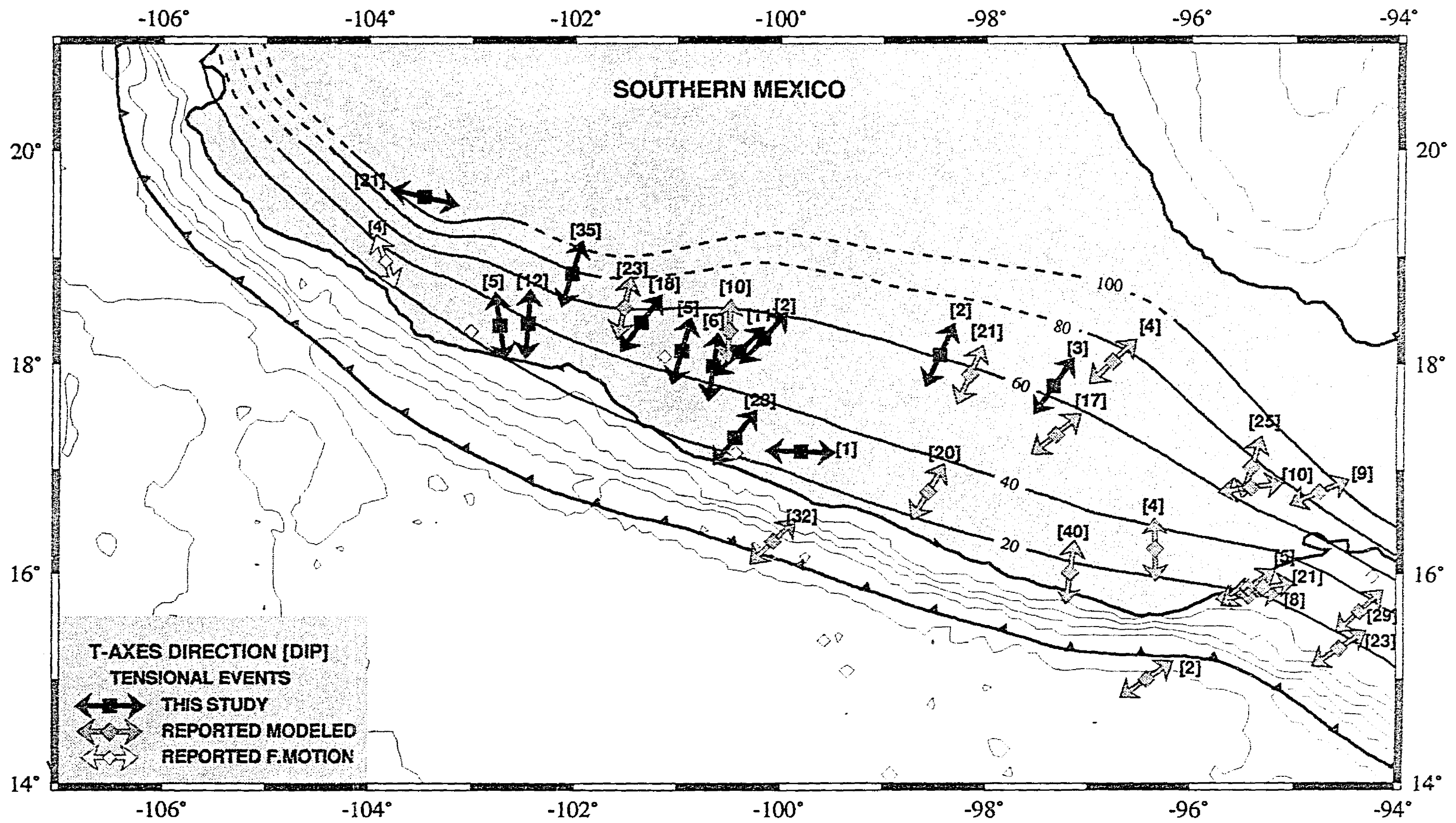


Fig. 7

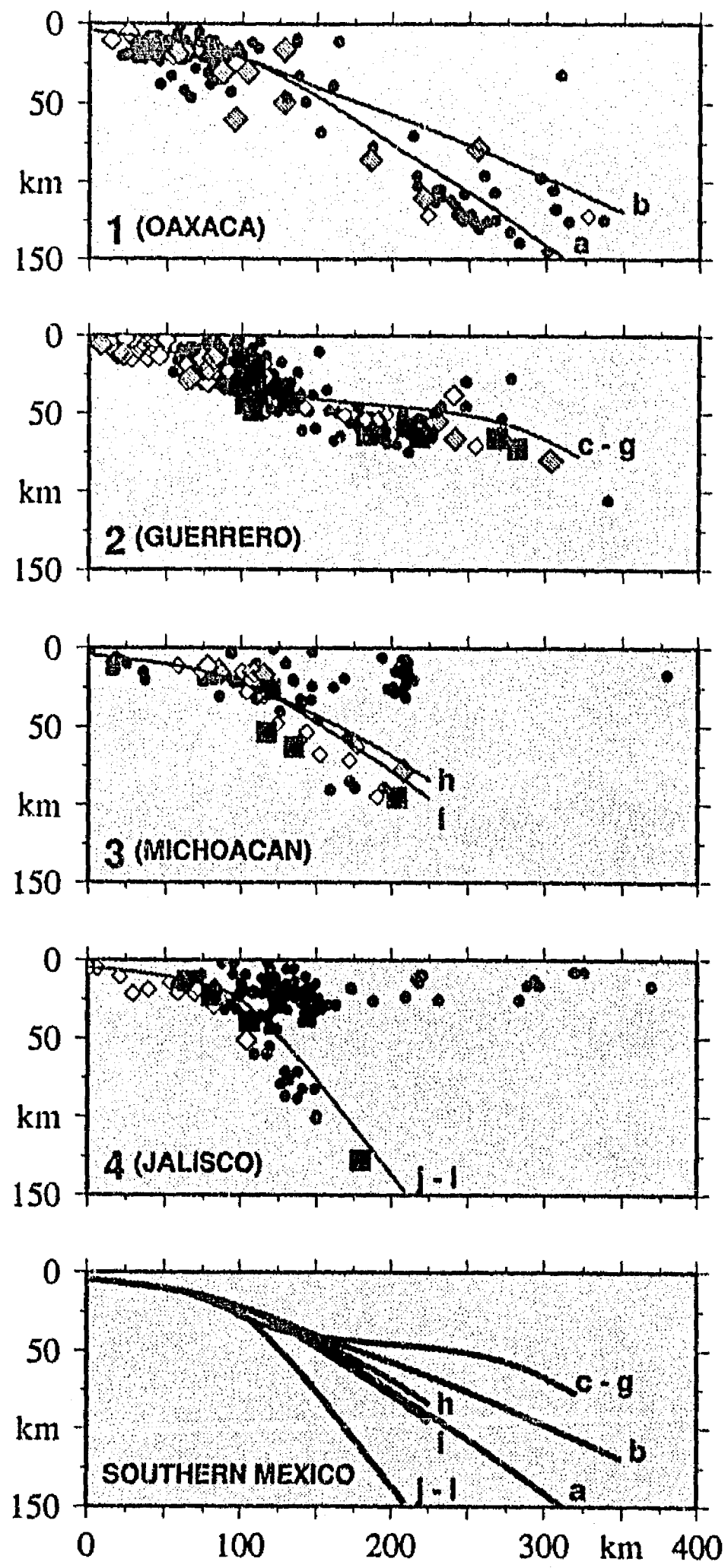


Fig. 8

APPENDIX A. *Relocated hypocenters and source parameters.*

Relocated hypocenters determined using the Joint Hypocenter Determination method [Dewey, 1971], with focal depth constrained from a formal body-wave inversion [Nábelek, 1984] for a subset of 26 events [Pardo and Suárez, 1993; This study]. Calibration events for different regions in southern Mexico and data used in the relocalization procedure are discussed in the text.

The catalog is not complete in time and magnitude, it include only the hypocentral locations that are considered reliable.

TABLE A1. Relocated Hypocenters and Source Parameters Used in this Study

N	DATE	TIME	LAT °N	LON °W	D km	m_b	Mo 10^{18} N-m	ϕ°	δ°	λ°
1	640227	113535.7	18.863	103.970	24.6	4.7				
2	640321	150811.2	18.503	103.228	16.0	5.1				
3	640402	015238.0	16.117	97.657	27.7	5.3		320	70	90 ^a
4	640604	042850.6	17.037	101.175	15.0	5.2				
5	640620	171217.1	18.463	105.440	5.0	5.0				
6	640706	072211.7	18.31	100.50	55.0	6.3	115.0 ^b	292	38	-63 ^b
7	641114	125246.4	18.002	105.589	9.0	5.1				
8	641225	162955.6	17.576	101.552	28.0	4.8				
9	650202	043032.7	16.846	94.797	121.8	5.2				
10	650403	112043.5	15.608	98.249	7.9	5.5		310	10	90 ^c
11	650823	194602.5	16.016	95.995	16.0	6.6		268	14	54 ^d
12	650824	010058.7	15.570	96.539	20.0	5.6		293	10	90 ^c
13	650924	171354.1	20.153	105.719	14.0	4.6				
14	650926	003618.3	18.004	101.459	46.0	4.7				
15	651209	060743.7	16.982	100.215	20.3	5.9	3.720 ^e	280	31	76 ^e
16	660402	015238.0	16.117	97.657	29.7	5.3				
17	660925	060226.4	18.119	100.958	59.3	5.6	0.612 ^e	290	50	-84 ^e
18	670413	195948.9	18.116	100.401	64.7	5.6	0.225 ^e	314	56	-92 ^e
19	670414	051830.9	17.156	100.431	23.0	5.0		160	48	-106 ^f
20	670607	070627.5	16.709	100.128	6.0	4.7				
21	670626	022234.4	18.226	105.410	5.0	5.3				
22	671015	183548.5	17.430	101.054	26.0	4.5				
23	680120	214110.0	16.037	105.500	10.0	4.8				
24	680203	053613.8	16.401	99.519	2.5	5.6		358	68	169 ^g
25	680426	174801.5	18.567	103.367	16.0	5.5		297	21	73 ^g
26	680510	092511.4	18.041	100.916	53.9	4.7				
27	680630	202128.5	17.766	105.935	5.0	4.8				
28	680702	034448.9	17.300	100.437	48.1	5.7	2.930 ^e	330	19	-61 ^e
29	680802	140641.7	16.273	97.976	16.0	6.3		287	12	76 ^d
30	680814	083846.9	18.306	103.008	20.0	5.7		318	84	-40 ^g
31	680816	182555.3	16.451	98.006	37.2	5.3		284	8	90 ^g
32	680816	212443.1	18.284	103.039	28.0	4.9				
33	681101	035553.2	18.220	105.778	13.0	4.7				
34	681128	103607.1	15.051	94.882	18.8	5.6		322	9	117 ^g
35	690430	150437.0	18.934	104.255	18.5	4.8				

36	690623	070829.3	18.304	104.564	11.0	5.5				
37	690831	234625.4	17.308	101.632	13.0	5.1				
38	690915	124723.6	17.683	101.437	18.0	5.0				
39	691020	152036.7	17.027	95.418	75.5	5.4		311	76	-60 ^a
40	700204	050846.7	15.364	99.561	8.0	5.9		21	80	-10 ^g
41	700710	131448.2	17.254	101.225	22.0	5.1				
42	700827	194440.0	15.135	95.947	5.1	5.4				
43	700907	180832.5	19.523	105.062	19.5	5.1				
44	710126	185901.4	18.714	103.013	53.3	4.8				
45	710205	052905.2	18.907	104.978	10.0	4.7				
46	710319	061233.7	16.831	95.425	85.1	5.4		320	44	-137 ^a
47	710716	214027.6	16.238	96.339	49.3	5.3		290	45	-60 ^a
48	711027	214916.9	18.068	100.516	58.7	5.0		326	60	-90 ^h
49	720102	215658.8	15.780	98.547	1.6	5.5		328	15	90 ^h
50	720708	121052.5	16.015	97.167	26.6	5.6		278	5	-90 ^a
51	720916	091432.5	14.994	96.422	9.1	6.0	2.57 ^a	320	47	-97 ^a
52	721110	145650.4	15.378	96.032	10.0	5.4		291	22	90 ^g
53	721113	044343.3	15.262	95.249	10.0	5.6		360	8	150 ^g
54	730122	003758.7	18.401	105.225	5.0	5.6				
55	730130	210113.9	18.383	103.004	16.7	6.1		266	17	55 ^d
56	730210	115328.1	18.410	103.631	11.0	5.6		246	16	39 ^g
57	730510	175055.9	18.860	104.683	18.6	5.1				
58	730521	152509.9	16.424	99.620	13.3	4.9		11	30	180 ^h
59	730703	035950.3	18.848	102.034	94.9	5.6	0.805 ^e	281	80	-98 ^e
60	730716	181255.8	17.093	100.841	29.3	5.6		303	10	90 ^f
61	730729	161633.7	19.563	103.466	127.4	5.0	0.527 ⁱ	352	71	-119 ⁱ
62	730828	095041.0	18.026	96.755	80.0	6.6	41.00 ^b	326	50	-76 ^b
63	731018	104939.0	19.337	104.945	13.5	6.0	1.200 ⁱ	296	33	86 ⁱ
64	731019	004953.2	19.281	105.035	14.1	4.9				
65	731108	131810.5	17.868	99.908	53.4	5.1				
66	731210	165533.8	17.885	106.028	5.5	4.8				
67	740126	053546.3	18.966	103.843	50.8	5.2		35	65	-145 ⁱ
68	740325	073709.6	18.088	103.491	11.0	4.7				
69	740625	084443.2	15.214	95.586	5.0	5.4		304	10	90 ^g
70	740718	192125.7	16.788	98.552	46.3	5.5		300	65	-90 ^a
71	740812	212712.9	17.213	100.715	23.6	5.0				
72	750222	004720.6	17.105	100.620	32.0	5.3				
73	750303	061909.7	17.229	101.260	16.1	4.5				
74	750411	193738.0	18.233	102.801	14.4	4.8				
75	750423	111450.1	16.156	99.055	15.7	5.9 ^o				
76	750625	055914.3	19.694	104.848	22.2	4.8				
77	750819	145714.1	15.977	94.233	90.8	5.6		320	80	-90 ^f
78	751029	045359.0	17.009	99.588	24.9	5.3	0.064 ^e	305	49	93 ^e
79	760201	111454.6	16.889	100.324	30.3	5.8		280	62	90 ^j
80	760307	214841.3	18.800	103.954	29.6	4.9				
81	760413	201748.5	18.537	104.798	5.0	5.3				
82	760607	142635.9	17.137	100.826	21.1	6.0	4.030 ^e	281	28	79 ^e
83	760701	213912.5	18.275	104.788	10.0	4.9				
84	760717	090212.8	19.280	104.744	13.3	5.2	0.059 ⁱ	311	12	115 ⁱ
85	760813	230440.6	17.335	101.554	24.3	4.6				
86	760905	201134.5	18.384	101.356	63.3	5.3	0.169 ^e	297	64	-102 ^e
87	760919	205805.6	17.975	100.652	62.3	5.5	0.209 ^e	295	54	-66 ^e
88	770418	185652.1	18.230	101.662	71.6	5.1				
89	780121	224026.7	18.165	103.353	14.5	4.8				
90	780319	013912.6	16.788	99.833	26.8	5.7	8.870 ^k	279	10	102 ^k
91	780326	195717.7	17.725	99.847	53.8	4.7				

92	780425	125610.3	19.219	104.100	38.8	5.3	0.060 ^e	282	34	105 ⁱ
93	780426	032820.1	16.870	99.537	22.9	5.0				
94	780705	201515.8	18.244	100.166	58.5	5.4	0.211 ^e	311	47	-92 ^e
95	780929	162137.3	18.380	102.464	62.8	5.4	0.196 ^e	281	33	-80 ^e
96	781004	055611.2	18.323	99.542	70.4	4.8				
97	781129	195249.0	15.770	96.800	18.0	6.3	527.0 ^k	270	14	54 ^d
98	781129	200446.3	15.908	96.901	16.0	5.2				
99	781129	204949.4	15.942	96.839	15.0	5.7				
100	781211	020756.7	16.307	100.069	5.0	5.4	0.264 ^k	306	13	-100 ^k
101	781211	024721.5	16.487	99.902	8.4	4.9				
102	781212	051424.2	16.605	100.065	5.8	4.9				
103	790126	100429.8	17.223	100.961	22.3	5.8	7.610 ^e	308	29	99 ^e
104	790126	120433.1	17.262	101.152	22.9	4.6				
105	790126	171041.4	17.257	101.200	19.5	5.4	0.574 ^k	302	22	99 ^k
106	790126	201735.7	17.213	101.185	20.3	5.4	0.239 ^k	319	21	117 ^k
107	790129	182147.8	17.314	101.225	24.7	5.2				
108	790129	182930.7	17.312	101.192	22.8	5.0				
109	790228	201016.0	17.315	101.203	19.8	5.2	0.493 ^k	303	22	101 ^k
110	790314	110711.0	17.454	101.455	13.6	6.5	270.0 ^d	293	14	87 ^d
111	790314	120118.8	17.371	101.611	21.2	5.5				
112	790314	153538.1	17.424	101.603	21.1	5.1				
113	790318	201230.9	17.356	101.120	25.1	5.3	0.332 ^k	316	27	116 ^k
114	790320	002751.3	17.245	101.442	16.9	5.0				
115	790322	122310.2	17.542	101.856	27.3	5.1				
116	790622	063056.0	16.787	94.751	110.0	6.2	29.20 ^k	310	62	-129 ^k
117	790826	210121.0	18.422	101.853	62.8	4.6				
118	800104	124648.0	17.291	101.227	22.4	5.1				
119	800121	131029.0	16.760	100.081	7.8	4.8				
120	800519	023437.5	17.252	101.335	20.8	5.0				
121	800531	194442.1	17.218	100.615	18.0	4.8				
122	801024	145335.7	17.901	98.152	65.4	6.3	64.90 ^k	311	26	-66 ^k
123	810207	053715.2	20.637	105.769	25.5	4.6				
124	810309	223853.0	18.762	103.935	22.4	5.9	0.644 ⁱ	260	28	60 ⁱ
125	810522	143002.0	19.396	105.463	21.1	4.8				
126	810522	143007.2	19.594	105.279	21.0	4.8				
127	810726	051424.8	17.965	102.051	48.6	5.4				
128	810801	111958.4	16.855	99.603	14.6	5.1				
129	810907	021157.0	17.000	99.955	16.8	4.5				
130	810917	095032.8	16.672	99.490	22.2	5.5				
131	811002	230044.3	17.918	104.637	10.0	5.2				
132	811025	032214.7	17.928	102.101	24.0	6.1	70.00 ^k	287	20	82 ^k
133	811101	231831.8	17.824	101.993	30.8	5.3				
134	820102	033054.4	16.589	100.248	12.0	5.4	0.202 ^k	275	18	68 ^k
135	820102	070552.0	16.495	100.166	11.0	5.3	0.074 ^k	271	24	26 ^k
136	820607	065235.8	16.253	98.245	20.0	5.8	29.00 ^k	268	10	48 ^k
137	820607	105939.0	16.324	98.453	11.4	6.0	20.9 ^l	315	24	103 ^l
138	820818	035822.0	18.011	105.697	5.0	4.9	0.153 ^k	281	90	180 ^k
139	820830	023255.4	16.853	102.143	8.0	4.9				
140	820930	060820.7	17.223	101.374	15.4	4.8				
141	821006	195048.1	17.189	101.338	11.0	5.0				
142	821025	145632.0	18.379	106.090	5.0	5.1				
143	821025	155520.5	18.361	106.057	5.0	5.1	0.114 ^k	311	89	169 ^k
144	830124	081741.3	15.873	95.448	60.0	6.3	20.60 ^k	110	54	-145 ^k
145	830125	203600.1	17.014	99.971	15.7	4.7				
146	830205	234104.7	15.795	95.449	30.0	5.6	0.11 ^a	150	59	-125 ^a
147	830207	115447.2	16.591	98.576	25.4	5.5	0.143 ^e	310	17	106 ^e

148	830222	093645.6	15.873	95.309	30.0	5.6	0.346 ^k	217	44	-18 ^k
149	830311	030549.7	19.014	104.443	21.4	4.8				
150	830527	062645.4	16.971	99.498	21.7	4.8				
151	830913	021930.9	17.873	100.763	51.1	5.1				
152	831208	102155.4	18.359	102.729	53.7	5.3	0.369 ^e	262	40	-90 ^e
153	831231	110209.8	17.293	101.649	28.5	4.6				
154	840128	192325.2	17.130	100.302	28.4	5.0				
155	840407	194311.1	16.623	99.992	10.9	4.9				
156	840604	043404.9	18.083	98.450	65.6	5.4	0.123 ^e	302	48	-79 ^e
157	840702	045042.8	16.592	98.638	26.5	5.8	1.630 ^e	302	26	94 ^e
158	840714	210347.6	17.168	99.802	43.8	5.3	0.172 ^e	31	55	-47 ^e
159	841013	171814.3	14.847	94.387	12.0	6.0	1.11 ^l	291	35	76 ^l
160	841219	085003.4	15.644	94.356	90.8	5.5	0.099 ^k	340	80	-62 ^k
161	850210	213749.8	18.761	102.938	67.3	4.8				
162	850310	082905.9	16.282	105.288	5.0	4.6				
163	850528	192750.9	18.687	102.020	94.4	5.1				
164	850915	075756.0	17.795	97.335	72.4	6.0	0.987 ^e	309	48	-85 ^e
165	850919	182936.3	18.066	101.703	48.6	5.1				
166	850920	033457.2	17.348	101.784	26.1	4.7				
167	850921	013713.5	17.621	101.765	31.1	6.3	249.0 ^k	296	17	85 ^k
168	850924	070317.4	18.011	101.877	59.0	4.5				
169	850928	035244.2	17.067	101.286	14.2	4.9	0.129 ^k	291	72	-176 ^k
170	860207	212651.7	17.730	101.665	37.3	5.0				
171	860407	224331.8	15.288	94.560	54.7	5.8	0.252 ^k	130	23	-112 ^k
172	860430	070723.1	18.396	102.950	26.0	6.1	14.70 ^e	303	16	105 ^e
173	860430	080903.1	18.221	103.213	15.0	4.9				
174	860430	081256.3	18.280	103.011	15.0	4.8				
175	860502	084705.5	18.388	103.128	15.3	4.9				
176	860505	054634.7	17.963	102.788	16.6	5.6	0.800 ^e	288	21	91 ^e
177	860506	131641.1	18.257	103.291	12.0	4.8				
178	860603	205512.3	17.973	105.731	10.0	4.9				
179	860611	213949.0	18.280	100.280	38.0	4.9	.002 ^m	201	54	-66 ^m
180	860619	043944.3	18.107	101.626	54.6	5.1				
181	870312	121814.7	15.422	94.702	47.8	5.7	1.510 ^k	281	19	98 ^k
182	870315	051120.0	15.444	94.703	51.1	5.5	0.746 ^k	297	24	73 ^k
183	870326	183828.4	16.892	100.027	19.2	4.7				
184	870607	133015.3	16.595	98.893	25.0	5.5	0.108 ^k	263	30	58 ^k
185	870715	071615.2	17.334	97.310	66.1	5.8	1.310 ^a	338	42	-65 ^a
186	870726	002242.2	18.530	101.520	74.1	5.0	0.055 ^k	280	68	-93 ^k
187	880208	135129.7	17.447	101.194	22.3	5.5	0.645 ^e	309	28	100 ^e
188	880529	061139.4	18.101	100.171	50.7	4.5				
189	880901	165249.7	16.704	99.539	18.2	5.0				
190	880908	111312.1	16.740	100.598	12.8	4.6				
191	880926	201200.8	17.134	101.138	24.2	5.0				
192	890309	101043.1	17.641	99.948	51.0	4.5				
193	890310	051950.4	17.411	101.128	26.6	5.2	0.135 ^k	251	35	47 ^k
194	890425	142900.2	16.606	99.426	15.5	6.8	12.3 ^l	255	29	51 ^l
195	890502	093017.6	16.680	99.415	14.6	5.4	0.22 ^l	286	19	79 ^l
196	890706	232101.7	17.327	101.506	19.0	4.8				
197	890812	153147.5	18.066	101.125	47.0	5.3	.085 ^m	270	71	-90 ^m
198	890817	005360.0	16.993	100.186	18.9	4.9				
199	891008	223238.1	17.055	100.165	20.0	5.0	0.047 ^k	252	50	106 ^k
200	891109	083640.4	16.795	99.620	23.5	5.1				
201	900113	020726.6	16.754	99.586	21.4	5.3	0.100 ^k	253	34	54 ^k
202	900511	234349.4	17.120	100.807	21.0	5.3	.088 ^m	317	19	100 ^m
203	900519	133735.8	17.211	101.279	21.3	5.0				

204	900531	073527.5	17.156	100.815	22.7	6.0	.600 ^m	317	19	100 ^m
205	900710	064449.3	16.746	99.619	13.8	4.5				
206	910725	152531.2	17.661	95.206	121.9	5.4				

References a, b, d, e, i, k and l report parameters from waveform modelling. Others, report focal mechanism from first motion of P waves.

- a Cruz and Suárez [1993]
- b Gonzalez-Ruiz [1986]
- c Molnar and Sykes [1969]
- d Chael and Stewart [1982]
- e This study
- f Lefevre and McNally [1985]
- g Dean and Drake [1978]
- h Molnar [1973]
- i Pardo and Suárez [1993]
- j Burbach et al. [1984]
- k Harvard Centroid Moment Tensor Solution Catalog
- l Pacheco et al. [1993]
- m Singh and Pardo [1993]

APPENDIX B. *Focal parameters determined in this study*

The parameters of the best fitting double-coupled point source of 21 events (Reference (e) on Appendix A) were determined using a formal inversion of long-period teleseismic P, SV and SH waveforms [Nábelek, 1984]. In each iteration we solve for the focal mechanism, centroid depth, seismic moment and source time function. For the less reliable solutions, the resulting uncertainties are within $\pm 10^\circ$ for the fault strike, dip and rake, ± 5 km for the centroid depth and $\pm 20\%$ for the seismic moment. Seismograms from the Global Digital Seismograph Network (GDSN) were used for the event that occurred before 1980, and from the World Wide Standardized Seismograph Network (WWSSN) for the events prior this date. The magnitude of all the events is within $5.0 \leq m_b \leq 6.1$ and a point source was used in all the inversions.

Figures B1 to B7 shows the results of the long-period body wave inversion determined in this study. Focal mechanisms in lower hemispheric projection showing observed (continuous line) and synthetic (dashed line) waveforms of: P-wave (Top), SV-wave (Middle) and SH-wave (Bottom). At the top are also shown the source time function and the date of the event. At the lower left bottom is shown the determined centroidal depth and at the right bottom the number of the event, keyed to Appendix A.

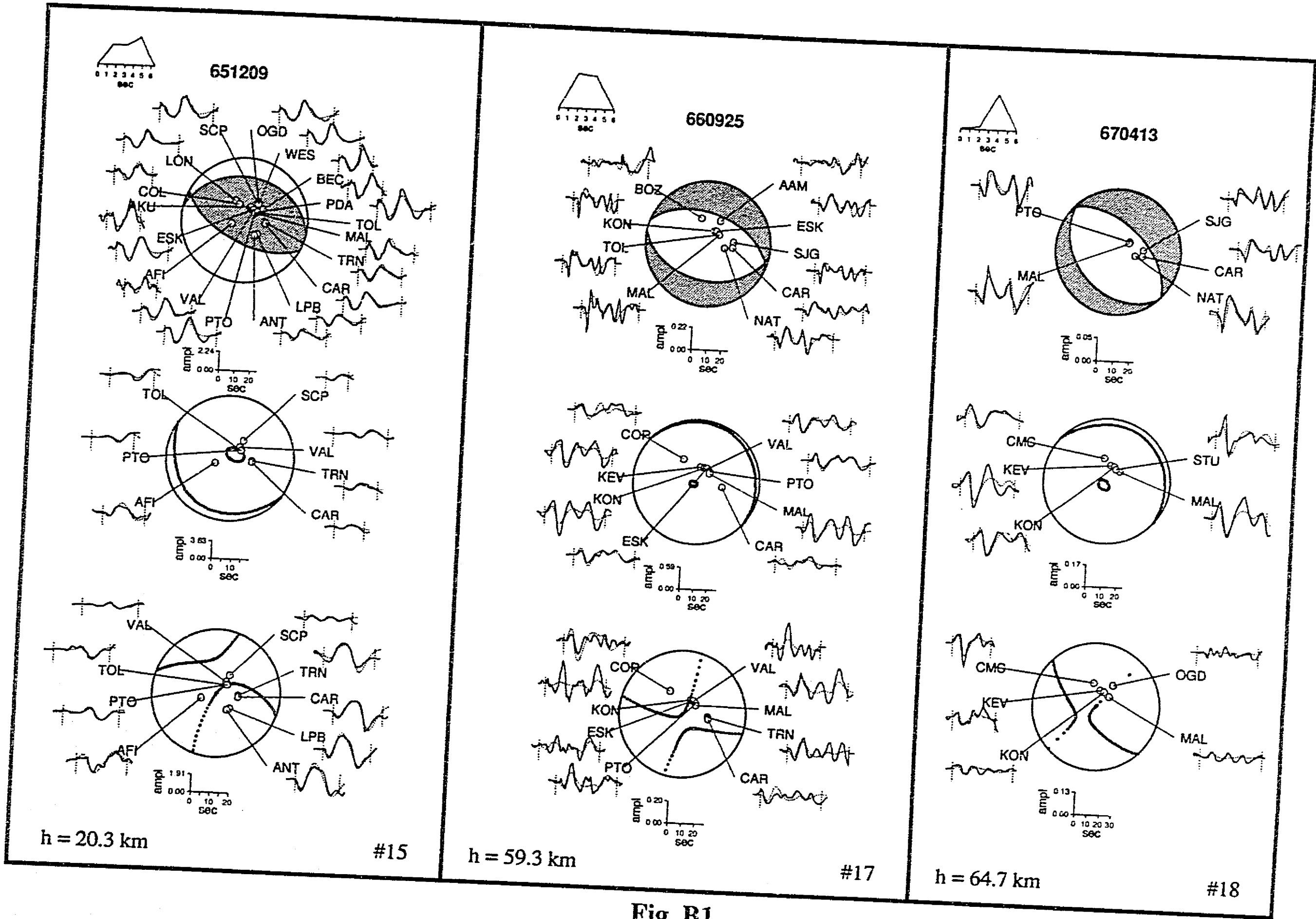


Fig. B1

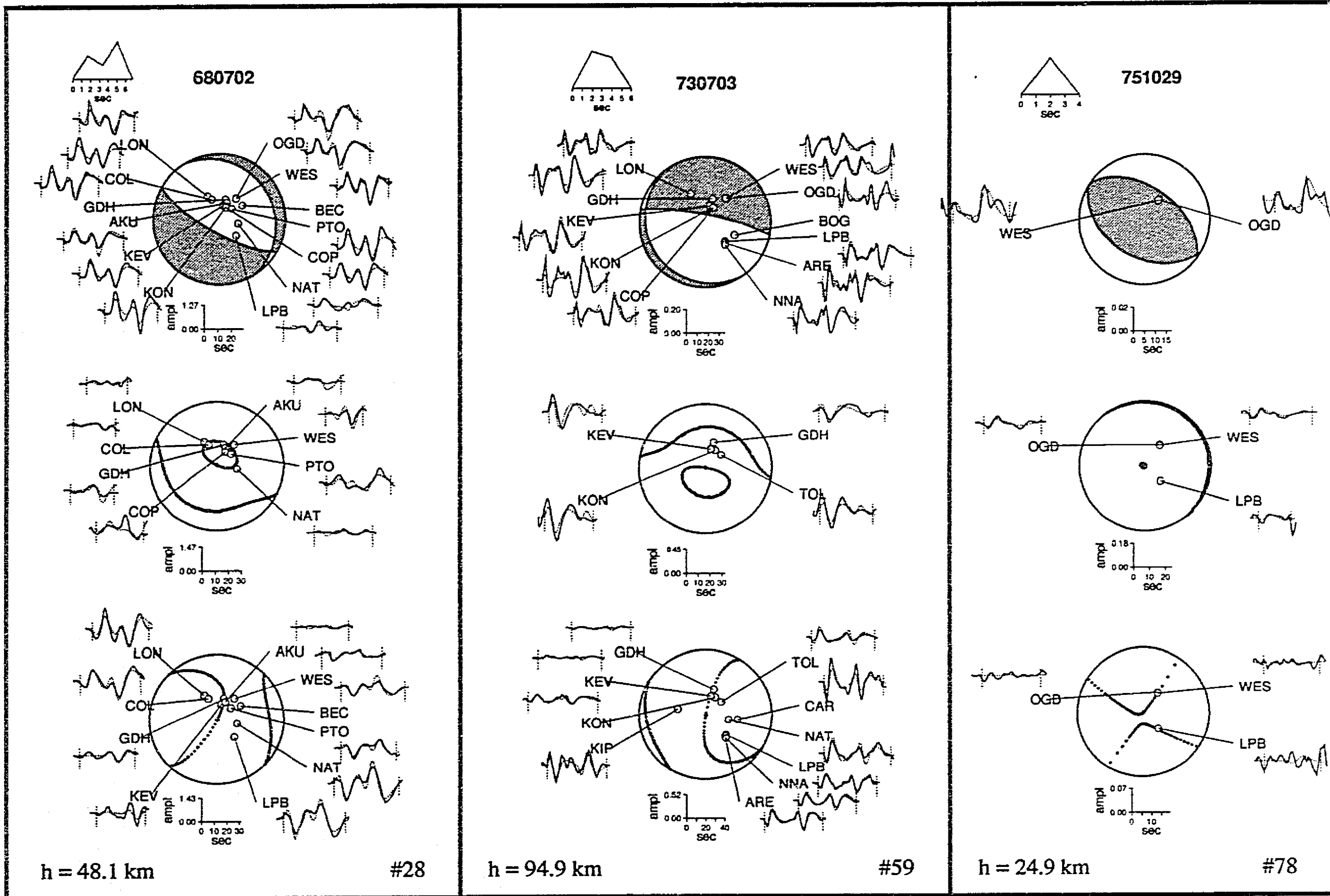


Fig. B2

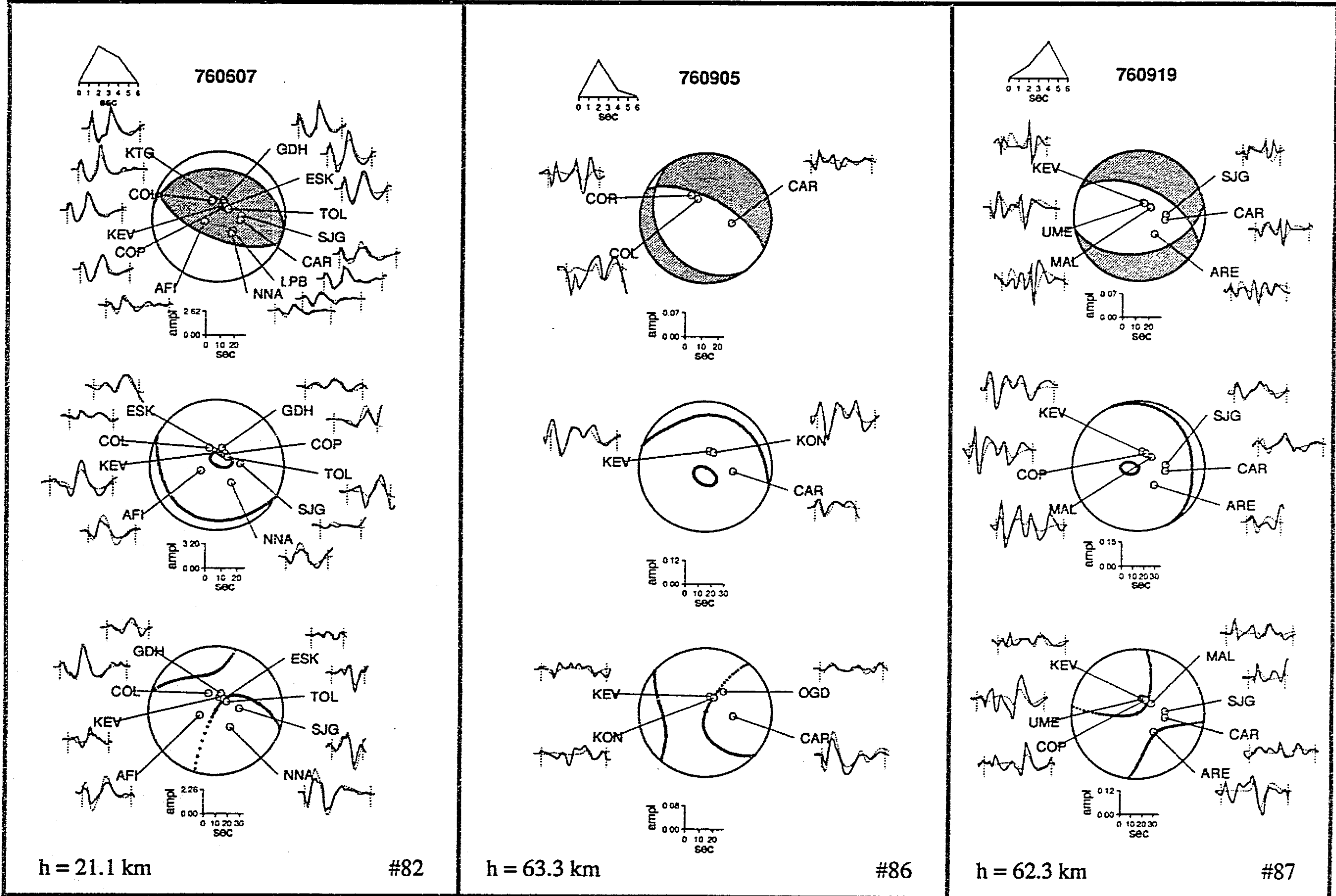


Fig. B3

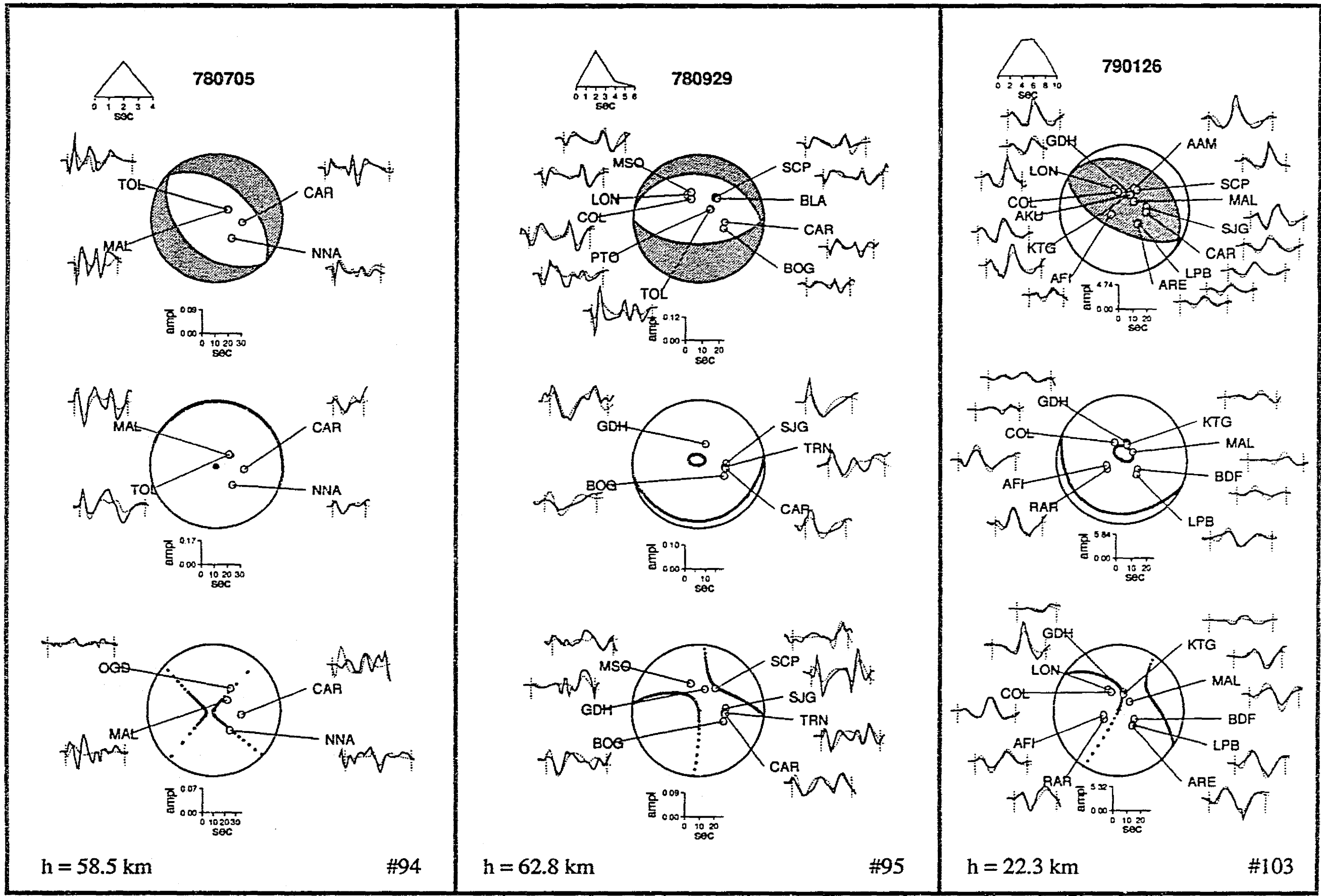


Fig. B4

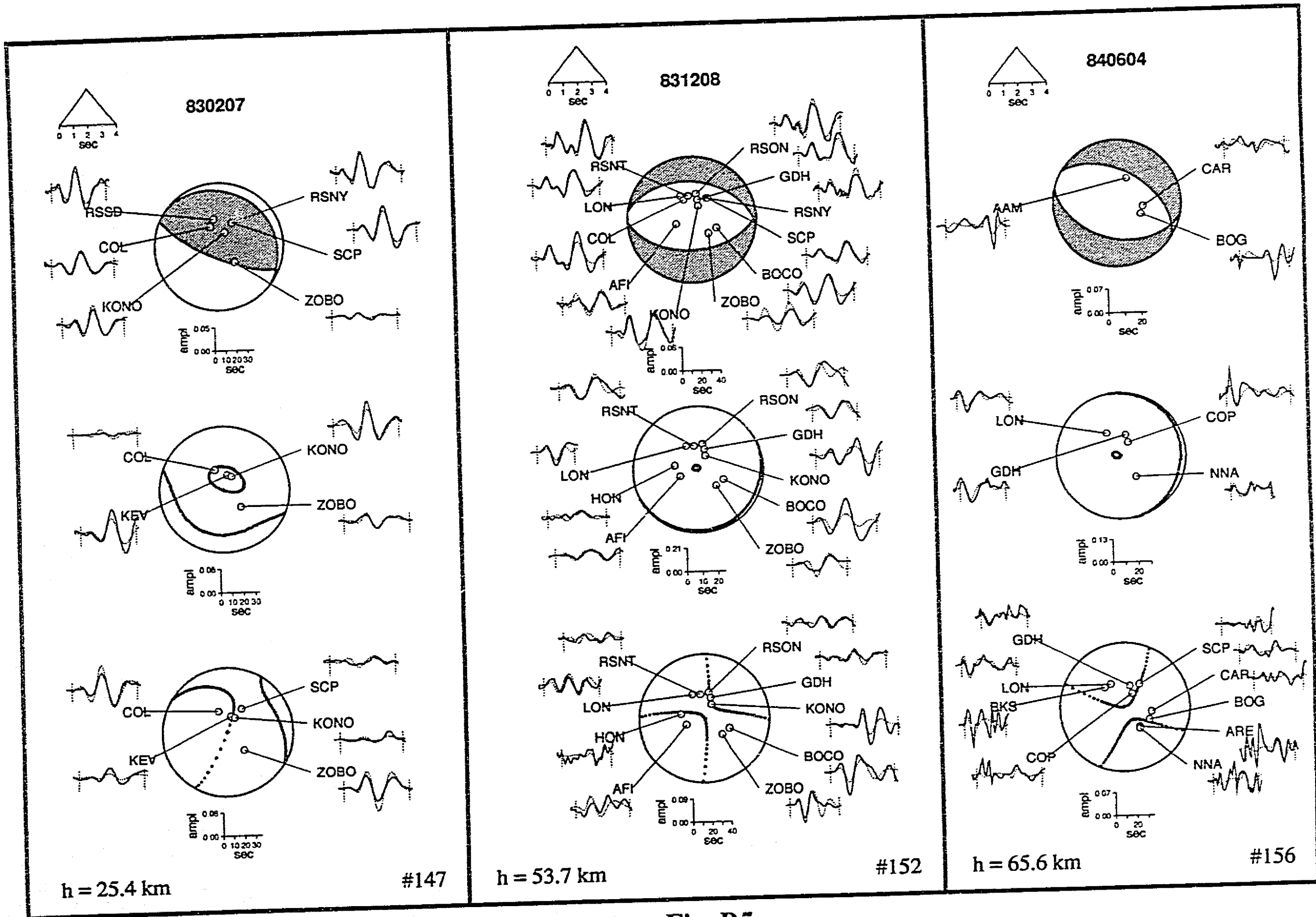


Fig. B5

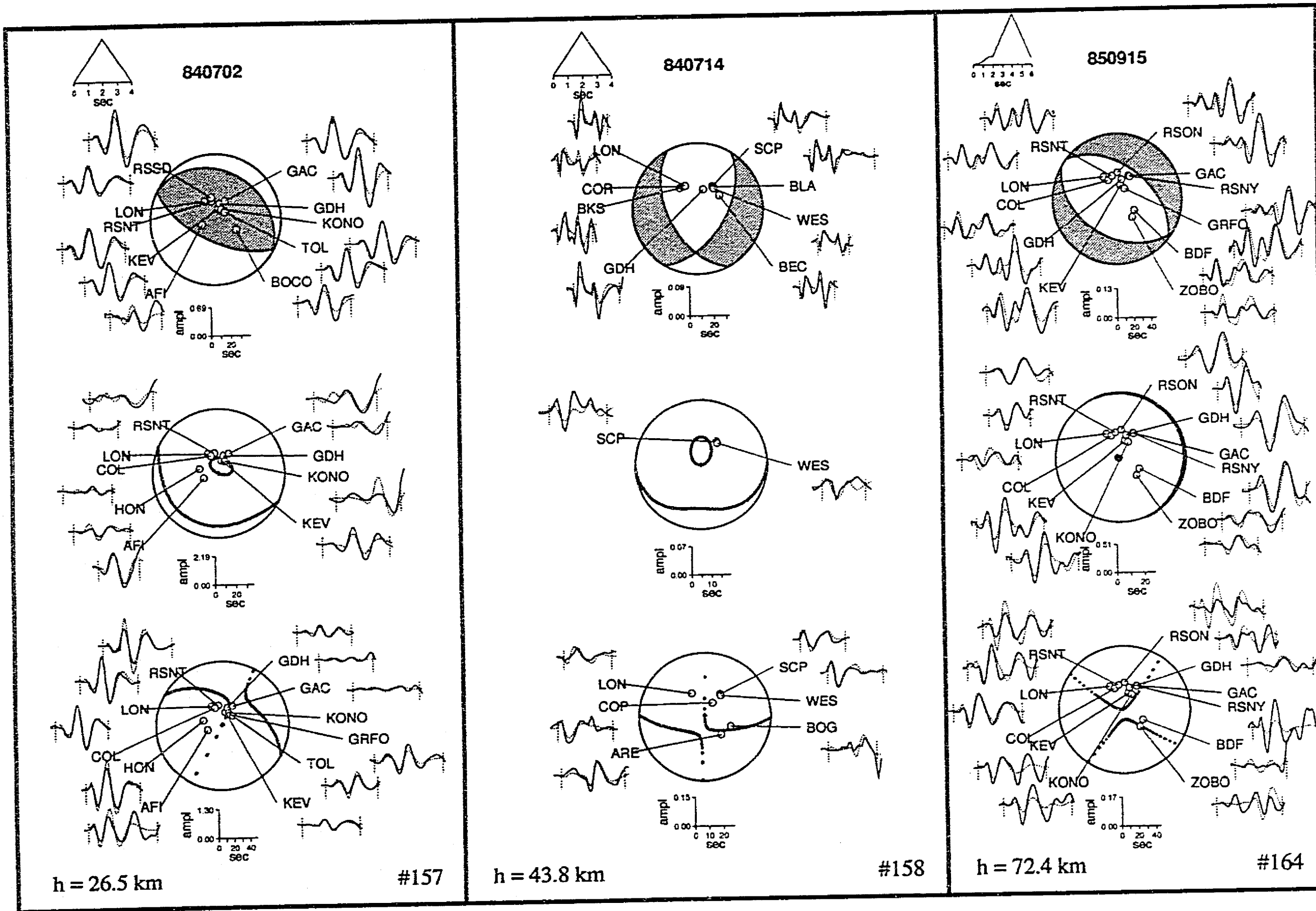


Fig. B6

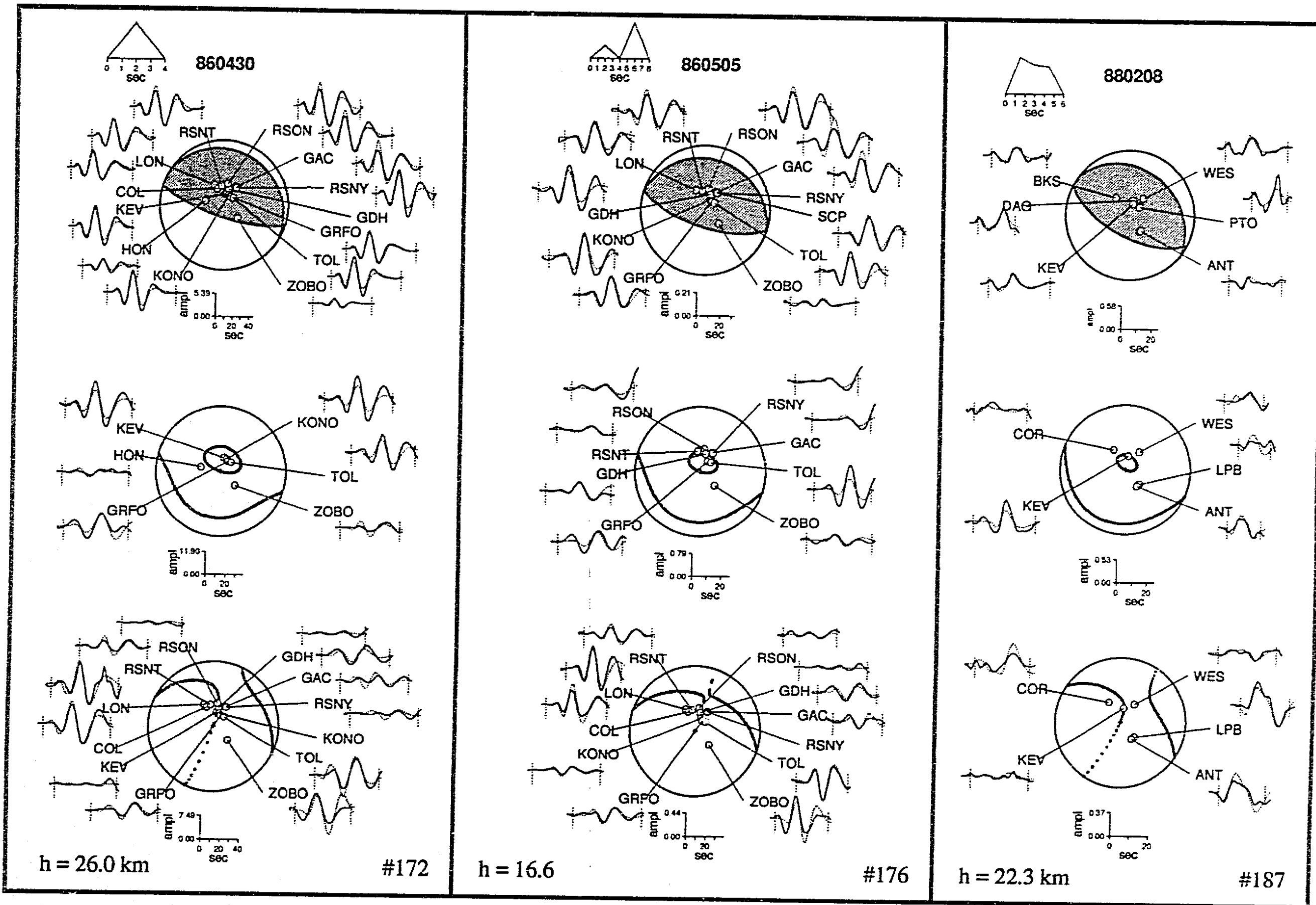


Fig. B7

**VI. Análisis Estadístico sobre la Existencia y Movimientos Relativos de los
Bloques de Jalisco y Sur de México**
(Enviado a: *Tectonics*, 1993)

**STATISTICAL EXAMINATION OF THE EXISTENCE AND RELATIVE
MOTIONS OF THE JALISCO AND SOUTHERN MEXICO BLOCKS**

William Bandy¹ and Mario Pardo^{1,2}

¹Instituto de Geofísica, Universidad Nacional Autónoma de México, México D.F., 04510.

²Departamento de Geofísica, Universidad de Chile, Casilla 2777, Santiago, Chile.

Abstract.. The continental lithosphere of Mexico south of the Trans-Mexican volcanic belt may consist of two lithospheric blocks; the Jalisco and Southern Mexico blocks. The existence of these two blocks can be examined employing the statistical F-test (formulated to test for the presence of significant misclosure around a plate circuit) to plate motion data derived from marine magnetic anomaly lineations, earthquake slip vectors and transform fault azimuths.

The result of the F-test applied to the Pacific-Cocos-North American plate circuit indicates that there is no significant (at the 99% confidence level) misclosure around this plate circuit. Therefore, if the Southern Mexico Block exists, its motion relative to the surrounding lithospheric plates is too small to be resolved from these data. In contrast, the result of the F-test applied to the Rivera-Pacific-North American plate circuit indicates the presence of a significant misclosure about the Rivera-Pacific-North American plate circuit; the cause of which is uncertain.

One interpretation of the misclosure around the Rivera-Pacific-North American plate circuit is that it is due to the presence of an independent Jalisco Block. However, it is more likely that this misclosure is, instead, primarily due to the effects of recent changes in the relative motion between the Pacific and Rivera plates.

Assuming The second explanation is correct, a new Rivera-North American Euler pole location (21.8°N, 110.4°W) is determinable solely from earthquake slip vectors located along the Rivera-North American boundary.

INTRODUCTION

The continental lithosphere of southern Mexico south of the Trans Mexican volcanic belt (TMVB) may consist of two small lithospheric plates or blocks. These are the Jalisco Block located northwest of the Colima Graben and the Southern Mexico Block located east

of the Colima Graben (Figure 1). Studies indicate that the Southern Mexico Block exhibits a left lateral motion relative to the North American (NA) plate along the TMVB [Pasquaré et al., 1986; Suárez and Singh, 1986; Urrutia-Fucugauchi and Böhnel, 1988], whereas the motion of the Jalisco Block relative to the NA plate is less clear. Several studies [Gastil and Jensky, 1973; Shurbet and Cebull, 1984; Luhr et al., 1985; Nieto-Obregón et al., 1985; Nieto-Obregón, 1990; Serpa et al., 1989, 1992; Carmichael, 1990; Allan et al., 1991; Bourgois and Michaud, 1991; Bandy, 1992] indicate a NW oriented, right lateral motion at a rate of 1.0 to 2.0 mm/yr, while other studies indicate either little or no motion [Böhnel and Negendank, 1988; Nieto-Obregón et al., 1992] or a SW oriented relative motion [Johnson and Harrison, 1989]. Presently, no Euler poles have been determined for either the Jalisco or Southern Mexico blocks relative to any of the surrounding major lithospheric plates.

The purpose of this study is to determine if the motions of both the Jalisco and Southern Mexico blocks are of sufficient magnitudes as to be resolvable using plate motion data derived from marine magnetic anomaly lineations, earthquake slip vectors and the azimuths of transform faults. Further, if their motions are resolvable employing these data, what are the Euler poles describing their motions relative to the surrounding major lithospheric plates; and can these poles be used to resolve the ambiguities in the previous studies of the relative motion between the Jalisco Block and the NA plate?

The results of the analysis suggest that the motions of both the Jalisco and Southern Mexico blocks relative to the NA plate are too small to be resolved from these data. Thus, no Euler poles describing their motions relative to the surrounding plates can be determined. However, due to the insignificant motion between the Jalisco Block and the NA plate, the location of the Rivera-NA Euler pole is determinable from earthquake slip vector data located along the Rivera-NA boundary. This pole location can be further constrained by comparing the morphology of the Rivera-Cocos plate boundary with Rivera-Cocos relative motion predicted employing this pole.

DATA AND METHODS

F-Tests and Plate Motion Inversions

The first step in the analysis is to determine if the motion of the Jalisco and southern Mexico blocks are resolvable using plate motion data derived from marine magnetic anomaly lineations, earthquake focal mechanism solutions and transform azimuths. To accomplish this, the statistical F-test as formulated by Gordon et al. [1987] is used. This

formulation tests for the presence of a significant misclosure around a plate circuit by comparing the magnitude of the weighted residuals (the difference between the observed data and the corresponding data predicted from the best fit poles divided by their assigned uncertainty) produced by two different models, or sets of Euler pole parameters. The two models differ solely in that one model invokes closure around a plate circuit (thus, in general, reducing the number of independent parameters by three), whereas closure is not invoked in the second model. Thus, the method tests whether there is a significant misclosure about the plate circuit which could be indicative of the presence of a plate which was not, but should have been, included in the circuit. It is important to note that the presence of a significant misclosure does not prove the existence of an additional plate since other factors such as erroneous data, systematic errors in the data (such as those produced by fluctuations in spreading rates), internal plate deformation and earthquake slip vectors which may be nonrepresentative of long term plate motions can also produce the misclosure. The Pacific-Rivera-NA plate circuit is employed in the test for the presence of the Jalisco Block. The Pacific-NA-Cocos plate circuit is employed in the test for the presence of the Southern Mexico Block.

The following data bases are used in these tests: (1) for the Rivera-Pacific and Cocos-Pacific plate pairs, the data base DB-1R (in which spreading rates are averaged over the last 0.83 Ma) of Bandy [1992] is used, (2) for the Cocos-NA and Pacific-NA plate pairs, the Nuvel-1 data base of DeMets et al. [1990] is used except that each Pacific-NA spreading rate of this data base is modified to reflect a spreading rate averaged over the past 0.73 Ma as determined by DeMets et al. [1987] (approximately 51 mm/yr), and (3) for the Rivera-NA plate pair, a new data base is constructed which consists of 8 earthquake slip vectors (Figure 2 and Table 1). Rivera-NA events 3, 6, 7, and 8 are obtained from the Harvard Data Base; event 5 is from Goff et al. [1987]; and events 1, 2 and 4 are new determinations using the long-period body wave inversion method of Nábelek [1984] (see Appendix for results of these waveform inversions). Assigned uncertainties for the slip directions of the Rivera-NA events, which are used as weights in the plate motion inversions, are 15° for all events. All spreading rates used in this study represent rates averaged over roughly the past 0.8 Ma.

The method used to determine Euler poles presented in this study is that of Minster et al. [1974]. The data used in the inversions of the present study are the same as that presented above.

Rivera-Cocos Azimuths

An analysis of the azimuth of relative motion between the Rivera and Cocos plates along their mutual boundary is also conducted; the results of which are presented in the discussion section. The objective of this analysis is to determine which of the permissible Rivera-NA Euler pole locations (i.e. pole locations within the 95% confidence ellipse associated with the best fit Rivera-NA Euler pole determined from the above mentioned Rivera-NA data base) predict compression, extension, or either compression or extension along this boundary. The location of the Rivera-NA pole can then be further constrained by comparing these predicted azimuths with the morphology of the Rivera-Cocos plate boundary.

To accomplish this, we first determine new Cocos-NA and Rivera-NA Euler poles from the above mentioned Rivera-NA, Pacific-NA, Pacific-Cocos and Cocos-NA data bases. Next, these poles are used to determine the possible azimuths of Rivera-Cocos relative motion at 18°N, 104.67°W (within the El Gordo Graben which forms the eastern portion of the Rivera-Cocos plate boundary [Bandy, 1992]). As the Rivera-NA data base contains no rate information, we herein assume that the angular rotation rate about the Rivera-NA Euler pole is 3.9°/m.y. as determined by Bandy [1992]. The uncertainties in this rate are unknown and are, therefore, not considered in this analysis.

To determine the range of azimuths, we first construct a 0.2° by 0.2° grid within the entire 95% confidence ellipse associated with the Rivera-NA Euler pole. Next, the Rivera-NA Euler pole is placed at one of these grid nodes. Then, three permissible azimuths of Rivera-Cocos relative motion are determined at 18°N, 104.67°W using this Rivera-NA pole in conjunction with a Cocos-NA pole located along the 95% confidence ellipse associated with the best-fit Cocos-NA Euler pole. Three different Cocos-NA angular rotation rates are employed; namely, the best fit rate, and the best fit rate $\pm 2\sigma_{\omega}$ (where σ_{ω} is the standard deviation associated with the best fit angular rotation rate). Next, keeping the Rivera-NA pole fixed at the same grid node, the location of the Cocos-NA pole is then moved to a new position located along the 95% confidence ellipse associated with the best fit Cocos-NA pole and three more azimuths are similarly calculated. This procedure is continued until the set of Cocos-NA poles completely samples the 95% confidence ellipse. All the calculated azimuths are then combined to determine the range of permissible azimuths of relative motion between the Rivera and Cocos plates at the 18°N, 104.67°W for a Rivera-NA pole located at the grid node. The resulting range of Rivera-Cocos azimuths is then compared to the orientation of the El Gordo Graben (N55°E) to determine if the permissible motion between the Rivera and Cocos plates at this point is extensional, compressional or either

extensional or compressional. This analysis is then carried out at each of the remaining grid nodes within the 95% confidence ellipse associated with the Rivera-NA Euler pole. Based on the extensional morphology of the El Gordo Graben, the locations of the Rivera-NA Euler pole for which the only permissible Rivera-Cocos motion at 18°N, 104.67°W is compressional are then ruled out as permissible pole locations.

Although a more exact method of determining the range of azimuths is to locate the various Cocos-NA Euler poles along the boundary of its error ellipsoid, the above method is desirable in that it leads to a wider range of permissible azimuths. The wider range of azimuths is desirable in that (1) it may accommodate the fact that we have not considered the uncertainties in Rivera-NA angular rotation rate and (2) it allows us to be more conservative as to which Rivera-NA pole locations can be excluded as permissible locations based on these azimuths.

RESULTS

Modification of the Rivera-North American Data Base

During the study it became apparent that the Rivera-NA event 6 (which exhibits slip directions greatly different from those of the other three events located along the Tres Marias Escarpment (TME)) was most likely produced by deformation either along the TME or within the Rivera plate; the deformation being related to the convergence of the two plates along the TME [DeMets and Stein, 1990, Couch et al., 1991; Bandy, 1992]. Therefore, the slip directions of this event do not represent relative plate motions. Thus, this event was excluded from the data base used in the following F-tests and plate motion inversions.

To illustrate this, we first invert all eight datums in the Rivera-NA data base. As Table 2 (inversion number 1) illustrates, this inversion results in unacceptably large residuals for the four events located along the TME (events 5, 6, 7 and 8). Further, the distribution of the normalized residuals (Figure 3a) clearly does not exhibit a Gaussian distribution with zero mean and unit variance. Next, we invert the Rivera-NA data base in which event 6 is excluded. The results of this inversion (Table 2, inversion number 2) yield acceptable residuals for all the remaining Rivera-NA events. Further, the distribution of the normalized residuals (Figure 3b) exhibits more closely a Gaussian distribution with zero mean and unit variance than does that of inversion 1.

F-Tests

The results of the F-test for the possible existence of the Jalisco (Rivera-Pacific-NA plate circuit) and Southern Mexico (Pacific-Cocos-NA plate circuit) blocks are presented in Table 3. In this table, N is the number of datums; R and $\chi^2(R)$ are the number of independent parameters and the resulting χ^2 value, respectively, for the model in which closure about the plate circuit was invoked; P and $\chi^2(P)$ are the number of independent parameters and the resulting χ^2 value, respectively, for the model in which closure about the plate circuit was not invoked; and $F_{P,R,N,P}$ is the resulting F-value.

For the Southern Mexico Block, the resulting F-value ($F_{2,164}=1.53$; Table 3) does not pass at either the 99% or the 95% confidence level indicating that there is more than a 5% risk that the improvement in fit is due solely to the additional independent parameters. In other words, the misclosure around this circuit is not significant at the 95% confidence level. Thus, the test indicates that the relative motion between the Southern Mexico Block and the NA plates is too small to be resolvable using the plate motion method employed in this study given the available data.

The resulting F-test value of the present study is much smaller than that calculated by DeMets et al. [1990] who found a significant misclosure about the Pacific-Cocos-NA plate circuit when global plate circuit closures are enforced. However, if only the Nuvel-1 Pacific-Cocos, Pacific-NA and Cocos-NA data are used, the results are consistent with our findings (C. DeMets, personal communication, 1993).

For the Jalisco Block, the resulting F-value ($F_{2,124}=6.64$; Test 1, Table 3) indicates that there is less than a 1% chance that the improvement in fit is due solely to the additional independent parameters. In other words, there is a misclosure around this plate circuit which is significant at the 99% confidence level. (Note: if event 1 is also excluded from the Rivera-NA data base as suggested by one of the reviewers, the resulting F-value ($F_{2,123}=5.21$) still indicates a significant misclosure).

The fits between the observed and predicted Rivera-Pacific, Rivera-NA and Pacific-NA datums for both closure and individual plate pair poles (Table 4) are illustrated in Figures 4, 5 and 6, respectively. These figures illustrate that the fit to the data located along both the Pacific-NA spreading center in the Gulf of California and along the Rivera-NA plate boundary clearly are adversely affected by invoking closure about the plate circuit; however, the predicted datums still lie within the limits of the data uncertainties. In contrast, invoking closure has no apparent effect on the fits along the other plate boundaries, with the possible exception of the fit to the Rivera-Pacific spreading rate data located closest to the best fit Rivera-Pacific Euler pole (Figure 4).

Euler Pole Determinations

The Rivera-NA data base is inverted to determine the location of the Euler pole which best fits these data. The parameters of the resulting pole and its associated 95% confidence ellipse are presented in Table 4 and illustrated in Figure 7. The angular rotation rate about this pole cannot be determined from the 2-plate inversion due to the lack of Rivera-Jalisco/Rivera-NA rate data. (Note: the exclusion of event #1 from the Rivera-NA data base does not result in a significant change in the pole location (21.8°N, 110.2°W) or in the parameters of the error ellipse ($L_{\max} = 2.16^\circ$; $L_{\min} = 0.61^\circ$; azimuth of $\sigma_{\max} = 88.4^\circ$; where L_{\max} is the length of the semi-major axis and L_{\min} is the length of the semi-minor axis).

Due to the ambiguity in the interpretation of the F-test, this pole may describe the relative motion between either the Rivera-Jalisco or Rivera-NA plate pairs. Specifically, if one interprets the misclosure around the Rivera-Pacific-NA plate circuit to be a result of the presence of an independent Jalisco Block, then the pole describes Rivera-Jalisco relative motion. Alternatively, if one interprets the misclosure as being due to other factors (such as the recent changes in spreading rate between the Rivera and Pacific plates) and not due to the presence of an independent Jalisco Block, then the pole describes Rivera-NA relative motion. The implications of these two different interpretations are discussed in the following section.

DISCUSSION

Interpretation 1: Significant Jalisco-North American Motion

The adverse effects on the fits along the Pacific-NA and the Rivera-NA plate boundaries noted above is interesting in that, if the proposal of Bourgois et al. [1988] and Bourgois and Michaud [1991] is correct, namely, that the segment of the Pacific-NA spreading center along which the Pacific-NA spreading rates were determined [DeMets et al., 1987] is in reality a boundary between the Pacific plate and the Jalisco Block, then only the fit to the data located along the boundaries of the proposed Jalisco Block are clearly adversely affected by invoking closure about the Rivera-Pacific-NA plate circuit. This supports the F-Test interpretation that the Jalisco Block may exist.

If the Jalisco Block exists (i.e. if it exhibits significant motion relative to the NA plate), then it is desirable to compare the Jalisco-NA motion predicted from the plate motion results with field observations along the Jalisco-NA boundaries. Two fairly well studied

areas are chosen for this comparison. The first is the area of the Santa Rosa Dam located within the Zacoalco Graben (20.91°N, 103.71°W). The second is the area of Lake Sayula located in the northern Colima Graben (20.15°N, 103.60°W).

Before presenting the analysis two complications need to be addressed. The first complication is that a discrepancy exists between the results of the F-test, which indicates the possibility of an independent Jalisco Block, and the overlap of the 95% confidence ellipses for the Rivera-NA and Rivera-Jalisco Euler poles (Figure 7), which indicates that the motion between the Jalisco and NA plates is insignificant. Such discrepancies between these two commonly used indicators of significance have been previously noted [Stein and Gordon, 1984] and were attributed to be the result of the errors assigned to the plate motion data; the assigned errors having a greater effect on the size of the 95% confidence ellipses than on the results of the F-test. It is also possible that in the formulation of the F-test used in the present study, the misclosure may not be due solely to the motion of the Jalisco block, but rather to a number of factors which, when combined, produce the misclosure. This possibility will be further addressed in the next section. The implication of this discrepancy is that if one accepts the interpretation that the Jalisco Block exhibits a significantly different motion than the NA plate, then the 95% confidence regions associated with the Rivera-Jalisco and Rivera-NA Euler poles cannot be used as meaningful indicators of the uncertainties associated with these poles.

The second complication is that a Jalisco-NA Euler pole is not obtainable due to both the lack of reliable plate motion data along the Jalisco-NA boundary and the lack of rate data along the Rivera-Jalisco boundary.

Because of these complications, the Jalisco-NA motion predicted from the Rivera-Jalisco and Rivera-NA Euler poles can only be determined via velocity vector diagrams, assuming that the rate of motion between the Jalisco and NA plates is small. Further, no meaningful confidence limits can be included in this analysis. For the following analysis we assume that the rate of relative motion between the Jalisco and NA plates is less than 5 mm/year at the two locations. Such a rate is consistent with the results of previous studies in this area [Nieto-Obregón et al, 1985; Carmichael, 1990; Allan, et al., 1991].

Within the area of the Santa Rosa Dam, field data indicates the presence of right lateral slip along generally NW-SE oriented faults at a rate of about 2 mm/yr [Nieto-Obregón et al., 1985; Carmichael, 1990; Allan et al., 1991]. Figure 8 illustrates the velocity vector diagram for this area which indicates that the predicted azimuth of relative motion of the Jalisco Block relative to a fixed NA plate ranges from 61° to 135° (azimuths measured clockwise from geographic north). This range of azimuths predicts either compression or left lateral strike slip motion along the NW-SE oriented faults. Thus, the predicted motions

are inconsistent with the field observations in this area.

Within the area of Lake Sayula, field data indicates recent normal faulting along N-S oriented faults (G. Suárez, Universidad Nacional Autónoma de México, unpublished manuscript, 1993); the rate of motion being only a few mm/year [Allan et al., 1991]. Figure 8 also presents the velocity vector diagram for this area which indicates that the predicted azimuth of relative motion of the Jalisco Block relative to a fixed NA plate ranges from 94° to 116° . This range of azimuths predicts compression along N-S oriented faults. Thus, the predicted motions are again inconsistent with field observations in this area.

Even though the Jalisco-NA motion predicted by the best fit Rivera-NA and Rivera-Jalisco Euler poles are inconsistent with field observations in the above mentioned area, the difference in the azimuths of Rivera-NA and Rivera-Jalisco motion are less than 10° at both locations. If the uncertainties in these azimuths are greater than about $\pm 5^\circ$ (which they probably are, given that an uncertainty of $\pm 15^\circ$ was assigned to the plate motion azimuth data) then no comparison of the predicted motions and the field observations is possible as a complete range in azimuths would then be permissible.

Interpretation 2: Insignificant Jalisco-North American Motion

Several observations noted in the previous section suggest that the misclosure around the Rivera-Pacific-NA plate circuit may not be produced by significant motion of the proposed Jalisco Block relative to the NA plate, but instead, to other factors. These observations are: (1) the overlap of the 95% confidence ellipses associated with the Rivera-Jalisco and Rivera-NA Euler poles, (2) the inconsistency between the field data and the Jalisco-NA motions predicted from the best fit Rivera-NA and Rivera-Jalisco Euler poles, (3) the observation that if both the Rivera-NA and Rivera-Jalisco azimuths calculated at the two sites located along the Jalisco-NA boundary exhibit at least $\pm 5^\circ$ of uncertainty (which is most likely), then no significant difference exists between the Rivera-Jalisco and Rivera-NA azimuths, and (4) the observation that even though the fits to the data are adversely affected by invoking closure, the predicted datums still lie within the limits of the data uncertainties.

This possibility is further suggested by the results of the study of Bandy [1992] whose Rivera-NA Euler pole is located in almost exactly the same location as our Rivera-Jalisco pole (Figure 7). The lack of an angular rotation rate about our Rivera-Jalisco Euler pole (2-plate) prevents us from stating emphatically that these two poles are identical. However, their almost identical location at least suggests this possibility.

Thus, instead of significant motion between the Jalisco Block and NA plate as being

responsible for the misclosure around the Rivera-Pacific-NA plate circuit, we suspect that other factors are responsible for the misclosure. The most likely factor is the recent changes in the relative motion between the Rivera and Pacific plates [Macdonald et al., 1980; Mammerrickx and Carmichael, 1989; Bandy and Yan, 1989, 1990; Lonsdale, 1989; DeMets and Stein, 1990; Bandy, 1992].

To investigate the effects of the recent changes in Rivera-Pacific relative motions on the misclosure about the Rivera-Pacific-NA plate circuit, a new F-test was performed in which the Rivera-Pacific spreading rate data was excluded from the test, and in which the angular rotation rate about the Rivera-Pacific Euler pole was fixed at $4.6^\circ/\text{m.y.}$ (the rate preferred by Bandy [1992]). The resulting F-value ($F_{2,104}=4.42$; Test 2, Table 3) results in an insignificant misclosure at the 1% risk level. This result, along with the previously mentioned observations, strongly suggest that the misclosure around the Rivera-Pacific-NA plate circuit is primarily due to recent fluctuations in Rivera-Pacific motion and that the motion of the Jalisco Block, like the Southern Mexico Block is too small to be resolvable using the plate motion method employed in this study given the available data.

The Location of the Rivera-North American Euler Pole

If the motion of the Jalisco Block relative to the NA plate is small, as it appears to be, then the Rivera-Jalisco Euler pole presented in Table 4 (individual plate pair) is roughly equivalent to the Rivera-NA Euler pole. Unlike previous studies [Minster and Jordan, 1979; DeMets and Stein, 1990; Bandy, 1992], the location of this Rivera-NA Euler pole is calculated directly from data located along the Rivera-NA plate boundaries. Because of this and the observed adverse effect of recent changes in the relative motion between the Rivera and Pacific plates on the F-test, it is useful to compare this pole with previous determinations of the Rivera-NA Euler pole, particularly those determined by invoking closure about the Rivera-Pacific-NA plate circuit.

As Figure 7 illustrates, the locations of the various Rivera-NA Euler poles all lie fairly close to each other. However, due to the close proximity of these poles to the Rivera plate, they (and other Euler poles derived from these poles) predict substantially different relative motions along the boundaries of the Rivera plate. By comparing the morphologies observed along the boundaries of the Rivera plate with the plate motions predicted along the boundaries by the various Euler poles, one can further constrain the location of the Rivera-NA Euler pole. The best boundary for this analysis is the Rivera-Cocos plate boundary, which consists of an $N55^\circ E$ oriented extensional structure (the El Gordo Graben) along its eastern extent [Bandy, 1992]. Although no well defined magnetic lineations are associated

with this feature, it contains a N55°E oriented central volcanic ridge which exhibits high heat flow (150 to 208 mW/m²) (L. A. Delgado-Argote, Centro de Investigacion Cientifica y de Education Superior de Ensenada, unpublished manuscript, 1993), suggesting that it is a recently active rift, and therefore, the most likely location of the Rivera-Cocos plate boundary.

Figure 7 illustrates three separate regions located within the 95% confidence ellipse associated with the best fit Rivera-NA Euler pole determined from the inversion of the Rivera-NA data Base. These regions delineate Rivera-NA pole locations which, when used in conjunction with our Cocos-NA Euler pole, predict extension, compression or either compression or extension between the Rivera and Cocos plates along the El Gordo Graben. The methods used to determine these zones is presented in the Data and Methods section. The Rivera-NA Euler pole determined in this study (2-plate model), along with that determined by Minster and Jordan [1979] and Bandy [1992] are all located in the zone within which Rivera-NA pole locations predict either compression or extension along the El Gordo Graben. Thus, these poles are all consistent with the observed extension along the eastern part of the Rivera-Cocos plate boundary. In contrast, the two Rivera-NA poles determined in the present study by invoking closure about the Rivera-Pacific-NA plate circuit and the pole of DeMets and Stein [1990] (which was also determined by invoking closure about the Rivera-Pacific-NA plate circuit) all lie in the zone for which pole locations predict only compression along the Rivera-Cocos plate boundary. Thus, these two poles are unlikely to truly represent Rivera-NA relative motion.

Although, the location of the Rivera-NA pole of DeMets and Stein [1990] is unlikely to represent Rivera-NA relative motion given the above analysis, it could be argued that the difference in angular rotation rates between their model ($\omega=3.32^\circ/\text{m.y.}$) and that used in the above analysis ($\omega=3.9^\circ/\text{m.y.}$) may permit their pole to remain permissible. To investigate this possibility a velocity vector diagram is constructed at the El Gordo Graben (insert on Figure 7). This diagram illustrates that the permissible azimuth of the relative motion of the Rivera plate with respect to a fixed Cocos plate ranges clockwise from 73° to 215°, again indicating that their pole predicts only convergence across the El Gordo Graben.

Therefore, it appears that the recent changes in the relative motion between the Rivera and Pacific plates have adversely affected both the Rivera-NA Euler pole determinations in which closure was invoked about the Rivera-Pacific-NA plate circuit (with the exception of the Minster and Jordan [1979] pole) and the F-test conducted about the Rivera-Pacific-NA plate circuit.

CONCLUSIONS

The main conclusions of this study are:

(1) The F-test for the existence of the Southern Mexico Block indicates no significant misclosure around the Pacific-Cocos-North American plate circuit. Thus, the relative motion between the southern Mexico Block and the North American plate is too small to be resolvable from plate motion studies employing data derived from the presently available marine magnetic, earthquake and bathymetric data.

(2) The F-test for the existence of the Jalisco block indicates a significant misclosure around the Rivera-Pacific-North American plate circuit. This misclosure may be due to the presence of an independent Jalisco Block or it may instead be due to the effects of recent changes in the relative motion between the Pacific and Rivera plates in combination with other factors known to affect closure, such as internal plate deformation or systematic errors in the data.

(3) It is most likely that the correct interpretation of the result of the F-test about the Rivera-Pacific-NA plate circuit is that the misclosure is primarily due to the effects of recent changes in the relative motion between the Rivera and Pacific plates and not to significant motion between the North American plate and the proposed Jalisco Block. This is suggested by the following. First, and most important, an F-test about the Rivera-Pacific-NA plate circuit in which the spreading rates between the Rivera and Pacific plates were excluded resulted in no significant misclosure about this plate circuit. Second, the 95% confidence ellipses associated with the Best fit Rivera-North American and Rivera-Jalisco Euler poles greatly overlap. Third, the motion of the Jalisco Block relative to the North American plate predicted from the best-fit Rivera-Jalisco Euler pole is inconsistent with field observations in the Zacoalco and northern Colima grabens. Further, a $\pm 5^\circ$ uncertainty in the Rivera-NA and Rivera-Jalisco azimuths calculated from these best fit poles results in no significant difference between these two azimuths. Fourth, the differences between the fits (observed data minus predicted data) to data lying along the boundaries of the proposed Jalisco Block obtained employing the 2-plate model and obtained by employing the closure model lie within the limits of uncertainty of the data. Lastly, the location of the Rivera-North American Euler pole of Bandy [1992] is identical to that of the best fit, 2-plate Rivera-Jalisco Euler pole determined in this study.

(4) Recent changes in the relative motion between the Rivera and Pacific plates adversely affects previous Rivera-North American Euler pole determinations which invoke closure about the Rivera-Pacific-North American plate circuit.

Acknowledgements. We thank Jaime Urrutia-Fucugauchi, Chuck DeMets and an anonymous reviewer for providing helpful suggestions on how to substantially improve the original manuscript.

REFERENCES

- Allan, J.F., S.A. Nelson, J.F. Luhr, I.S.E. Carmichael, M. Wopat, and P.J. Wallace, Pliocene-Recent rifting in SW Mexico and associated volcanism: an exotic terrain in the making, in *The Gulf and Peninsular Province of the California's*, Memoir 47, edited by J.P. Dauphin, and B.R.T. Simoneit, AAPG, Tulsa, Oklahoma, 1991.
- Bandy, W.L., *Geological and Geophysical Investigation of the Rivera-Cocos Plate Boundary: Implications For Plate Fragmentation*, Ph.D. Dissertation, Texas A&M University, College Station, Texas, 1992.
- Bandy, W.L., and C.-Y. Yan, Change in Pacific-Rivera relative plate motion between 0.95 and 1.77 Ma (abstract), *EOS Trans. Am. Geophys. Un.*, 71, 635, 1990.
- Bandy, W.L., and C.-Y. Yan, Present-day Rivera-Pacific and Rivera-Cocos relative plate motions (abstract), *EOS Trans. Am. Geophys. Un.*, 70, 1342, 1989.
- Böhnell, H., and J.F.W. Negendank, Paleomagnetism of the Puerto Vallarta intrusive complex and the accretion of the Guerrero terrain, Mexico, *Phys. Earth Planet. Inter.*, 52, 330-338, 1988.
- Bourgeois, J., and F. Michaud, Active fragmentation of the North American plate at the Mexican triple junction area off Manzanillo, *Geo-Marine Letters*, 11, 59-65, 1991.
- Bourgeois, J., V. Renard, J. Aubouin, W. Bandy, E. Barrier, T. Calmus, J.C. Carfantan, J. Guerrero, J. Mammerickx, B. Mercier de Lepinay, F. Michaud, and M. Sosson, Active Fragmentation of the North American plate: offshore boundary of the Jalisco Block off Manzanillo, *C.R. Acad. Sci. Paris*, 307, 1121-1130, 1988.
- Carmichael, I.S.E., The Jalisco Block: a tectonic and petrologic entity (abstract), paper presented at the symposium on *The Tectonics, Geophysics, and Volcanism of Mexico*, University of New Orleans and Tulane University, New Orleans, April 12-14, 1990.
- Couch, R.W., G.E. Ness, O. Sanchez-Zamora, G. Calderón-Riveroll, P. Doguin, T. Plawman, S. Coperude, B. Huehn, and W. Gumma, Gravity anomalies and crustal structure of the gulf and peninsular province of the Californias, in *The Gulf and Peninsular Province of the Californias*, AAPG Memoir 47, edited by J.P. Dauphin and B.R.T. Simoneit, pp. 25-45, AAPG, Tulsa, Oklahoma, 1991.
- DeMets, C., and S. Stein, Present-day kinematics of the Rivera plate and implications for tectonics in southwestern Mexico, *J. Geophys. Res.*, 95, 21931-21948, 1990.
- DeMets, C., R. G. Gordon, D.F. Argus, and S. Stein, Current plate motions, *Geophys. J. Int.*, 101, 425-478, 1990.
- DeMets, C., R.G. Gordon, S. Stein, and D.F. Argus, A revised estimate of Pacific-North American motion and implications for western North America plate boundary zone

- tectonics, *Geophys. Res. Lett.*, 14, 911-914, 1987.
- Dewey, J.W., *Seismicity studies with the method of Joint Hypocenter Determination*, Ph.D. Thesis, University of California, Berkeley, 1971.
- Gastil, G.R., and Jency, J., Evidence for strike slip displacement beneath the Trans-Mexican volcanic belt, *Stanford Univ. Press. Conf. 13*, 171-180, 1973.
- Goff, J.A., E.A. Bergman, and S.C. Solomon, Earthquake source mechanisms and transform fault tectonics in the Gulf of California, *J. Geophys. Res.*, 92, 10,485-10,510, 1987.
- Gordon, R.G., S. Stein, C. DeMets, and D.F. Argus, Statistical tests for closure of plate motion circuits, *Geophys. Res. Lett.*, 14, 587-590, 1987.
- Johnson, C.A., and C.G.A. Harrison, Tectonics and volcanism in central Mexico: a landsat thematic mapper perspective, *Remote Sens. Environ.*, 28, 273-286, 1989.
- Lonsdale, P., Geology and tectonic history of the mouth of the Gulf of California, in *The Geology of North America, Vol N, The Eastern Pacific Ocean and Hawaii*, edited by E.L. Winterer, D.M. Hussong, and R.W. Decker, pp. 499-521, The Geological Society of America, Boulder, Colorado, 1989.
- Luhr, J.F., S.A. Nelson, J.F. Allan, and I.S.E. Carmichael, Active rifting in southwestern Mexico: manifestations of an incipient eastward spreading-ridge jump, *Geology*, 13, 54-57, 1985.
- Macdonald, K.C., S.P. Miller, S.P. Huests, and F.N. Spiess, Three-dimensional modelling of a magnetic reversal boundary from inversion of deep-tow measurements, *J. Geophys. Res.*, 85, 3670-3680, 1980.
- Mammerickx, J., and I.S.E. Carmichael, A spreading incursion in the continent near the Rivera Plate and Jalisco Block ? (abstract), *EOS Trans. Am. Geophys. Un.*, 70, 1318-1319, 1989.
- Minster, J.B., and T.H. Jordan, Rotation vectors for the Philippine and Rivera plates (abstract), *EOS Trans. Am. Geophys. Un.*, 60, 958, 1979.
- Minster, J.B., T.H. Jordan, P. Molnar, and E. Haines, Numerical modelling of instantaneous plate tectonics, *Geophys. J. R. Astron. Soc.*, 36, 541-576, 1974.
- Nábelek, J.L., *Determination of Earthquake Source Parameters From Body Waves*, Ph.D. Dissertation, MIT, Cambridge, Massachusetts, 1984.
- Nieto-Obregón, J., Recent structural deformation in west-central Mexico, Paper presented at the symposium on the *Tectonics, Geophysics and Volcanism of Mexico*, University of New Orleans-Tulane University, New Orleans, April 12-14, 1990.
- Nieto-Obregón, J., J. Urrutia-Fucugauchi, E. Cabral-Cano and A. Guzman de la Campa, Listric faulting and continental rifting in western Mexico - A paleomagnetic and

- structural study, *Tectonophysics*, 208, 365-376, 1992.
- Nieto-Obregón, J., Delgado-Argote, L. and Damon, P.E., Geochronologic, petrologic, and structural data related to large morphologic features between the Sierra Madre Occidental and the Mexican volcanic belt, *Geof. Intern.*, 24, 623-663, 1985.
- Pardo, M., and G. Suárez, Steep subduction geometry of the Rivera plate beneath the Jalisco block in western Mexico, *Geophys. Res. Lett.*, in press, 1993.
- Pasquaré, G., Forcella, F., Tibaldi, A., Vezzoli, L. and Zanchi, A., Structural behavior of a continental volcanic arc: the Mexican volcanic belt, In F.-C. Wezel (Editor), *The Origin of Arcs*, Elsevier, Amsterdam, pp. 509-527, 1986.
- Serpa, L., S. Smith, C. Katz, C. Skidmore, R. Sloan and T. Palvis, A geophysical investigation of the southern Jalisco block in the State of Colima, Mexico, *Geof. Intern.*, 31, 475-492, 1992.
- Serpa, L., C. Katz, and C. Skidmore, The southeastern boundary of the Jalisco Block in west-central Mexico (abstract), *EOS Trans. Am. Geophys. Un.*, 43, 1319, 1989.
- Shurbet, D.H., and S.E. Cebull, Tectonic interpretation of the Trans-Mexico volcanic belt, *Tectonophysics*, 101, 159-165, 1984.
- Stein, S., and R.G. Gordon, Statistical tests of additional plate boundaries from plate motion inversions, *Earth Planet. Sci. Lett.*, 69, 401-412, 1984.
- Suárez, G., and Singh, S.K., Tectonic interpretation of the Trans-Mexican volcanic belt, Discussion, *Tectonophysics*, 127, 155-160, 1986.
- Urrutia-Fucugauchi, J., and H. Böhnel, Tectonics along the Trans-Mexican volcanic belt according to paleomagnetic data, *Phys. Earth Planet. Inter.*, 52, 320-329, 1988.

APPENDIX: NEW SOURCE MECHANISM DETERMINATIONS

The parameters of the best fitting double-couple point source of three events (number 1, 2, and 4; Table 1) were determined using a formal inversion of long-period teleseismic P, SV and SH waveforms [Nábelek, 1984]. In each iteration we solve for the focal mechanism, centroid depth, seismic moment and source time function. The resulting uncertainties are within $\pm 5^\circ$ - 10° for the fault strike, dip and rake, ± 2 km for the centroid depth and $\pm 20\%$ for the seismic moment. Seismograms from the Global Digital Seismograph Network (GDSN) were used for the event that occurred in 1981, and from the World Wide Standardized Seismograph Network (WWSSN) for the other two events. The epicenters of these earthquakes were relocated using the JHD method [Dewey, 1971] with constrained focal depth from the body-wave inversion (Pardo and Suárez, 1993).

Figure A1 illustrates the fit between the observed P, SV and SH waveforms from these earthquakes and the synthetic waveforms for the best fitting point source.

Table 1. Rivera-North America Data Base

EQ #	DATE Y/M/D	LAT °N	LONG °W	CENTROID DEPTH km	m_b	M_0 N-m 10^{18}	STR °	DIP °	RAKE °	SLIP VECTOR	S.D.
1 ^a	810309	18.76	103.94	22	5.9	0.64	260	28	60	N23E	15
2 ^a	760717	19.28	104.74	13	5.2	0.06	311	12	115	N15E	15
3	891208	19.25	104.42	15	5.1	0.19	13	22	162	N30E	15
4 ^a	731018	19.34	104.95	14	6.0	1.20	296	33	86	N31E	15
5 ^b	760209	21.63	106.59	11	5.6	0.71	95	52	86	N09E	15
6	890131	22.19	107.32	15	5.2	0.12	276	74	173	N82W	15
7 ^c	910401	22.31	107.04	15	4.8	0.33	303	10	132	N09W	15
8	821208	22.71	106.82	15	5.0	0.09	160	90	180	N20W	15

Epical and magnitude data are taken from ISC; centroid depth, mechanism and seismic moment are taken from Harvard data base, except where noted.

^a New determination. Relocated epicenter.

^b Determination from Goff et al. [1987]

^c Location from NEIC data base.

Table 2: Residuals

EQ #	Inver. 1	Inver. 2
1	7.9°	4.3°
2	14.9°	10.9°
3	-1.6°	-4.9°
4	-0.4°	-4.7°
5	-18.6°	-6.4°
6	45.4°	-----
7	-25.6°	-0.7°
8	-20.2°	4.4°

Table 3: F-Test Results

Plate Circuit	N	P	R	$\chi^2(P)$	$\chi^2(R)$	$F_{P-R,N-P}$	F(95%)	F(99%)
Pac-Cocos-NA:								
	172	8	6	70.6921	72.0129	1.53	3.05	4.73
Pac-Riv-NA:								
Test 1	132	8	6	43.1051	47.7246	6.64	3.07	4.79
Test 2	111	7	5	34.6985	37.7023	4.42	3.08	4.80

Table 4. Euler Vectors

PLATE PAIR		LAT.	LONG.	ω^*	ERROR ELLIPSE**			σ_ω^{***}
moving	fixed	(°N)	(°E)	(°/Ma)	L_{\max}	L_{\min}	azm	(°/Ma)
<u>Individual Plate Pair</u>								
Rivera	Jalisco	21.8	-110.4	-----	2.18	0.64	90.1	-----
Rivera	Pacific	27.9	-104.3	4.10	1.31	0.33	14.5	0.441
Noam	Pacific	49.6	-76.7	0.78	3.05	1.51	66.2	0.047
<u>Rivera-Pacific-North American Circuit</u>								
Rivera	Noam ^a	22.1	-108.5	3.67	0.44	0.27	106.4	0.365
Rivera	Noam ^b	22.5	-108.5	3.44	0.81	0.41	142.8	0.449
Rivera	Pacific ^a	27.4	-104.5	4.34	0.88	0.27	19.5	0.347
Rivera	Pacific ^b	27.9	-104.3	4.10	1.32	0.31	14.5	0.441
Noam	Pacific ^a	49.6	-77.0	0.81	3.01	1.43	63.9	0.046
Noam	Pacific ^b	49.6	-76.7	0.78	3.05	1.51	66.2	0.047
<u>Cocos-Pacific-North American Circuit</u>								
Cocos	Noam	27.2	-121.6	1.56	2.04	0.93	103.1	0.089
Cocos	Pacific	36.3	-110.0	2.22	1.15	0.95	138.4	0.070
Noam	Pacific	49.6	-76.9	0.79	3.04	1.51	65.9	0.046

* Angular rotation rate, positive counter-clockwise

** 95% error ellipse determined from the model covariance matrices. Length of the semi-major (L_{\max}) and semi-minor (L_{\min}) axes are geocentric angles in degrees. The azimuth of the semi-major axis (azm) is in degrees, positive clockwise from geographic north. $L = \sigma\sqrt{2}$.

*** Rotation rate uncertainty; determined from the standard deviation of a marginal distribution.

^a Includes Rivera-North America data base.

^b Excludes Rivera-North America data base.

FIGURE CAPTIONS

Fig. 1. Location map of study area. The abbreviations shown on figure are: RP = Rivera Plate, JB = Jalisco Block, SMB = Southern Mexico Block, ZG = Tepic-Zacoalco Graben, CG = Colima Graben, EG = El Gordo Graben, TME = Tres Marias Escarpment, MAT = Middle America Trench, TMVB = Trans Mexican Volcanic Belt.

Fig. 2. Earthquake focal mechanism solutions (lower hemispheric projection) which comprise the Rivera-North American data base employed in this study.

Fig. 3. Histograms of normalized residuals for (a) the inversion of entire Rivera-North American data base and (b) the inversion of Rivera-North American data base excluding event #6. Continuous curve on both figures is the theoretical ideal Gaussian distribution with zero mean and unit variance.

Fig. 4. Plot of observed Rivera-Pacific data (symbols) versus datums (continuous curve) predicted by the best fit Rivera-Pacific Euler poles determined by invoking closure about the Rivera-Pacific-North American plate circuit (on left) and from the Rivera-Pacific data base (on right). Vertical lines through the observed data are the assigned uncertainties. For the azimuth plots, asterisks and open circles denote azimuths derived from earthquake slip vectors and transform faults, respectively.

Fig. 5. Plot of observed Rivera-North America data (symbols) versus datums (continuous curve) predicted by the best fit Rivera-North American Euler poles determined by invoking closure about the Rivera-Pacific-North American plate circuit (on left) and from the Rivera-North American data base (on right). Vertical lines through the observed data are the assigned uncertainties. Asterisks denote azimuths derived from earthquake slip vectors.

Fig. 6. Plot of observed Pacific-North America data (symbols) versus datums (continuous curve) predicted by the best fit Pacific-North American Euler poles determined by invoking closure about the Rivera-Pacific-North American plate circuit (on left) and from the Pacific-North American data base (on right). Vertical lines through the observed data are the assigned uncertainties. For the azimuth plots, asterisks and open circles denote azimuths derived from earthquake slip vectors and transform faults, respectively.

Fig. 7. Plot of various Rivera-North American pole locations and associated 95% confidence ellipses (see figure index for references). The three regions within the 95% confidence ellipse associated with the 2-plate Rivera-North American Euler pole designate areas where a Rivera-North American pole location, used in conjunction with our Cocos-North American pole (also shown on figure), predicts extension (region west of shaded area), compression (region east of shaded area) or either extension or compression (shaded area) at the El Gordo Graben (circle at 18°N , 104.67°W). Velocity vector diagram within the insert illustrates the range of possible Rivera-Cocos azimuths predicted by the Rivera-North American Euler pole of DeMets and Stein (1990) and the Cocos-North American Euler pole determined in this study. The two small arrows in the insert mark the upper and lower bounds of this range. Error ellipses presented in the insert are derived from the 95% confidence limits associated with each pole.

Fig. 8. Map illustrating the velocity vector diagrams used to determine the direction of motion of the Jalisco Block relative to a fixed North American Plate at the Santa Rosa Dam (20.91°N , 103.71°W) and Lake Sayula (20.15°N , 103.60°W). Vectors are determined from the best fit Rivera-Jalisco pole (derived from the Rivera-North American data base) and the best fit Rivera-North American pole determined by invoking closure about the Rivera-Pacific-North American plate circuit.

Fig. A1. Results of waveform inversion for Rivera-North American events 1, 2, and 4. Focal mechanisms in lower hemispheric projection showing observed (continuous line) and synthetic (dashed line) waveforms.

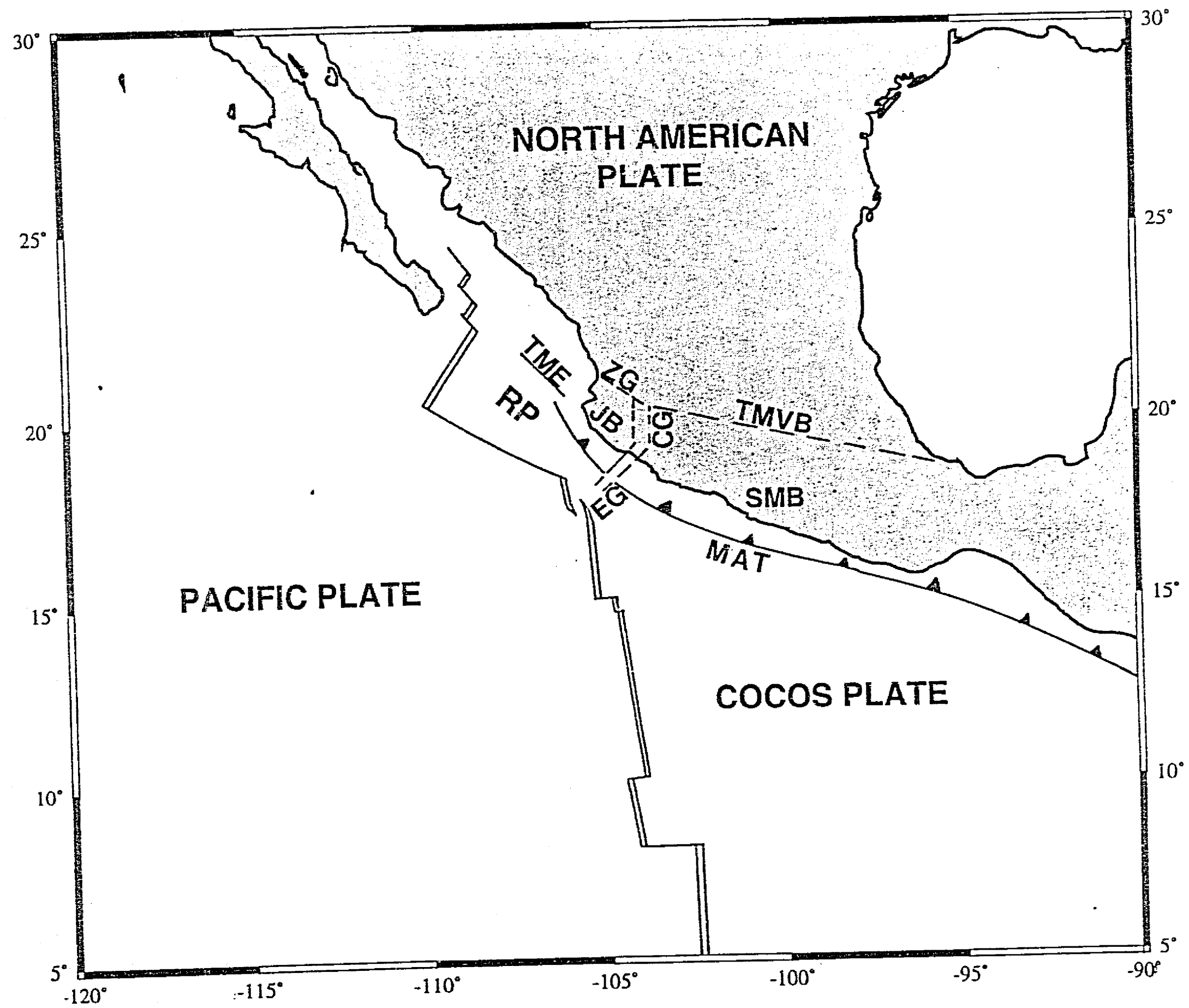


Fig. 1

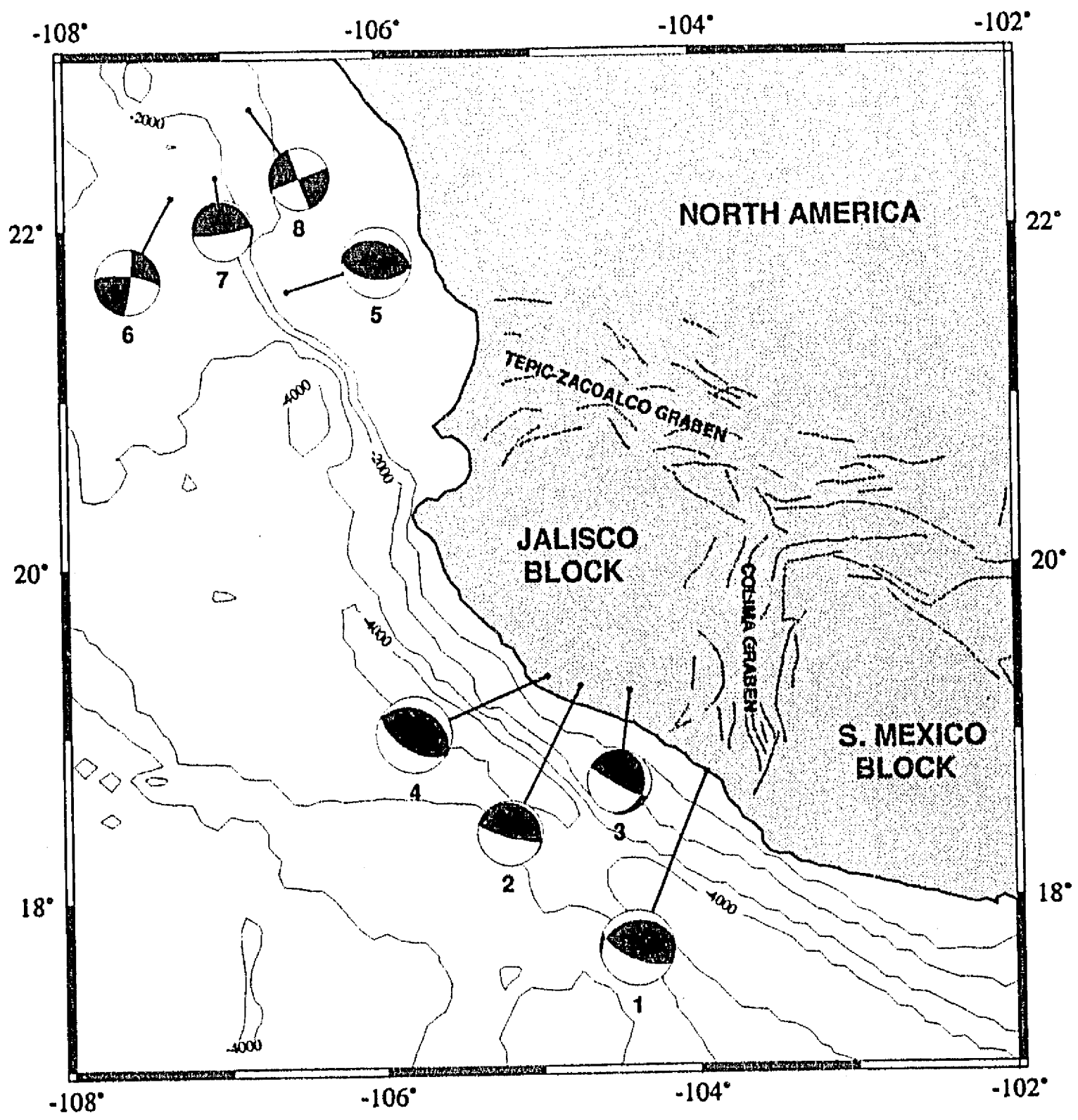


Fig. 2

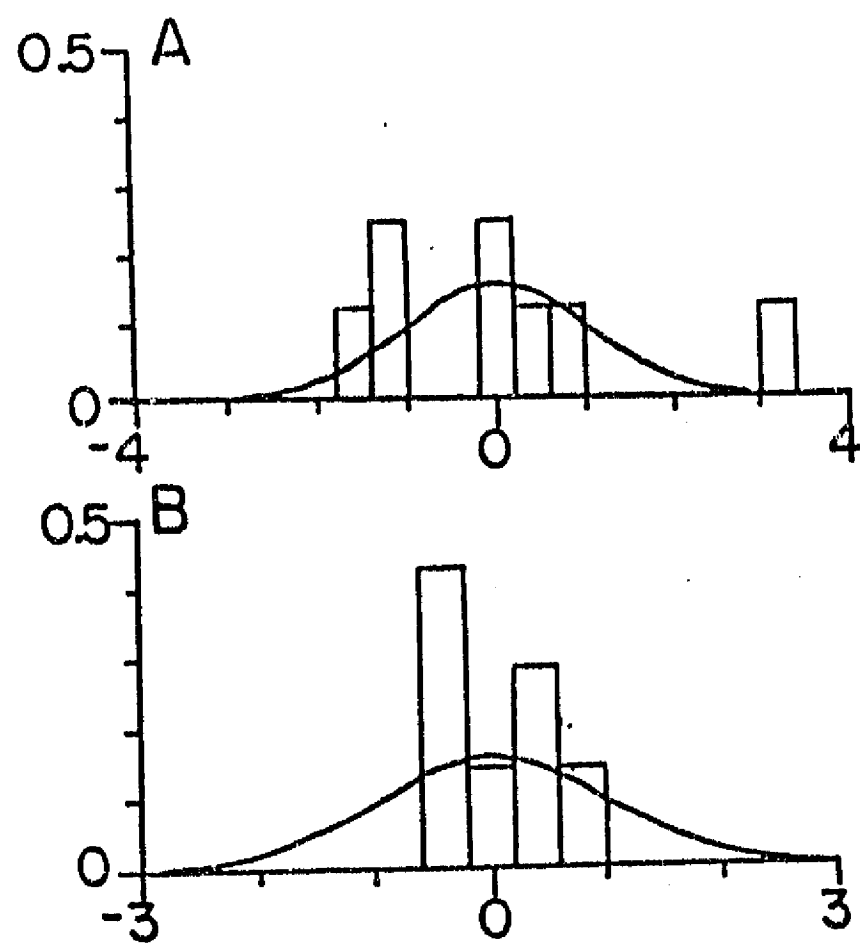


Fig. 3

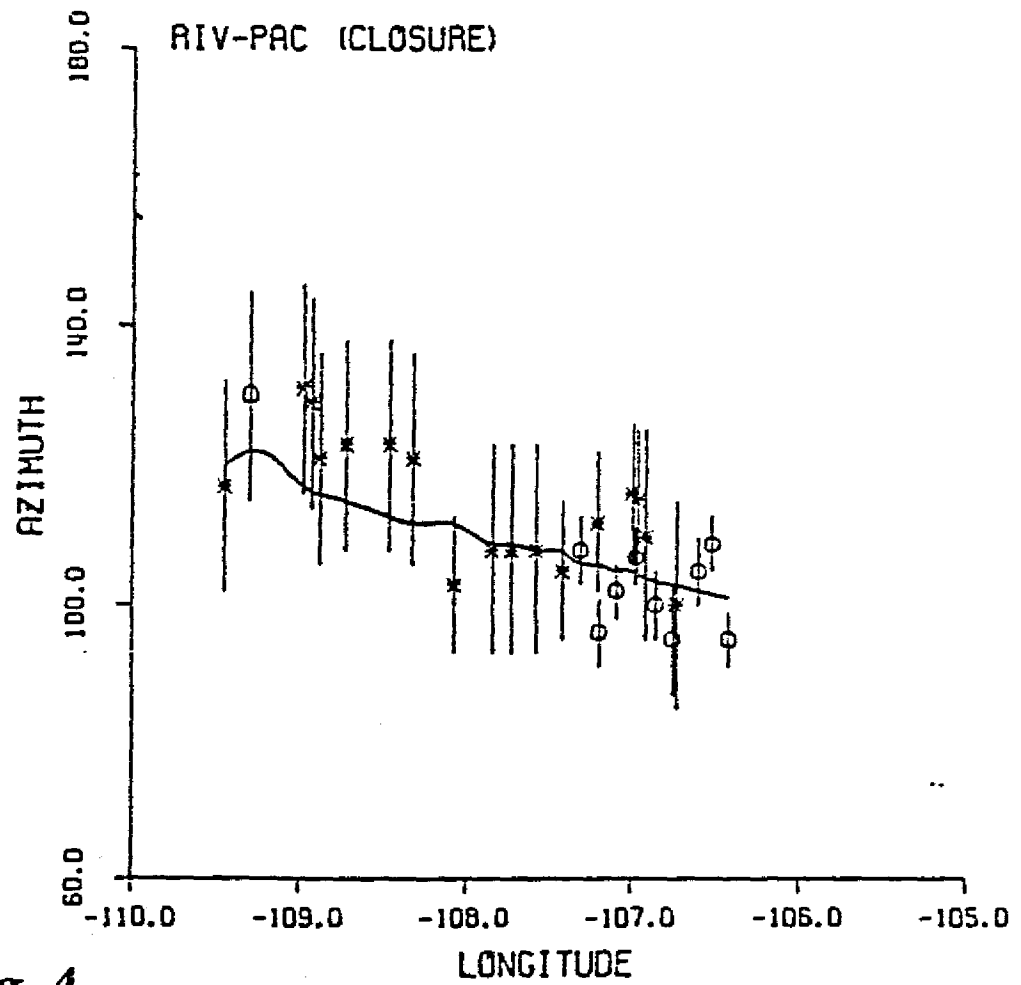
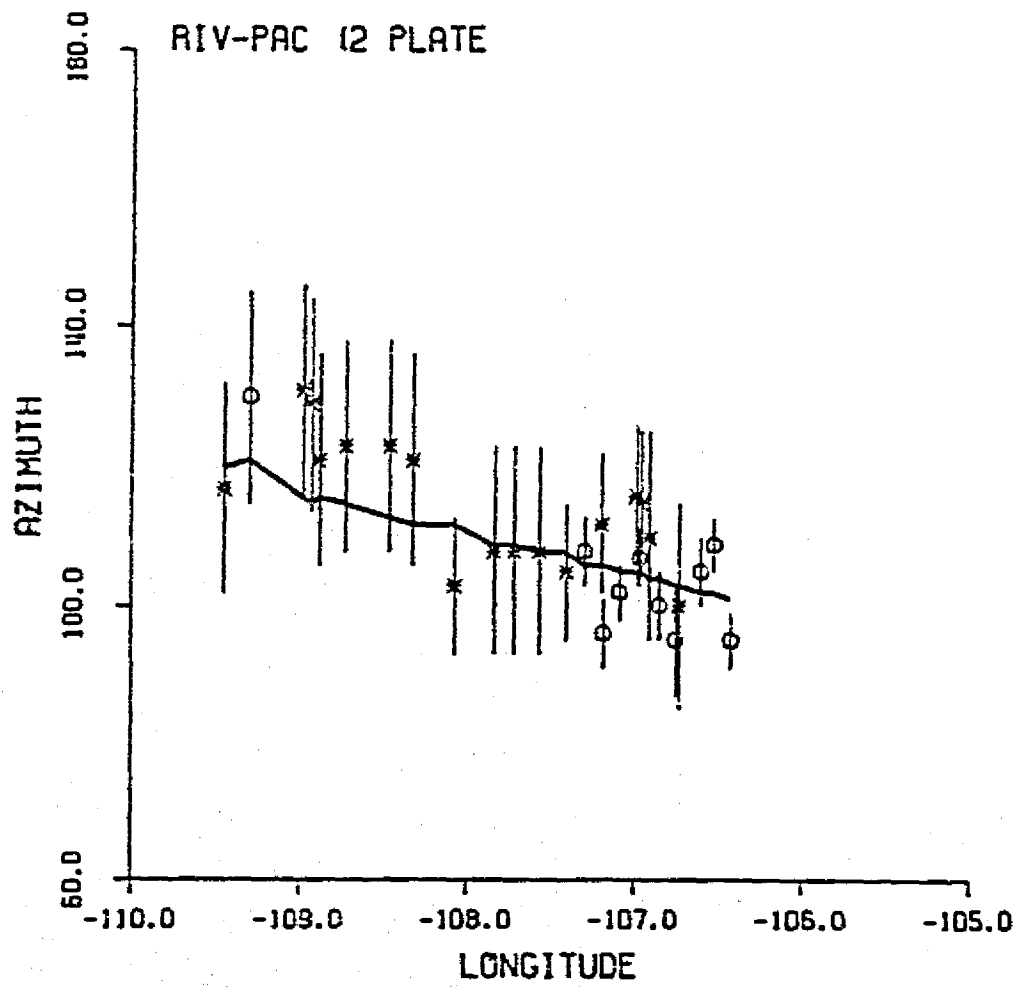
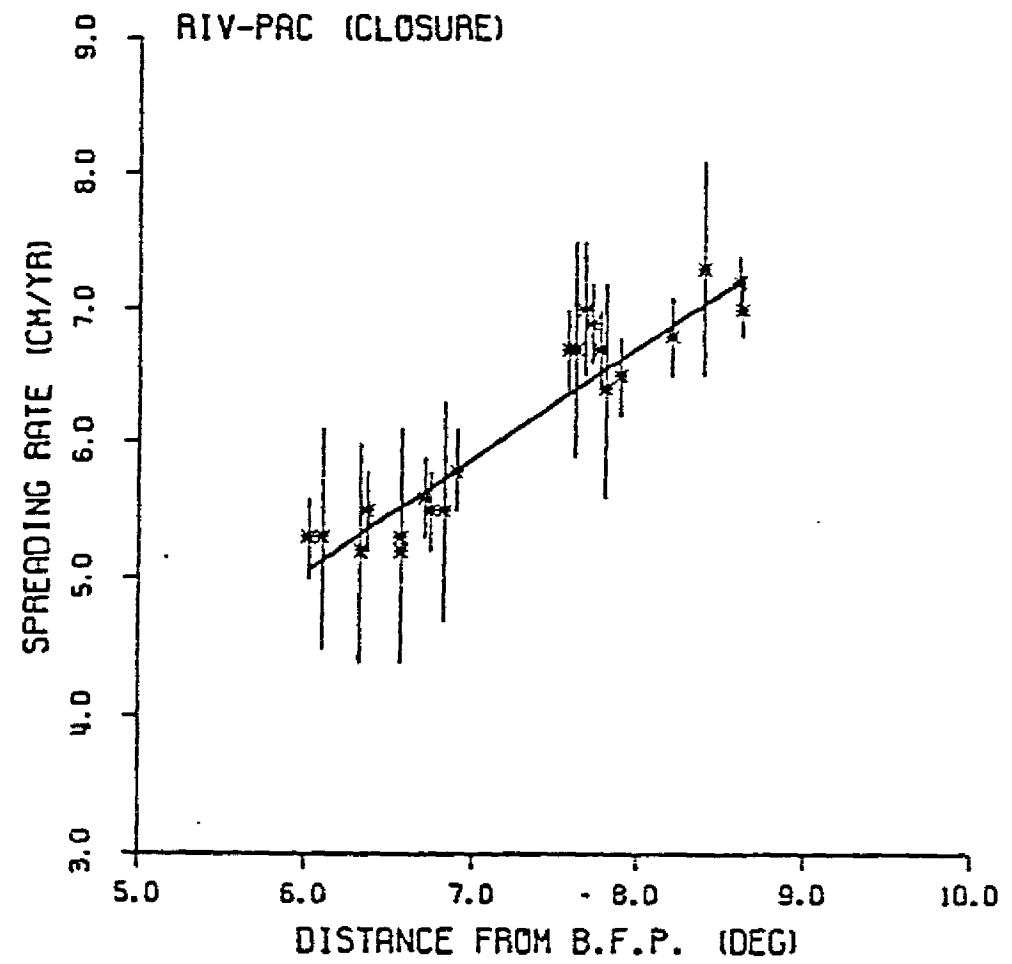
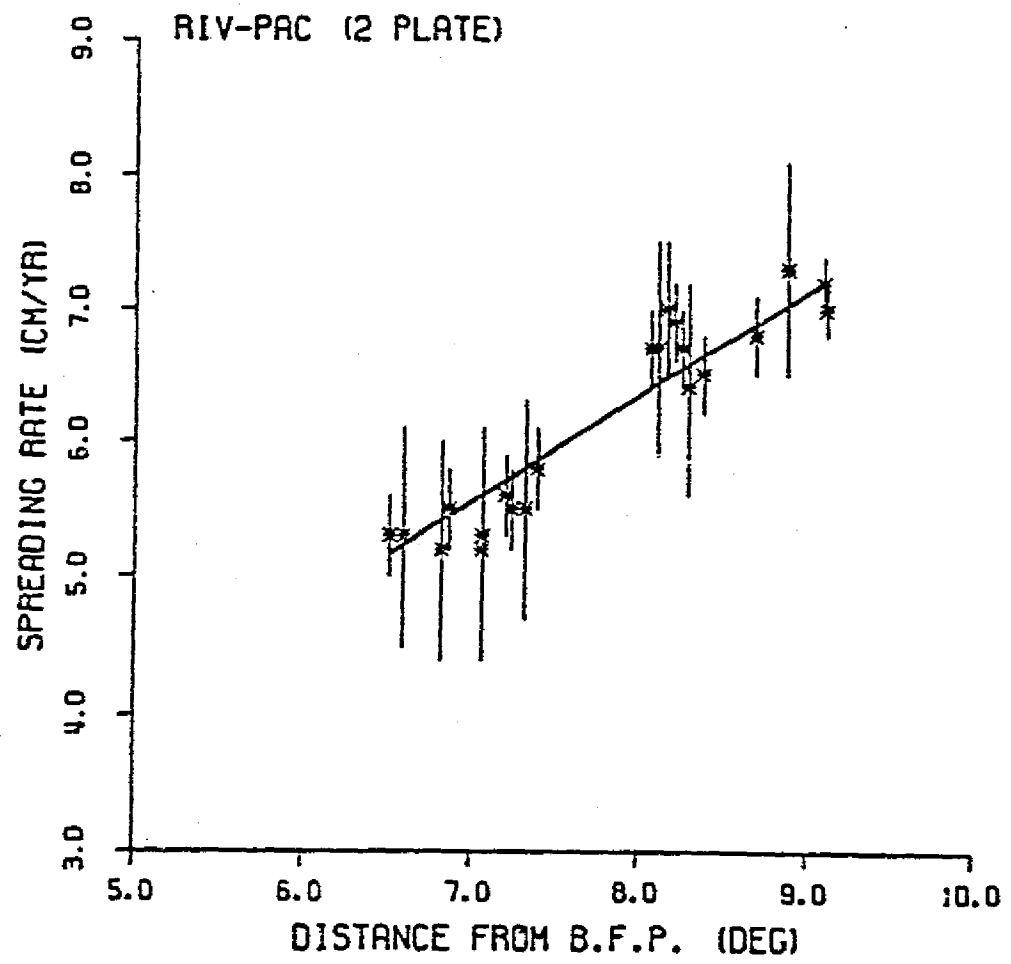


Fig. 4

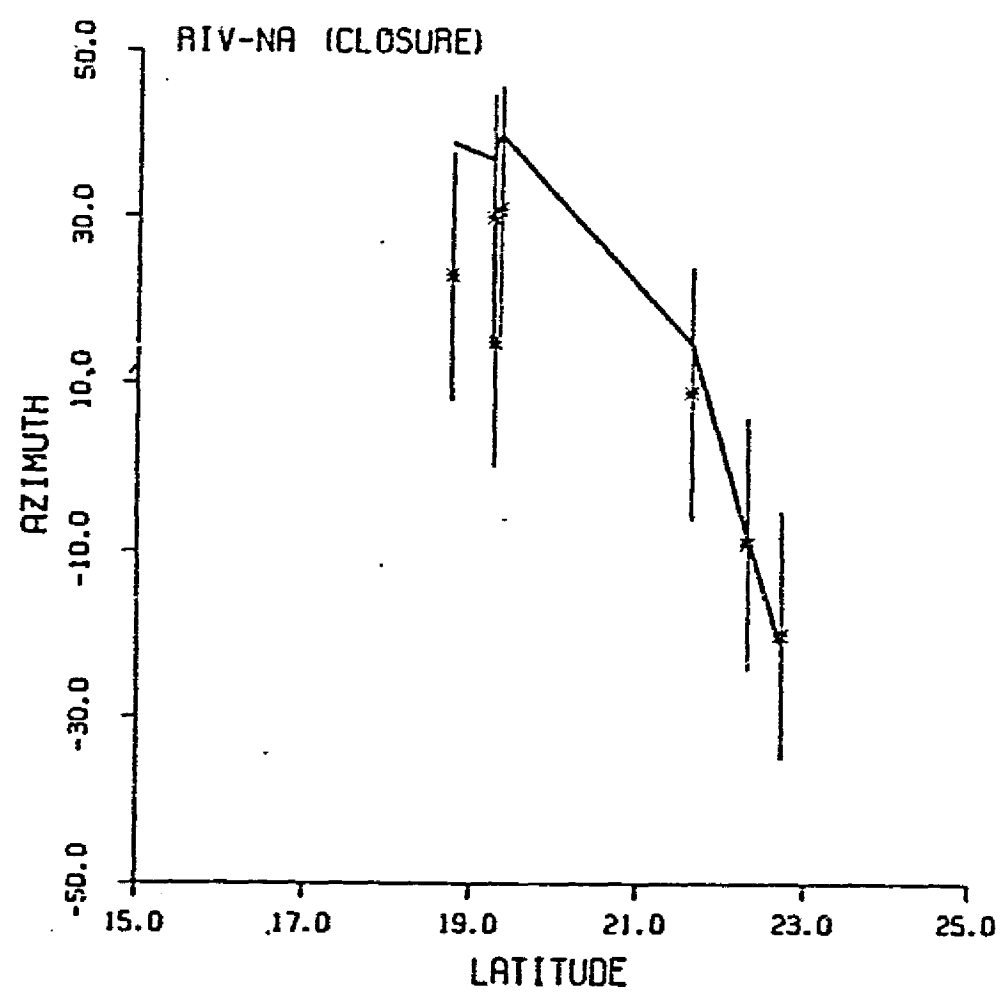
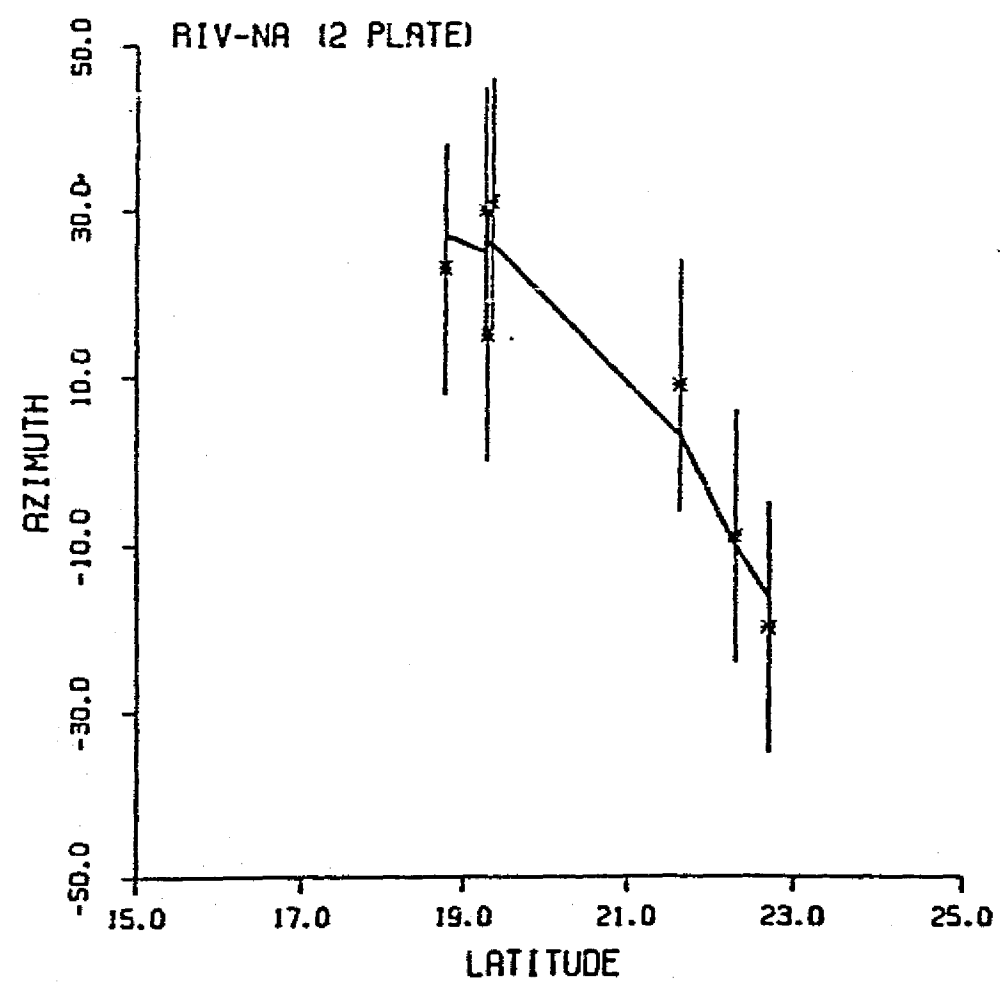


Fig. 5

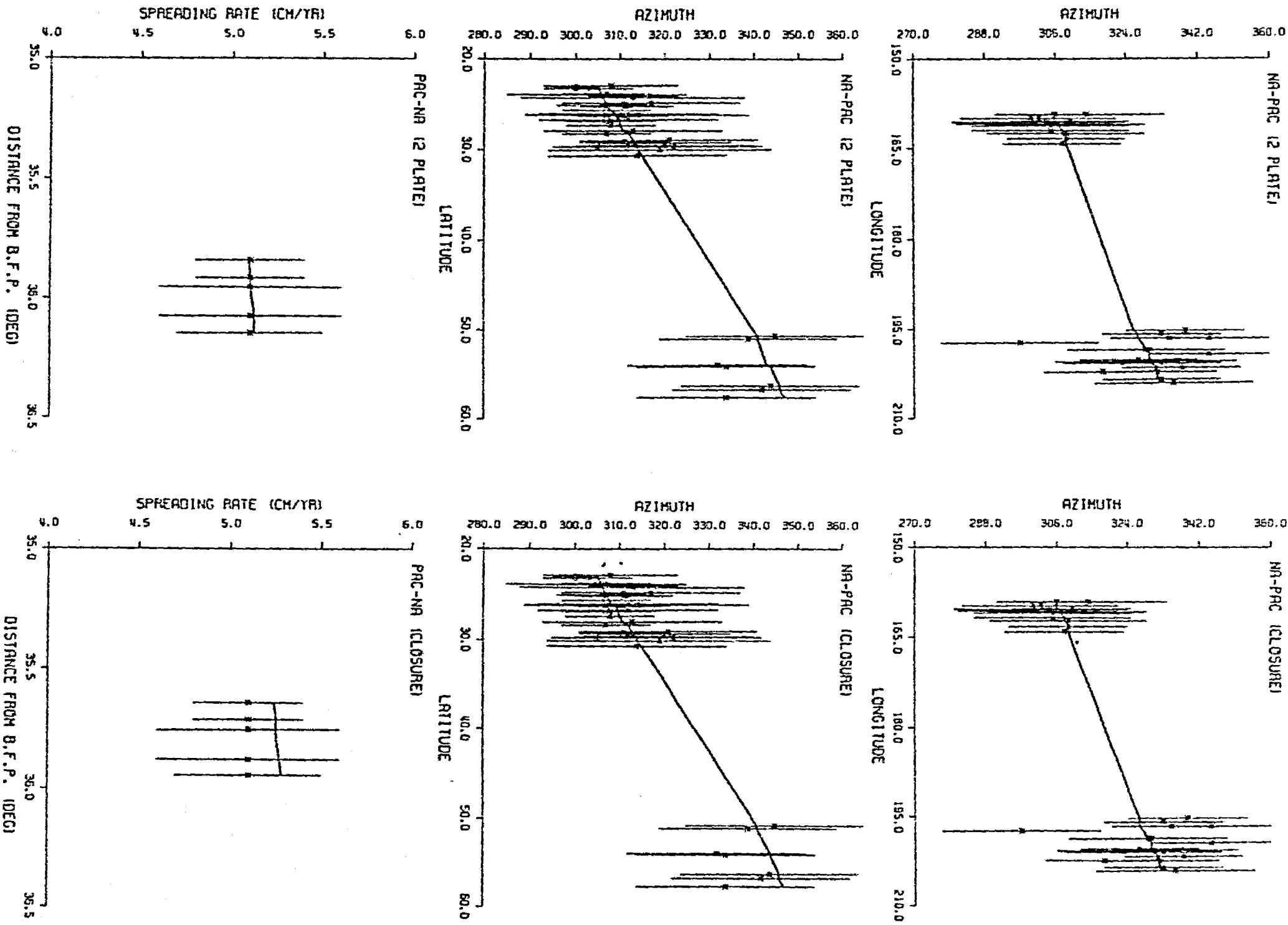


Fig. 6

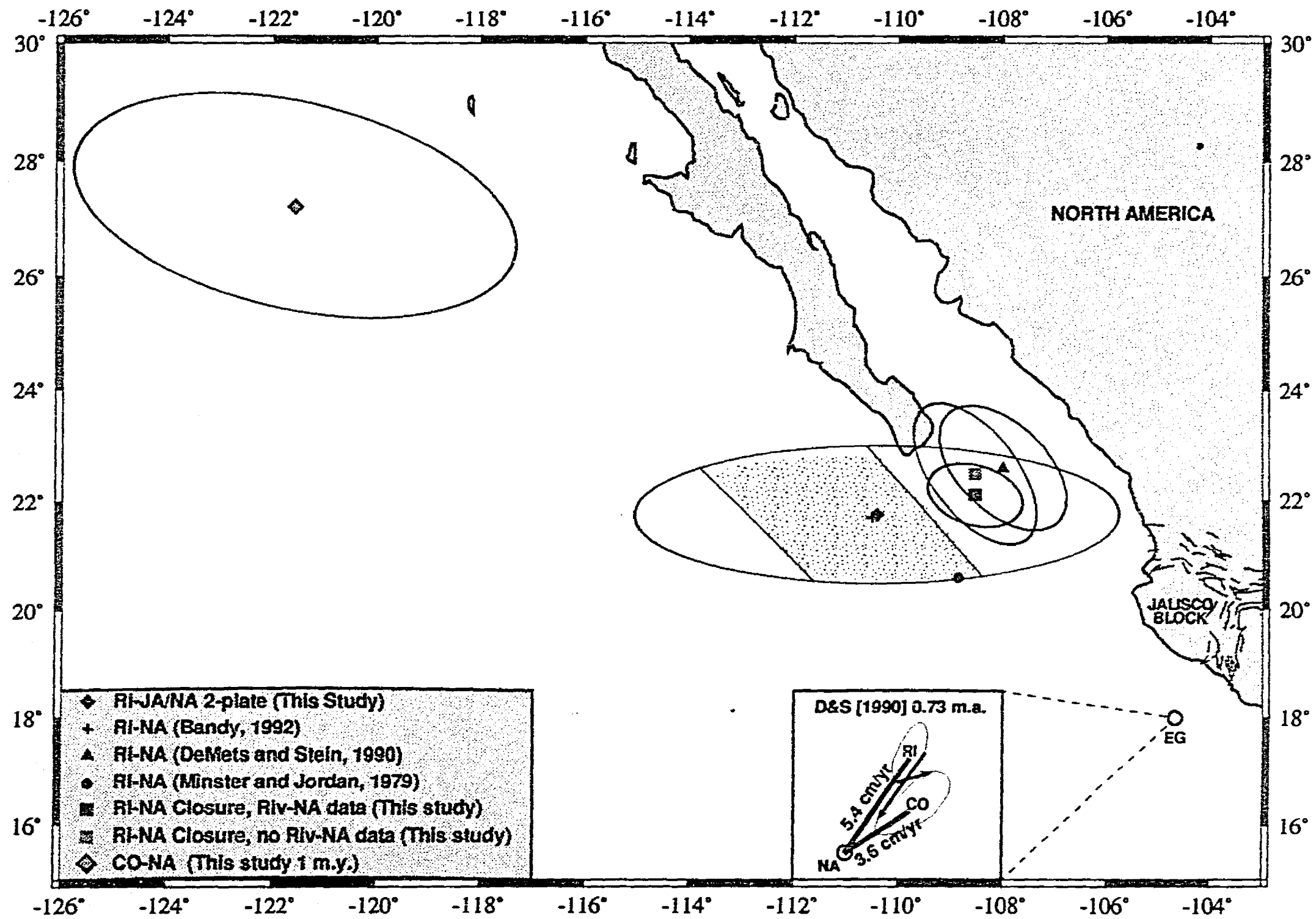


Fig. 7

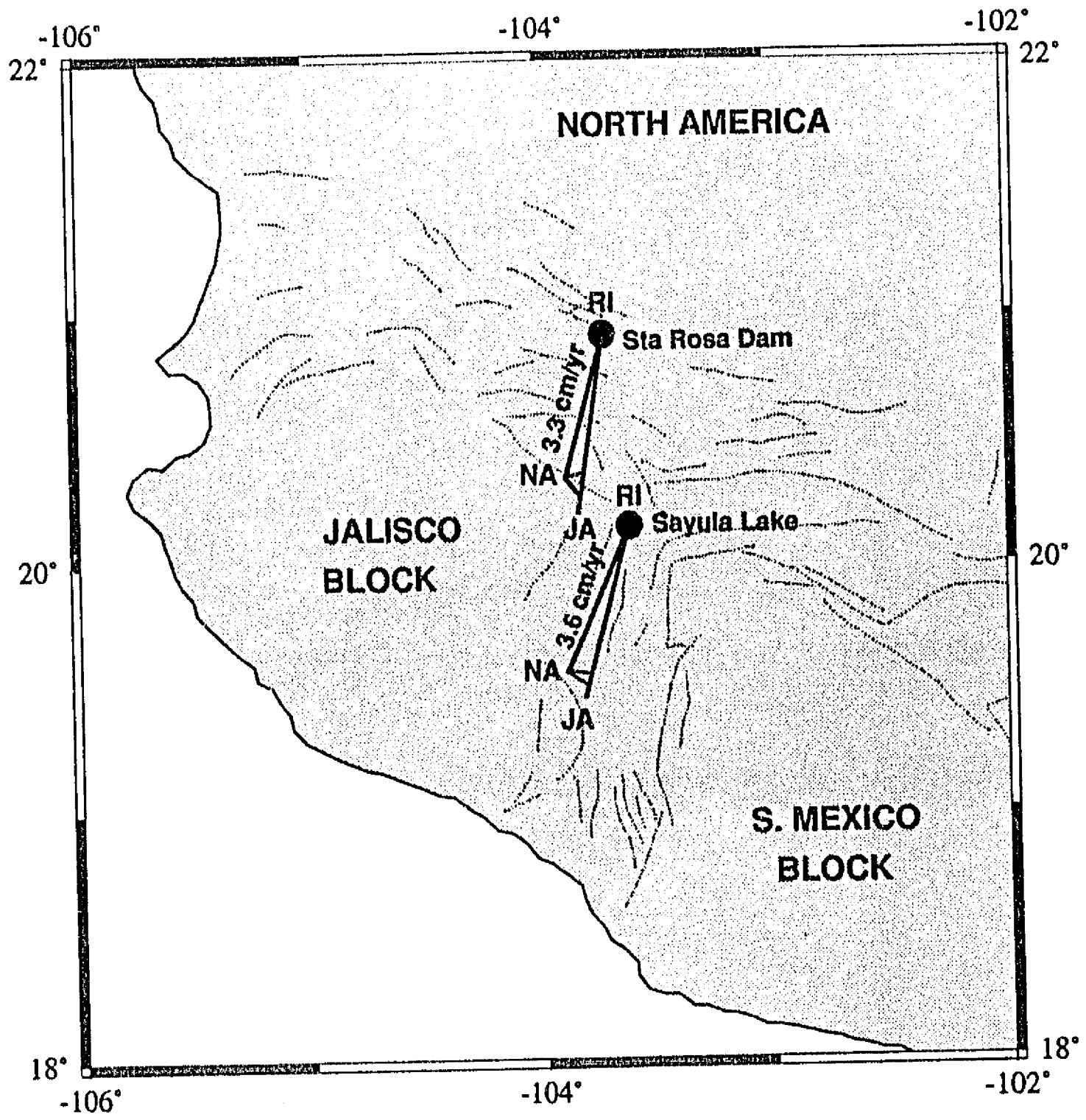


Fig. 8

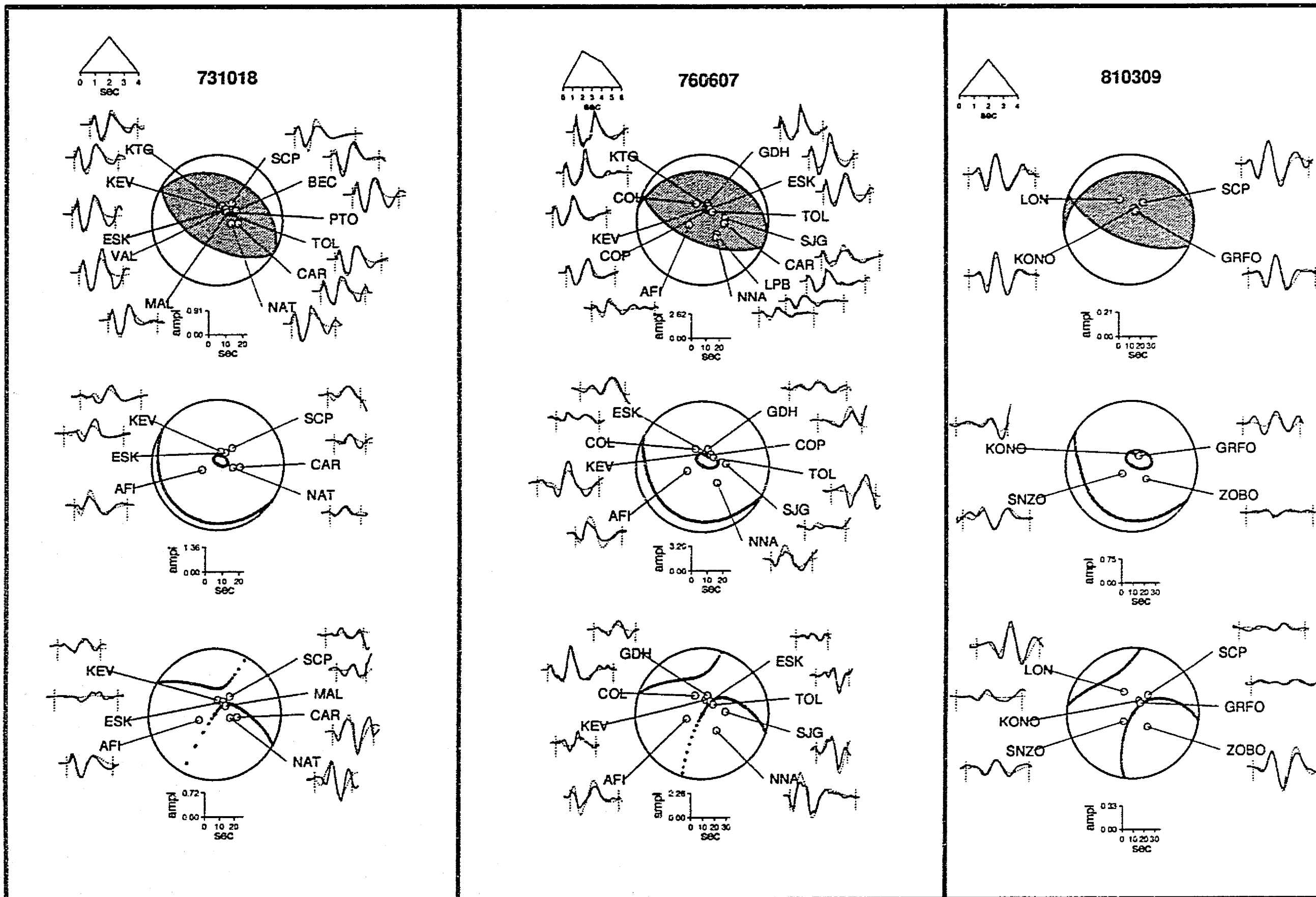


Fig. A1

VII. CONCLUSIONES

Se analizan las características de la subducción de las placas de Rivera y Cocos bajo la placa de Norte América en el sur de México, utilizando hipocentros y mecanismos focales de eventos registrados por redes locales y telesísmicas.

Las principales conclusiones de este estudio son las siguientes:

- La sismicidad base en el contacto sismogénico de zonas de subducción es proporcional a la edad de la placa en la trinchera y a la velocidad relativa de convergencia. Se define la sismicidad base como el número de sismos superficiales ($h \leq 70$ km) con magnitud $m_b \geq 5$ que ocurren en un área de 1000 km^2 por año, excluyendo los eventos que ocurren un mes antes y tres meses después de un sismo con magnitud $M_s \geq 7$. En el caso del sur de México se observa que la sismicidad base aumenta lateralmente hacia el sur-este debido a las variaciones de edad y velocidad de convergencia de las placas de Rivera y Cocos.
- No se observa una relación entre la sismicidad base y el grado de acoplamiento en zonas de subducción a nivel mundial. El grado de acoplamiento, relacionado con la magnitud máxima M_w esperada en la zona, es directamente proporcional a la velocidad de convergencia, pero inversamente proporcional a la edad de la placa en la trinchera.
- El ángulo de subducción de la placa de Cocos bajo Norte América es subhorizontal entre los 110-275 km de distancia de la trinchera, alcanzando una profundidad media de 50 km en la región de Guerrero. Este resultado confirma los modelos anteriormente propuestos para la zona.
- En la región de Guerrero, los mecanismos de foco de la sismicidad intraplaca continental indican que, en general, la placa de Norte América está sometida a un régimen de esfuerzos tensional
- La subducción de la placa de Rivera en la región oriental de México, bajo el bloque de Jalisco, comienza con un buzamiento suave de 10° hasta los 20 km de profundidad y luego aumenta gradualmente hasta alcanzar un buzamiento constante de 50° bajo los 40 km de profundidad. Este ángulo de subducción es mayor que el observado en la subducción de la placa de Cocos bajo Norte América, pero es similar al observado para la placa de Cocos bajo la placa del Caribe en Centro América.

- El volcán de Colima de carácter andesítico calco-alkalino, está directamente asociado a la subducción de la placa de Rivera. El frente volcánico Cuaternario de tipo andesítico, observado hacia el noroeste, paralelo a la trinchera, también puede ser explicado por la subducción de la placa de Rivera bajo el bloque de Jalisco.

- Se determinó un modelo integral de la geometría de la subducción de las placas de Rivera y Cocos bajo la placa de Norte América en el sur de México (oeste de 94°W), que considera una placa de Cocos boyante subduciendo en forma subhorizontal bajo Norte América, con condiciones de frontera de placas con geometría más inclinada en los bordes, correspondientes a la placa de Rivera bajo Norte América hacia el oeste y la placa de Cocos bajo la placa del Caribe hacia el este.

- Este modelo explica la sismicidad y el campo regional de esfuerzos. En la zona del contacto sismogénico, se observan eventos compresionales con profundidades máximas de ~ 30 km en la placa de Cocos y ~ 40 km en la placa de Rivera. Cuando se desacoplan las placas oceánica y continental, se observa una zona doble de esfuerzos con eventos tensionales más profundos que los eventos compresionales, alcanzando hasta 45 km de profundidad, que podrían estar relacionados con las flexiones que sufre la placa oceánica durante el proceso de subducción. Hacia el interior del continente se observa una zona asísmica con un ancho inversamente proporcional al buzamiento de la placa oceánica, seguida de una zona de eventos de fallamiento tensional de la litósfera oceánica en profundidad, relacionados con la acción de la gravedad sobre la placa al hundirse en el manto.

- No se observan cambios laterales en el buzamiento de la placa oceánica en la zona acoplada interplaca hasta 30 km de profundidad. No existe, aparentemente, una relación de la geometría interplaca con la subducción de rasgos batimétricos importantes en la zona, donde ocurren cambios en la edad de la placa en subducción a lo largo de la trinchera y en la velocidad de convergencia debido a la cercanía de los polos de rotación.

Sólo se observan cambios importantes en la geometría de la litósfera oceánica en subducción cuando ésta se desacopla de la placa continental, sugiriendo que a partir de la transición de la zona de acoplamiento las características de edad y velocidad de convergencia comienzan a ser parámetros importantes en la dinámica de la placa oceánica.

Los cambios notables observados en el ángulo de subducción a lo largo de la zona estudiada, se pueden correlacionar con la subducción de rasgos batimétricos importantes en la zona.

- El sur de México se puede dividir en cuatro regiones con diferentes características sismotectónicas, en base a la sismicidad, la geometría y sus cambios en el buzamiento:

1) La región de Jalisco que presenta una subducción inclinada de la placa de Rivera, similar a la observada bajo Centro América. Esta región comprende la zona de subducción de Rivera hasta la subducción del graben de El Gordo, límite propuesto entre Rivera y Cocos. La profundidad máxima de sismos observados en esta región es de 130 km.

2) La región de Michoacán comprendida entre el graben de El Gordo y la subducción de la zona de fractura de Orozco. Esta región corresponde a una zona de transición entre la subducción inclinada de la placa de Rivera y la subducción horizontal observada en Guerrero. La máxima profundidad de sismos en la región es de 100 km.

3) La región de Guerrero ubicada entre la subducción de las zonas de fractura de Orozco y de O'Gorman. La geometría de la subducción de la placa de Cocos bajo esta región es casi subhorizontal, con actividad sísmica hasta los 70 km de profundidad.

4) La región de Oaxaca comprendida entre la subducción de la zona de fractura de O'Gorman y la dorsal de Tehuantepec. Esta región corresponde a una zona de transición entre la subducción casi horizontal en Guerrero y la subducción inclinada de la placa de Cocos bajo la placa del Caribe. La profundidad máxima de sismos en la región aumenta gradualmente desde 70 km cerca de O'Gorman hasta 180 km bajo Tehuantepec.

- Los cambios en la geometría de la subducción que ocurren en torno a los límites de las regiones propuestas, parecen ser contorsiones suaves sin fallamiento de la litósfera oceánica en subducción, excepto en el caso del límite entre las placas de Cocos y Rivera donde se observa un cambio rápido en el buzamiento de la placa oceánica. Sin embargo, con los datos disponibles no es posible resolver si existe en esta zona una fractura o una contorsión en la placa oceánica.

- Los contornos de 80-100 km de profundidad de la geometría de la subducción en el sur de México se correlacionan bien con el frente de la faja volcánica transmexicana, indicando una asociación directa entre la faja volcánica con la litósfera oceánica en subducción en la zona. El no paralelismo de la faja volcánica con la dirección de la trinchera se debe fundamentalmente a la geometría de la subducción de las placas de Rivera y Cocos bajo Norte América en el sur de México.

- Se ha postulado una fragmentación de la placa de Norte América en dos bloques tectónicos, Jalisco y Sur de México, localizados al sur de la faja volcánica transmexicana.

Para verificar la posible existencia y movimientos relativos de estos bloques, se realizaron análisis estadísticos para determinar la existencia de diferencias significativas en el cierre de un circuito de placas tectónicas, con datos de movimientos de placas derivados de alineamientos de anomalías magnéticas, vectores de deslizamiento de mecanismos focales y azimuts de fallas transformadas. Los resultados indican que:

a) No existe diferencia significativa en el cierre del circuito Pacífico-Cocos-Norte América, implicando que el movimiento del bloque del Sur de México es insignificante relativo a las placas litosféricas circundantes. Por lo que puede ser considerado como parte de la placa de Norte América.

b) Existe una diferencia significativa en el cierre del circuito Rivera-Pacífico-Norte América. Esto implica dos posibles interpretaciones:

1) Existe el bloque de Jalisco con un movimiento relativo a Norte América muy lento y menor que 5 mm/a y es independiente de las placas circundantes.

2) No existe en forma independiente el bloque de Jalisco, el que sería parte de la placa de Norte América. En este caso las diferencias significativas en el cierre del circuito de placas se deberían a efectos generados por cambios recientes en el movimiento relativo entre las placas de Rivera y Pacífico.